

AD-A074 782

CONTROL DYNAMICS CO HUNTSVILLE AL*
APPLICATION OF DISCRETE GUIDANCE AND CONTROL THEORY.(U)
AUG 79 S M SELTZER

F/G 17/7

UNCLASSIFIED

CDC-79-2

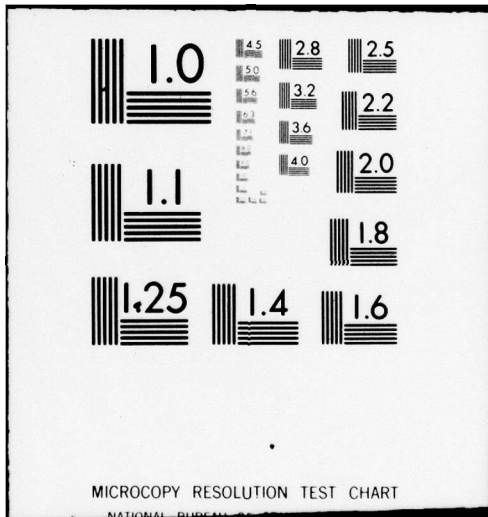
DAAK40-78-C-0226

NL

1 of 3

ADA
074782





MICROCOPY RESOLUTION TEST CHART

NATIONAL BUREAU OF STANDARDS-1963-A

AD A 074782

LEVEL III

2
B. 4

6 APPLICATION OF DISCRETE GUIDANCE AND CONTROL THEORY.

by

10 S. M. Saltzer Principal Investigator

9 Final Technical Report

This research was performed for the
United States Army Missile Research and Development Command
Redstone Arsenal, Alabama 35809

under

Contract No. DAAK1-78-C-226

15

DDC
RECEIVED
OCT 8 1978
E

14 CDC-79-2

Control Dynamics Company
701 Carlett Drive Suite 2
Huntsville, Alabama 35802

12 225

DDC FILE COPY

This document has been approved
for public release and sale; its
distribution is unlimited.

11 CDC-79-2
Aug 1979

394 628

MTI

70 08 17 006



DISCLAIMER NOTICE

**THIS DOCUMENT IS BEST QUALITY
PRACTICABLE. THE COPY FURNISHED
TO DDC CONTAINED A SIGNIFICANT
NUMBER OF PAGES WHICH DO NOT
REPRODUCE LEGIBLY.**

2

DDC
OCT 10 1979
E

ABSTRACT

This technical report covers Task II of a two-task investigation into the application and implementation of advanced discrete guidance and control theory and analysis to a United States Army missile system of the future. Task I was completed during the period 7 August through 30 September 1979 and is described in Applied Control Systems Dynamics Company Report ACSD-78-2, dated September 1978. 8034571

During Task II a stability analysis, summary, and implementation associated with the discrete control for a missile system was performed via the parameter space technique. Emphasis was placed upon the development of analytical tools to perform the design and analysis of the system. The three design tools developed under this contract are described:

1. SAM; an Alternative to Sampled-Data Signal Flow Graphs;
2. Determination of Digital Control System Response by Cross-Multiplication; and
3. Sampled-Data Analysis in Parameter Space.

The three techniques have been cast in a form amenable to implementation within digital computers or desktop calculators.

Also, during Task II, a technical seminar was conducted for selected members of the Guidance and Control Directorate. In addition, summarized within the report are the presentations prepared by Dr. Seltzer and trips undertaken in its behalf.

This document has been approved for public release and sale; its distribution is unlimited.

TABLE OF CONTENTS

	Page
SECTION I. INTRODUCTION	1
A. Study Objective	1
B. Study Schedule	2
C. Contents of Report	2
SECTION II. DEVELOPMENT PROGRAM FOR ADVANCED GUIDANCE & CONTROL SYSTEM	4
SECTION III. SURVEY OF PERTINENT STATE-OF-THE-ART	6
SECTION IV. PERFORMANCE REQUIREMENTS	7
SECTION V. GUIDANCE AND CONTROL LAW EXTENSION	8
A. Introduction	8
B. Design Tool Development	8
C. Survey and Implementation of Discrete Control for Missile Systems via the Parameter Space	14
SECTION VI. TECHNICAL SEMINAR	29
SECTION VII. AMERICAN INSTITUTE OF AERONAUTICS & ASTRONAUTICS ACTIVITIES	33
SECTION VIII. SIG-D EVALUATION	34
SECTION IX. HELLFIRE WHITE PAPER	35
SECTION X. PRESENTATIONS	36
SECTION XI. TRIPS	37
SECTION XII. SUMMARY	38
SECTION XIII. CONCLUSIONS	40
SECTION XIV. REFERENCES	41
SECTION XV. FIGURES	42

Accession For	<input checked="" type="checkbox"/> <input type="checkbox"/> <input type="checkbox"/>	DTIC GRA&I DDC TAB Unannounced Justification	Distribution/ Availability Codes	Avail and/or special <div style="text-align: center; font-size: 2em; font-family: cursive;"> 33P </div>
BY				1st <div style="text-align: center; font-size: 2em; font-family: cursive;"> 33P </div>

- APPENDIX A. SAM. AN ALTERNATIVE TO SAMPLED-DATA SIGNAL FLOW GRAPHS
- APPENDIX B. DETERMINATION OF DIGITAL CONTROL SYSTEM RESPONSE BY CROSS-MULTIPLICATION
- APPENDIX C. SAMPLED-DATA ANALYSIS IN PARAMETER SPACE
- APPENDIX D. PARAMETER SPACE PROGRAM: STABILITY REGIONS
- APPENDIX E. SYSTEM RESPONSE PROGRAM
- APPENDIX F. AIAA PAPER: "GUIDANCE LAWS FOR SHORT RANGE TACTICAL MISSILES"
- APPENDIX G. SIG-D EVALUATION
- APPENDIX H. HELLFIRE WHITE PAPER
- APPENDIX I. PRESENTATION TO DR. HUFF AND DR. HARTMAN
- APPENDIX J. PRESENTATION TO ADVANCED SENSORS DIRECTORATE
- APPENDIX K. PLANT MODEL FOR ADVANCED GUIDANCE AND CONTROL SYSTEM

SECTION I. INTRODUCTION

A. Study Objective

The purpose of this study is to investigate the application and implementation of advanced discrete guidance and control theory and analysis to a United States Army Missile System of the future. An aim of this investigation is to achieve modularity of the guidance and control system functions. The end result of this study is the analysis and preliminary design of a discrete (or digital) guidance and control system (or systems) that can be used for a U. S. Army Guided Missile System.

The study effort is composed of two tasks described in the Scope of Work, contained in Technical Requirement T-0107, entitled "Application of Discrete Guidance and Control Theory." The requirements imposed by these two tasks are contained in the referenced contract document and re-stated (for convenience of the reader) below.

Task I requirements:

2.1 Obtain or derive several candidate guidance and control laws applicable to boost, coast, and terminal flight phases of a long range ground-to-ground missile system.

2.2 Obtain or derive mathematical models of the missile system applicable to the three flight phases identified in Subsection I.1 above. The models shall include significant dynamics of missile plant, sensors, effectors, on-board computer or processor, and external disturbances (such as aerodynamics). In particular, identify any significant nonlinearities in the model. Since a major portion of this modeling already exists in-house, this task shall be oriented to extending that currently available.

2.3 Mathematically cast the several candidate guidance and control laws, Subsection I.1 above, in a form amenable to their implementation in an on-board computer or processor.

Task II requirements:

2.4 Extend the guidance and control laws of Subsection 2.1 and Subsection 2.3 via the parameter space technique for the analysis and design of digital control systems. Investigate the capabilities and limitations of this technique to the discrete control system of the missile developed in Subsection 2.3 and compare the results obtained through the use of extant sampled-data techniques.

2.5 Combine the outputs resulting from Subsections 2.2, 2.3, and 2.4 above so the dynamics of each system may be determined analytically, using both existing and newly-developed digital and sampled-data techniques.

2.6 Deleted by Contract Amendment, Modification No. P00002, dated 31 January 1979.²

2.7 Document in complete detail the modeling, analysis, and simulation results described in Subsections 2.1 through 2.6 above.

2.8 Conduct a technical seminar for selected members of the Guidance and Control Analysis Group, Guidance and Control Directorate (DRDMI-TGN).² The purpose of the seminar is to develop a design expertise among members of the Group to enable them to design and evaluate discrete guidance and control systems. Both existing and newly-developed sampled-data techniques will be described and discussed in detail with practical applications conducted during the course of the seminar conference.

B. Study Schedule

The requirements of Task I were completed during the period, called Phase I, 7 August 1978 (date of contract initiation) through 30 September 1978. They are reported upon in Applied Control Systems Dynamics Company Report ACDS-78-2, dated September 1978, entitled: "Application of Discrete Guidance and Control Theory. Technical Report: Phase I."³

The requirements of Task II are to be completed during the period, called Phase II, that culminates in twelve (12) months duration. This is construed to mean the period ending 6 August 1979. It began with Amendment 1, Modification P00001, effective 20 October 1978.⁴

C. Contents of Report

This technical report covers the effort performed in completing the requirements of Task II of the study, i.e., Phase II. As stated in the referenced contract requirements, the documentation of this technical report shall include, but not be limited to,⁵

a. A stability analysis, summary and implementation of the discrete control for the missile system applicable via the parameter space technique. The results and comparisons made for the extant sampled-data technique shall be documented.

- b. Any simulation initializing operations.
- c. Any simulation input parameters required and their formats.
- d. Any analytic results produced.
- e. Operating instructions for a user of the computer simulation(s) generated.
- f. (deleted)
- g. Summary of computer simulation runs, results, and analyses performed.

The documentation shall cover work done to perform Task II from 20 October 1978 (beginning of Modification P00001 of the contract) until completion of contract. The required documentation shall be a technical report to be delivered to the Guidance and Control Analysis Group (DRDMI-TGN).

SECTION II. DEVELOPMENT PROGRAM FOR ADVANCED GUIDANCE & CONTROL SYSTEM

The definition of the development program for the Advanced Guidance and Control System was developed during Task I and may be found in the referenced technical report: Phase I.³ The original development program, then entitled "Development Program for an Optimal Digital Guidance and Control System for U. S. Army Future Missiles" is included as Appendix A of that report. That development program comprises the framework within which the study is being performed. A summary follows of that program.

The U. S. Army Missile Research and Development Command (MIRADCOM) recently embarked on a task to develop an Advanced Guidance and Control (G&C) System for future U. S. Army Modular Missiles. The intent is to "leapfrog" systems currently under development. The reason for embarking on this task is that existing weapon systems may be seriously degraded in engagements against targets with predicted characteristics of the 1990's and beyond and in the battlefield environments of the time frame. It has been established that the guidance laws currently in use may not be adequate to control these dynamically elusive threats. Thus, it is projected that fundamental advances in G&C systems theory are required to enhance the effectiveness of future weapon systems. Additionally, missile airframe and propulsion systems may require advances commensurate with predicted target scenarios. In particular, air defense weapons currently in R&D may be seriously hampered in the combat scenarios envisioned. From an overall system viewpoint, this task shall address the issue of creating new theory in the G&C area to meet the high performance threats of the future. From the systems requirements, the objective clearly emerges to develop and validate research that will enable the digital optimal guidance and control of future U. S. Army Modular Missiles. The work that has taken place to meet this objective began in fiscal year 1979. It began with a continuing definition of the dynamics of predicted future targets. This was followed by performing and documenting an extensive search of literature pertaining to the theory and implementation of missile guidance laws. A trade study was conducted to compare capabilities of the guidance law classes, leading to the selection of an optimal formulation of the advanced guidance law. Development began of analytical models of candidate future missile and subsystems (to enable realistic G&C system research). New digital control theory also was developed with an eye toward simplifying elusively difficult mathematical tools for designing digital systems. For example, an alternative to the usually difficult and cumbersome digital signal flow graph method of design already has been developed. In fiscal year 1980, it is planned to further extend and develop new digital (sampled-data) theory. Computer software will be developed to implement these (and other) theoretical advanced analysis tools. Guidance law performance indices

will be evaluated, and the need for on-board state estimation techniques will be determined. Parallel to this effort, fluidics technology will continue to be developed. Beyond fiscal year 1980, candidate advanced G&C systems configurations will be defined and a figure of merit developed. Advanced analysis and simulation techniques will be used to evaluate the candidate G&C systems. Additionally, the merits of advanced electronics, fluidics, and distributed controllers will be evaluated.

The foregoing G&C efforts are being conducted within the Technology Laboratory of MIRADCOM. The Advanced G&C System program is defined within the G&C Directorate. It is being implemented by both in-house engineers and by contracted effort at universities and local industry. It is to support this Advanced G&C System program that the contract described by this technical report was made.

The participation of the G&C Analysis Group in the Advanced G&C System development has been through the assignment of particular areas of research and development. The assignments are indicated in Appendix A of Technical Report: Phase I and in Appendices I and J of this report. Progress has been indicated by individual oral quarterly reports to Mr. Russell T. Gambill. It is planned to formalize a progress report at the end of fiscal year 1979 by the Guidance and Control Analysis Group.

SECTION III. SURVEY OF PERTINENT STATE-OF-THE-ART

As reported in the Technical Report: Phase I, the U. S. Air Force presently is investigating and developing advanced digital guidance and control concepts for air-to-air missiles. Dr. Seltzer has maintained close liaison with the principal investigators at the U. S. Air Force Armament Laboratory, Eglin Air Force Base. Of particular interest has been their development of an algorithm to predict "time-to-go" (remaining time of flight). This important parameter is needed by both optimal guidance law formulations and Disturbance Accommodating Control formulations. It presently is being investigated for applicability and ease of implementation.

An awareness of the rapidly changing state-of-the-art has been maintained by Dr. Seltzer, partially through his participation in American Institute of Aeronautics and Astronautics (AIAA) conferences pertinent to the subject at hand (see Section VII). This is augmented by extensive selected reading of pertinent literature and technical publications.

SECTION IV. PERFORMANCE REQUIREMENTS

As a result of extensive studies of predicted future target characteristics conducted by personnel of the Guidance and Control Analysis Group, Dr. Seltzer conducted extensive discussions and analyses of the gathered information with these personnel and personnel of the Department of Defense (see Section XI). The results were the following:

1. The surface targets of the 1990's era probably will be capable of being engaged by surface-to-surface missiles now in the field or presently under development.

2. The aerial targets of the 1990's era that may be too elusive dynamically for surface-to-air missiles presently under development are:

- a. Tactical ballistic missiles;
- b. Aircraft (manned or unmanned);
- c. Cruise missiles; and
- d. Remote pilotless vehicles (RPV's).

The predicted large number of RPV's probably dictates their engagement by less expensive weapons than a guided missile. Hence, the first three predicted future target classes are considered to be those that must be engaged by an Advanced Guidance and Control System. Hence, it is their characteristics that are used to define the necessary performance characteristics of the Advanced G&C System and its missile. To this end, a design point for the proposed future missile is developed as follows:

Mach No.: 4
Lateral g's: 12
Altitude: 70,000 feet.

It is expected that these values will be exceeded by a significant margin, e.g., perhaps 20 g's.

In an attempt to determine analytically if such performance requirements are feasible, the Aeroballistics Directorate was contacted. Members of that Directorate are now investigating three possible candidate missile configurations with the hope of determining one (or more) that can meet the desired characteristics. They are shown in Appendix K.

SECTION V. GUIDANCE AND CONTROL LAW EXTENSION

A. Introduction

Mathematical models of candidate guidance laws were categorized and described in Section IV of the Technical Report: Phase I.³ A means of extending guidance and control laws is developed in Part B of this section. It is then applied - via the parameter space technique in particular - to a selected model of a future missile system, using as a basis Section IV of the Technical Report: Phase I. This is performed in Part C of this section. The results are then compared with those that would be obtained by extant sampled-data techniques.

B. Design Tool Development

As a means of meeting Section 2.4 of the referenced Scope of Work in Technical Requirement T-0107, three new design and analysis tools were developed by Dr. Seltzer. They are described summarily in the following three subparagraphs and in detail in Appendices A, B, and C of this report.

1. SAM: An Alternative to Sampled-Data Signal Flow Graphs.

In Appendix A, an alternative to the use of Signal Flow Graphs (SFG's) and Mason's Gain Rule (Formula) is presented to use in the analysis of complicated sampled-data digital control systems. Usually in such systems, block diagram algebraic manipulation may become unwieldy, particularly when such systems include multiple loops and samplers. The Systematic Analysis Method (SAM) may be applied to such systems (as well as to simple single-loop feedback systems, of course). This is shown in Section II of Appendix A. Also shown is how to apply SAM to make use of Modified Z - transforms (Section V of Appendix A).

The advantages of using SAM are that the cumbersome application of Mason's Gain Formula can be avoided. Further, the entire method of drawing Signal Flow Graphs may be circumvented. Since only the equations describing the system are needed for SAM, even the customary block diagram is not needed.

If the analyst prefers to use one of the Signal Flow Graph (SFG) methods, a modified SFG technique is also described (Section III of Appendix A). It is simpler and less cumbersome to apply than the conventional SFG method which, for purposes of comparison, is described in Section IV of Appendix A.

All three techniques are applied to two examples in Appendix A. This is done to better describe the application of SAM and the modified SFG and to help provide a basis for the following comparison of the three methods.

The Systematic Analysis Method (SAM) can be used to determine the states of a digital system in terms of that system's transfer functions and the inputs to the system. This, of course, can also be done by the application of other methods, such as signal flow graph (SFG) techniques. The usual advertised advantages of the latter, when they are compared to block diagram or algebraic manipulation, are that they are particularly amenable to the analysis of complicated systems.

It is demonstrated in Appendix A of this report that SAM can handle digital system analysis as capably as can SFG methods. It has the advantage of not requiring the cumbersome Mason's Gain Rule. It hence avoids the oft-committed errors associated with SFG analysis; such as over-looked closed-loops, non-obvious forward paths, etc.. As with SFG's, a block diagram is not needed - the system equations are sufficient.

Finally, it is demonstrated that SAM is easy to implement. It appears to take less lengthy analytical manipulation.

If the analyst prefers using SFG's to either block diagrams or algebraic manipulations, a modified SFG technique is presented. It is based on SAM techniques. As such, it is systematic. While the SFG's produced by this technique are usually different from those produced by standard SFG techniques, they yield the same results. Mason's Gain Rule is only applied at one stage of the analysis in the modified SFG technique - as opposed to the standard SFG technique which requires several applications of Mason's Gain Rule.

In conclusion then, an alternative to the Signal Flow Graph (SFG) technique has been presented and compared to a standard and a modified SFG. The alternative, termed Systematic Analytical Method or SAM, is claimed herein to be simpler and more straightforward to implement than the SFG methods. Not only does it appear to be quicker to use in system analysis, but it obviates the cumbersome use of Mason's Gain Rule. For the analyst who desires to use SFG techniques, a modified SFG technique is presented. It is systematic and reduces the number of required applications of Mason's Gain Rule.

2. Determination of Digital Control System Response by Cross-Multiplication.

In Appendix B, a means is described for obtaining the response of a digital control system from its closed-loop transfer function. It is assumed that the closed-loop transfer function is available in the z - or modified z -transform domain. The numerator and denominator of each side of the transfer function are cross-multiplied. The Real Translation Theorem is then applied to the result, yielding a difference equation in the time-domain. This may be solved for the system response in terms of the reference (or other) input(s) to the system as well as in terms of system state initial conditions.

Two different modifications to the basic technique are described: one using the submultiple method and one using the modified z -transform technique. These are applied when it is desired to determine the intra-sampling responses of the system.

All three techniques are applied to a single example. A summary of the techniques and their application is provided at the conclusion of the report.

It has been assumed that a given digital or sampled-data system can be described by a closed-loop transfer function that relates a single controlled output of the system to a single reference input. If there is more than one input, the technique can also be applied to the resulting sum of closed-loop transfer functions relating the controlled output to each of the inputs. Although the report refers only to a single controlled output, the technique can be applied to find any system state if it is related to the inputs to the system in the z -domain. These relationships may be derived by using any of the standard techniques (such as signal flow graphs) or by the newly developed Systematic Analytical Method (SAM) technique.

Several analytical techniques for obtaining the response of a digital control system have been described. They are based on a single principle: cross-multiplication followed by applications of the real translation theorems. Each is applied to a single example. As a starting point for application of each of the techniques, it is required that the dynamics of the digital control system be described in the z - or modified z -domain.

The advantages of the three techniques over extant classical methods are:

- a. The response may be obtained for any deterministic reference input into the system as long as its value is known at the sampling instants. It need not be described by a differential equation, and the z -transform for a specific reference input need not be determined before obtaining an expression for the response.

b. Initial conditions and instantaneous changes can be accommodated readily by the equations obtained through use of the cross-multiplication methods.

c. The difference equations obtained are particularly amenable to programming on a desktop calculator or digital computer.

d. A detailed knowledge of the theory underlying digital or sampled-data control systems is not required (although it certainly is helpful) by the analyst in order to apply the recipes described herein.

3. Sampled-Data Analysis in Parameter Space

In essence, the parameter space technique provides the digital guidance and control system designer with a means for determining the stability and dynamic characteristics of a digital control system in terms of several selected system parameters. The method requires that the system characteristic equation be available in the complex z -domain. It is this capability that makes the method more powerful than most design techniques (which describe stability in terms of only one variable parameter or gain).

The parameter space method provides an analytical tool developed for use in control system analysis and synthesis. Although not necessary, its application is facilitated by augmenting the analytical results with graphical portrayals in a selected multi-parameter space. The method requires that the control system be described by a characteristic equation which, for sampled-data or digital systems, may be expressed in the z -domain. The technique is based on the analysis and synthesis methods for linear and nonlinear control system design which are amply described in Siljak's excellent monograph on the subject.⁶ Reference 7 describes the application of the technique to the analysis and synthesis of linear sampled-data control systems.

Once the system characteristic equation has been obtained, the parameter plane method enables the designer to evaluate graphically the locations of roots of the equation. Hence, he may design the control system in terms of the chosen performance criteria; e.g., absolute stability, damping ratio, and settling time. He is able to see the effect on the characteristic equation roots of changing two adjustable

parameters. Siljak further simplified the design procedure by introducing Chebyshev functions into the equations, thereby putting them in a form particularly amenable to their solution by a digital computer. The method has been extended to portray the effect of varying the sampling period. The extended method permits one to see the effect of the choice of values assigned to the sampling period on absolute and relative stability. Also, the recursive formulas shown therein are simpler in form than the Chebyshev functions of Reference 7. The resulting formulation is deliberately cast in a form that makes it particularly amenable to solution by a digital computer or a desk calculator, again emphasizing the interplay between analysis and computing machines. When portrayed graphically, the results show the dynamic relation between the selected parameters and the characteristic equation roots, as a function of the nondimensional independent argument, $\omega_n T$. Hence one readily can deduce the dynamic effect upon the system of various combinations of values of the selected parameters defining the parameter space.

The history of the continuous-time domain version of the parameter plane technique is well-described with suitable references in Reference 6. Briefly summarizing that history, in 1876 I. A. Vishnegradsky of the Leningrad School of Theoretical and Applied Mechanics developed and used the first version of the parameter plane techniques to portray system stability and transient characteristics of a third order system on a two-parameter plane. In 1949 Professor Yu I. Neimark of the Russian School of Automatic Control generalized Vishnegradsky's approach to permit the decomposition of a two-parameter domain (D) describing an nth order system into stable and unstable regions. The technique was called D-decomposition. During the period 1959 through 1966, Professor D. Mitrovic, founder of a Belgrade group of automatic control, extended the method to enable the analyst to relate the system's variable parameters to the system response, using the last two coefficients of an nth order characteristic equation. Beginning in 1964, Professor D. D. Siljak, then a student of Mitrovic's at the University of Belgrade, generalized the method and called it the Parameter Plane method. His method permitted the analyst to select an arbitrary pair of characteristic equation coefficients (or parameters appearing within the coefficients) and portray both graphically and analytically the dependence of the system response upon the selected parameters. The method was extended subsequently by Siljak and others to encompass a host of related problems. In 1967 Professor J. George modified the D-decomposition method to enable the portrayal of the absolute stability region in a multi-parameter space (George also showed how to portray contours of relative stability, as did Siljak). All of the foregoing work is carefully and completely referenced within Reference 6. In 1966 and subsequently,

Seltzer has applied the parameter space method to the design of missile, aircraft, and satellite controllers including systems containing one or two nonlinearities; the analysis of the dynamic effects of the nonlinear "Solid Friction" (Dahl) model for systems with ball bearings, such as control moment gyroscopes and reaction wheels; and the specification by the system designer of the dynamic structural flexibility constraints to the structural designer. Most of this work has appeared in the technical journals of the IEEE, the AIAA, the International Journal of Control, and the journal, Computers and Electrical Engineering. A portion of the history that has not been reported upon previously (with one exception to be noted) is the control system work conducted by the German rocket scientists in the early 1940's at Peenemunde. There, Dr. W. Hausermann and others applied the D-decomposition technique to the design of the V-2 Rocket, following Dr. Hausermann's earlier (pre-World War II) application to the control of an underwater torpedo. This work was not published in the open literature because of national security constraints. When the group came to the United States to work with the Army Ballistic Missile Agency (first at Fort Bliss, Texas, then at Redstone Arsenal, Huntsville, Alabama), Dr. Hausermann and his associates continued to apply the method to U. S. Army Missiles (and later to NASA space vehicles). Again, national security (this time, another nation) precluded publication in the open literature until 1957.¹⁰

In 1964 Professor Siljak published the first application of the parameter plane technique to sampled-data systems.⁷ As mentioned above, this was extended in References 8 through 9. In 1971 Seltzer presented an algorithm for systematically solving the Popov Criterion applied to sampled-data systems. Applications of these sampled-data parameter space techniques are found in References 8, 9, and 11.

In summary, an analytical method for portraying stability regions in a selected parameter space is described for a digital system. The method requires that the system characteristic equation be available and expressed in the complex z-domain. It also is possible to apply pole placement to obtain desired dynamic characteristics using this modified parameter space technique. The advantage of the technique over existing classical sampled-data methods is that the stability and dynamic response characteristics are expressed in terms of several (rather than merely one) selected parameters. Also, the sampling period, T, need not be expressed numerically before the design technique begins, giving the system designer one more degree of freedom.

C. Survey and Implementation of Discrete Control for Missile Systems via the Parameter Space.

1. Introduction

In this section, the results of mathematical models of Sections IV and V of the Technical Report: Phase I are used to demonstrate the application of the newly-developed digital and sampled-data techniques. A simplified planar model of a missile system is used to demonstrate the application of the three design and analysis techniques described in Part B, above. It is described by the block diagram of Figure 1, where $G(s)$ is used to portray the transfer function describing the characteristics of the plant. For lucidity, aerodynamics are neglected and the coefficients of the equations describing the dynamics of the system are assumed to be time-invariant. The symbol $G_{ho}(s)$ is used to represent the transfer function associated with a zero order hold in a digital computer. Trapezoidal integration is used to approximate the mathematics associated with taking an integral of a state and is represented by the transfer function (in the complex z -domain), $D(z)$. These three transfer functions may be written as

$$G(s) = \frac{-c_2}{s} , \quad (IV-1)$$

$$G_{ho}(s) = \frac{1 - e^{-sT}}{s} , \quad (IV-2)$$

and

$$D(z) = \frac{T(z+1)}{2(z-1)} . \quad (IV-3)$$

The onboard digital computer sampling period is represented by the symbol T , and symbols s and z represent the complex Laplace (s) and z variables, where

$$z = e^{sT} . \quad (IV-4)$$

On Figure 1, control gains are represented by symbols a_1 , a_0 , and a_{-1} . The attitude of the missile is represented by θ , and the overdot represents the time derivative of the symbol beneath it.

The approach taken in this section is to:

- a. First determine the system closed-loop transfer function.
- b. Then determine conditions to ensure system stability.
- c. Finally, determine representative system responses to given inputs to the system.

In each of the three portions to the approach, the methods developed under this contract will be applied. It is at this point that one sees the logical need for the development of three tools. "SAM" was developed to provide a better means for obtaining the closed-loop transfer function. The parameter space technique was developed to provide an efficient means for determining conditions that ensure stability (and that also can ensure a desired system response). The cross-multiplication technique was developed to provide a relatively simple means for determining the system response. It is stated that these three techniques appear to be superior to known extant methods. An indication of this superiority will be provided summarily within this section at the conclusion of each of the above three steps.

2. System Closed-Loop Transfer Function.

The system closed-loop transfer function will now be derived by applying the "SAM" technique described in Appendix A. The System Equations (see Step No. 1 of the SAM procedure) may be written directly upon inspection of Figure 1.

$$E = X_1 = X + X_8 \quad (IV-5)$$

$$E^* = X_2 = X_1^* \quad (IV-6)$$

$$\bar{E} = X_3 = G_{ho} X_2 \quad (IV-7)$$

$$a_{-1} \int E^* dt = X_4 = a_{-1} D^* X_2 \quad (IV-8)$$

$$a_{-1} \int \bar{E} dt = X_5 = G_{ho} X_4 \quad (IV-9)$$

$$B_c = X_6 = a_0 X_3 + X_5 + a_1 X_{10} \quad (IV-10)$$

$$\dot{\theta} = X_7 = G X_6 \quad (IV-11)$$

$$\theta = X_8 = X_7/s \quad (\text{IV-12})$$

$$\dot{\theta}^* = X_9 = X_7^* \quad (\text{IV-13})$$

$$\overline{\dot{\theta}} + X_{10} = G_{ho} X_9 \quad (\text{IV-14})$$

The overbar over a state indicates that the state's value at the beginning of any sampling period is held (at that value) until the beginning of the sampling period. The asterisk following a state indicates the instantaneous value of the state at the instant of the assumed sampling impulse, i.e., it indicates the pulsed transform of the variable. All states are considered to be written in the Laplace domain, i.e., the usual notation $X_j(s)$ has been shortened to X_j for convenience.

The Modified System Equations (see Step No. 2 of the SAM procedure) corresponding to the above System Equations may be written directly from the System Equations.

$$E = X_1 = X + X_8 \quad (\text{IV-5M})$$

$$E^* = X_2 = X_1^* \quad (\text{IV-6M})$$

$$X_3 = G_{ho} X_1^* \quad (\text{IV-7M})$$

$$X_4 = a_{-1} D^* X_2 \quad (\text{IV-8M})$$

$$X_5 = a_{-1} G_{ho} D^* X_1^* \quad (\text{IV-9M})$$

$$X_6 = a_0 X_3 + X_5 + a_1 X_{10} \quad (\text{IV-10M})$$

$$\dot{\theta} = X_7 = (GG_{ho})(a_0 X_1^* + a_{-1} D^* X_1^* + a_1 X_7^*) \quad (\text{IV-11M})$$

$$\theta = X_8 = a_0 (GG_{ho}/s) X_1^* + a_{-1} (GG_{ho}/s) D^* X_1^* + a_1 (GG_{ho}/s) X_7^* \quad (\text{IV-12M})$$

$$\dot{\theta}^* = X_9 = X_7^* \quad (\text{IV-13M})$$

$$\overline{\dot{\theta}} = X_{10} = G_{ho} X_7^* \quad (\text{IV-14M})$$

The Pulsed System Equations (see Step No. 3 of the SAM procedure) corresponding to the above equations may be written directly from the System Equations.

$$E^* = X_1^* = X^* + X_9^* \quad (\text{IV-5P})$$

$$X_2^* = X_1^* \quad (\text{IV-6P})$$

$$X_3^* = G_{ho}^* X_1^* \quad (\text{IV-7P})$$

$$X_4^* = a_{-1} D^* X_2^* \quad (\text{IV-8P})$$

$$X_5^* = a_{-1} D^* G_{ho}^* X_1^* \quad (\text{IV-9P})$$

$$X_6^* = a_0 X_3^* + X_5^* + a_1 X_{10}^* \quad (\text{IV-10P})$$

$$X_7^* = G G_{ho}^* (a_0 X_1^* + a_{-1} D^* X_1^* + a_1 X_7^*) \quad (\text{IV-11P})$$

$$E^* = X_8^* = G G_{ho}^* / s (a_0 X_1^* + a_{-1} D^* X_1^* + a_1 X_7^*) \quad (\text{IV-12P})$$

$$X_9^* = X_7^* \quad (\text{IV-13P})$$

$$X_{10}^* = G_{ho}^* X_7^* \quad (\text{IV-14P})$$

For convenience, one may define $G_1(s)$ as

$$G_1 \stackrel{d.}{=} G G_{ho}^* / s = -\frac{c_2}{s} \cdot \frac{1}{s} \cdot \frac{1 - e^{-sT}}{s}, \quad (\text{IV-15})$$

which leads to

$$\begin{aligned} G_1(z) &= \mathcal{Z} \left\{ G_1(s) \right\} = (1-z^{-1}) \left\{ \frac{-c_2}{s^2} \right\} \\ &= -\frac{c_2 T^2 (z+1)}{(z-1)^2} \end{aligned} \quad (\text{IV-15Z})$$

One may define $G_2(z)$ as

$$\begin{aligned} G_2(z) &\stackrel{d.}{=} G G_{ho}(z) = (1-z^{-1}) \left\{ \frac{-c_2}{s^2} \right\} \\ &= -c_2 T / (z-1) \end{aligned} \quad (\text{IV-16})$$

The trapezoidal approximation for the integration operation (see Section V of the Technical Report: Phase I) may be written in the z-domain as:

$$D(z) = \frac{1}{2}T(z+1)/(z-1) \quad (IV-17)$$

Making use of these definitions, one may substitute them into the Pulsed System Equations to obtain

$$X_1^* = \frac{G_2^*(a_0 + a_{-1}D^*)X_1^*}{1 - a_1 G_2^*} \quad (IV-18)$$

and, after some algebraic manipulation, one obtains the closed-loop transfer function,

$$\frac{\theta(z)}{X(z)} = \frac{-\left[\frac{1}{2}c_2T^2 \frac{(z+1)}{(z-1)^2}\right] \left[a_0 + \frac{1}{2}a_{-1}T \frac{(z+1)}{(z-1)}\right]}{\frac{a_1c_2T}{(z-1)} + \frac{1}{2}c_2T^2 \frac{(z+1)}{(z-1)^2} \left[a_0 + \frac{1}{2}a_{-1}T \frac{(z+1)}{(z-1)}\right]} \quad (IV-19)$$

If one defines the dimensionless gains, k_p , k_i , k_d , as

$$k_p = \frac{d.}{2} a_0 c_2 T^2, \quad (IV-20)$$

$$k_i = \frac{d.}{4} a_{-1} c_2 T^3, \quad (IV-21)$$

and

$$k_d = \frac{d.}{2} a_1 c_2 T, \quad (IV-22)$$

one may rewrite Equation (IV-19) as

$$\frac{\theta(z)}{X(z)} = \frac{(k_p + k_i)z^2 + 2k_i z - (k_p - k_i)}{C.E.(z)} = \frac{\sum_{j=0}^2 d_j z^j}{C.E.(z)} \quad (IV-23)$$

where the denominator C.E.(z) of the closed-loop transfer function is the characteristic equation for the system, i.e.,

$$\begin{aligned} C.E.(z) &= z^3 + (k_p + k_i + k_d - 3)z^2 + (2k_i - 2k_d + 3)z + (-k_p + k_i + k_d - 1) \\ &= \sum_{j=0}^3 d_j z^j \quad (IV-24) \end{aligned}$$

The characteristic equation will be used in the sequel to determine conditions to ensure system stability. The closed-loop transfer function will be used to determine the response of the system.

The question is now asked: "How well does SAM compare to other methods for determining the closed-loop transfer function?" Several means will be examined briefly for comparative purposes. They are (1) the well-known and oft-used Signal Flow Graph (SFG) method; and (2) block diagram manipulation.

Even if the modifications put forth in Section III of Appendix A are implemented, the SFG method is tedious and amenable to mistakes (such as not recognizing the existence of loops on the graph). Using the System Equations (IV-5) through (IV-14) and the Pulsed System Equations (IV-5P) through (IV-14P), one may construct the modified SFG found in Figure 2. Mason's Gain Rule (also found in Appendix A) is then applied as follows.

There are three loops on the SFG.

Loop No. 1: A closed-loop beginning and ending at X_7^* with a gain of $K_1 = a_1 G_2^*$.

Loop No. 2: A loop passing through X_1^* , X_7^* , X_8^* , and back to X_1^* with a gain of $K_2 = a_1 G_1^* G_2^* (a_0 + a_{-1} D^*)$.

Loop No. 3: A loop passing through X_1^* , X_8^* , and back to X_1^* with a gain of $K_3 = G_1^* (a_0 + a_{-1} D^*)$.

It is observed that Loops No. 1 and No. 3 do not touch each other. The value of Δ (actually, the characteristic equation) is found to be

$$\begin{aligned} \Delta &= 1 - K_1 - K_2 - K_3 + K_1 K_3 \\ &= 1 - a_1 G_2^* - (a_0 + a_{-1} D^*) G_1^* (a_1 G_2^* + 1) \\ &\quad + a_1 G_1^* G_2^* (a_0 + a_{-1} D^*) \\ &= 1 - a_1 G_2^* - (a_0 + a_{-1} D^*) G_1^* \end{aligned} \tag{IV-25}$$

This may be shown to be identical to Equation (IV-24) which is the system characteristic equation found by applying SAM.

Returning to the SFG, one sees that there are two forward paths from X^* to Θ^* . Along the first forward path (the upper of the two),

$$M_1 = a_1 G_1 * G_2 * (a_0 + a_{-1} D^*) \quad (\text{IV-26})$$

and

$$\Delta_1 = 1 \quad (\text{IV-27})$$

Along the second forward path (the lower one),

$$M_2 = G_1 * (a_0 + a_{-1} D^*) \quad (\text{IV-28})$$

and

$$\Delta_2 = 1 - K_1 \quad (\text{IV-29})$$

The expression for the closed-loop gain between X^* and Θ^* is

$$\begin{aligned} \frac{\Theta^*}{X^*} &= \frac{M_1 \Delta_1 + M_2 \Delta_2}{\Delta} \\ &= \frac{a_1 G_1 * G_2 * (a_0 + a_{-1} D^*) + G_1 * (a_0 + a_{-1} D^*) (1 - a_1 G_2^*)}{\Delta} \\ &= \frac{G_1 * (a_0 + a_{-1} D^*)}{1 - a_1 G_2^* - (a_0 + a_{-1} D^*) G_1^*} \quad (\text{IV-30}) \end{aligned}$$

It is seen that Equation (IV-30) may be manipulated so that it is identical to Equation (IV-19) obtained by using SAM.

The same result may be obtained by block diagram and/or algebraic manipulation. Since this technique is well known, it will not be described here. Suffice it to say, it can become tedious.

The advantages that SAM appears to possess are that it can be applied to a system having any level of complexity or order. It is not subject to not recognizing a path or closed-loop (not always obvious) on a SFG. Because it is systematic, it is less amenable to errors by the user.

3. System Stability

The conditions for stability of the system are now determined by using the parameter space technique described in Appendix C. It will be applied to the characteristic equation (IV-24). Since it is a third order polynomial, it has three roots - either all three are real or one is real and two are complex conjugates.

The $z=1$ boundary is found by substituting the value of unity for z in Equation (IV-24), yielding

$$k_i = 0 \quad . \quad (IV-31)$$

The $z=-1$ boundary is found by letting $z=-1$ in Equation (IV-24), yielding

$$k_d = 2 \quad . \quad (IV-32)$$

The complex conjugate root boundary (associated with the unit circle in the z -domain) is found by substituting the value,

$$z^j = R_j + i I_j (1 - B^2)^{\frac{1}{2}} \quad (IV-33)$$

for each value of z^j (where j is an integer) appearing in Equation (IV-24), where values of R_j and I_j corresponding to the unit circle boundary may be found from Table 1 (see Appendix C for how these values may be obtained) and B is defined as $\cos \omega T$. (Recall s may be defined as $s = \sigma + i\omega$).

TABLE 1.
Values of R_j , I_j , and γ_j

j	R_j	I_j	γ_j
0	1	0	$-k_p + k_i + k_d - 1$
1	B	1	$2k_i - 2k_d + 3$
2	$2B^2 - 1$	$2B$	$k_p + k_i + k_d - 3$
3	$4B^3 - 3B$	$4B^2 - 1$	1

The result is an equation containing both real and imaginary quantities. If the reals and the imaginaries are separated into two equations, one obtains the following two simultaneous algebraic equations:

$$R = \delta_3 R_3 + \delta_2 R_2 + \delta_1 R_1 + \delta_0 R_0 = 0 \quad (\text{IV-34R})$$

and

$$I = \gamma_3 I_3 + \gamma_2 I_2 + \gamma_1 I_1 + \gamma_0 I_0 = 0 \quad (\text{IV-34I})$$

Substituting the values from Table 1 into Equations (IV-34), one may obtain

$$R = (B+1)(B-1)k_p + B(B+1)k_i + B(B-1)k_d + (B-1)^2(2B+1) = 0 \quad (\text{IV-35R})$$

and

$$I = Bk_p + (B+1)k_i + (B-1)k_d + (B-1)(2B-1) = 0 \quad (\text{IV-35I})$$

Since there are two equations, they may be solved for any two parameters contained within. The two control gains, k_p and k_d , may be the selected two. If one uses Cramer's Rule to solve for k_p and k_d , one may obtain the Jacobian,

$$J = \begin{vmatrix} (B+1)(B-1) & B(B-1) \\ B & (B-1) \end{vmatrix} = 1 - B > 0 \forall B < 1 \quad (\text{IV-36})$$

The parameters (control gains) may be solved for, obtaining

$$k_p = \frac{\begin{vmatrix} -B(B+1)k_i - (B-1)^2(2B+1) & B(B-1) \\ -(B+1)k_i - (B-1)(2B-1) & (B-1) \end{vmatrix}}{J} = 1 - B \quad (\text{IV-37})$$

and

$$k_d = \frac{\begin{vmatrix} (B+1)(B-1) & -B(B+1)k_i - (B-1)^2(2B+1) \\ B & -(B+1)k_i - (B-1)(2B-1) \end{vmatrix}}{J} = \frac{(1+B)}{(1-B)} k_i + (1-B) \quad (\text{IV-38})$$

A summary of the three stability boundaries in the k_p, k_i, k_d parameter space is:

$$z=+1: k_i = 0 ,$$

$$z=-1: k_d = 2 ,$$

$$z=e^{-i\omega T}: k_p = 1-B ,$$

$$k_d = \frac{(1+B)}{(1-B)} k_i + (1-B) .$$

Although these may readily be shown in three-space with proper graphics, they are shown in this report in a k_p, k_d two-space (or plane) on Figure 3 for several values of k_i (i.e., $k_i = 0, 0.1, \text{ and } 0.5$). The shading rules described in Appendix C are applied to determine the stable and unstable regions. The number of stable roots in a particular region are denoted by an encircled number. The program for obtaining numerical values for generating these curves, using a Hewlett-Packard 9100B calculator, is found in Appendix D.

If the root locus technique were used to plot the dynamic characteristics of the system, this could be accomplished only after two of the three parameters were assigned numerical values, thus losing a considerable amount of potential information. Also, the numerator and denominator of the root locus equation would have to be factored into first and second order terms to determine locations of poles and zeros. For example, if k_d were selected as the variable parameter (gain), the root locus equation (obtained from the characteristic equation) would be:

$$G(z) = \frac{(z^2 - 2z + 1) k_d}{z^3 + (k_p + k_i - 3)z^2 + (2k_i + 3)z + (k_p + k_i - 1)} . \quad (\text{IV-39})$$

The corresponding root locus equation for the selection of k_p is equally cumbersome:

$$G(z) = \frac{(z^2 - 2z + 1) k_p}{z^3 + (k_i + k_d - 3)z^2 + (2k_i - 2k_d + 3)z + (k_i + k_d - 1)} . \quad (\text{IV-40})$$

If one were to use a Bode plot, one would also have to factor the appropriate equations into first and/or second order parts, again having (in most cases) to resort to numerical values. Such is the nature of most classical techniques, whereas the parameter space technique permits the retention (and hence generality) of several generic (rather than numerical) values of gains. In this study, the dynamic characteristics of the system have not been specified, although Appendix C tells how this can be done (essentially using pole placement technique). In that case, the parameter space technique provides additional strength, since a numerical value of the sampling period (T) need not be specified before design commences.

If one wishes to resort to array techniques (i.e., the sampled-data analogue of the Routh-Hurwitz Criterion), one may use the Schur-Cohn Method, the more versatile Jury's Test, or the considerably more versatile Raible's Test.¹² Even in the case of the latter, the use of the table (when implemented with a digital calculator or by hand analysis) is cumbersome, as shown in Table 2.

TABLE 2.
Raible's Test

a_3 a_0k_a	a_2 a_1k_a	a_1 a_2k_a	a_0 -	$k_a = a_0/a_3$
b_0 b_2k_b	b_1 b_1k_b	b_2 -	-	$k_b = b_2/b_0$
c_0 c_1k_c	c_1 -	-		$k_c = c_1/c_0$
d_0	-			

The values of the coefficients in Table 2 are found in Table 3.

TABLE 3.
Raible's Test Coefficients

j	a_j	b_j	c_j	d_j
0	$-k_p + k_i + k_d - 1$	$a_3 - a_0 k_a$	$b_0 - b_2 k_b$	$c_0 - c_1 k_c$
1	$2k_i - 2k_d + 3$	$a_2 - a_1 k_a$	$b_1 - b_1 k_b$	-
2	$k_p + k_i + k_d - 3$	$a_1 - a_2 k_a$	-	-
3	1	-	-	-

To use the Raible's Array of Table 2 for determining the conditions that ensure stability, one determines the values of parameters that cause b_0 , c_0 , and d_0 to always be greater than unity. While on the surface this appears to be simple, the actual implementation requires great algebraic effort (unless numerical values - with their attendant decrease in generality - are used).

4. System response

The system response to an input is now determined, using the cross-multiplication method described in Appendix B. It will be applied to the closed-loop transfer function of Equations (IV-23) through (IV-24). Cross-multiplication of the terms in Equation (IV-23) leads directly to the equation,

$$z^3\theta(z) + \gamma_2 z^2\theta(z) + \gamma_1 z\theta(z) + \gamma_0\theta(z) = -\delta_2 z^2 X(z) - \delta_1 z X(z) - \delta_0 X(z) \quad (IV-41)$$

If one solves Equation (IV-41) for the value of $\theta(z)$ that is the coefficient of the highest power of z (in this case, three), one obtains

$$\theta(z) = - \left[\delta_2 z^{-1} X(z) + \delta_1 z^{-2} X(z) + \delta_0 z^{-3} X(z) \right] - \left[\gamma_2 z^{-1} \theta(z) + \gamma_1 z^{-2} \theta(z) + \gamma_0 z^{-3} \theta(z) \right] \quad (IV-42)$$

Equation (IV-42) may be put in the form of a difference equation, where the symbol θ_k denotes the value of $\theta(t)$ at the instant, $t=kT$, k an integer, and x_k denotes the value of $X(t)$ at time $t=kT$:

$$\theta_k = - [\delta_2 x_{k-1} + \delta_1 x_{k-2} + \delta_0 x_{k-3}] - [\gamma_2 \theta_{k-1} + \gamma_1 \theta_{k-2} + \gamma_0 \theta_{k-3}] \quad (IV-43)$$

The power of the difference equation is respectable in the era of digital machinery. For example, in the case of Equation (IV-43), any value of $\theta(kT)$ may be found if only the next earlier values of θ are known. This may be done for any reference input signal, $X(t)$, whose value is known at the sampling instants $t=kT$. In other words, contrary to many existing methods for determining system response, $X(t)$ need not be specified in mathematically closed-form. Let us dwell on this power briefly. Suppose the initial condition for the missile system under study herein is denoted as θ_0 , i.e., the value of the missile attitude at the instant of time $t=0$. Using Equation (IV-43) and assuming that $t=0$ was selected (as it surely can be) at an instant before which the state θ is at rest, or zero, one obtains the value of θ at the next sampling instant, $t=T$:

$$\theta_1 = \delta_2 x_0 - \gamma_2 \theta_0 \quad (IV-44)$$

Knowing θ_1 , one may again use Equation (IV-42), this time to find the value of θ at time $t=2T$, i.e.,

$$\theta_2 = \delta_2 x_1 + \delta_1 x_0 - (\gamma_2 \theta_1 + \gamma_1 \theta_0) \quad (IV-45)$$

Similarly, values of θ may be determined at later sampling instants of time in this recursive manner. This form obviously is amenable to implementation in a digital computer or calculator.

As a simple example of the application of the technique, assume the system is commanded to follow a unit step input applied at time $t=0$, i.e.,

$$X(t) = 1 \quad \forall t \geq 0 \\ = 0 \quad \forall t < 0 \quad (IV-46)$$

The response to the step input may be determined readily from Equation (IV-43) as:

$$(k=0) \quad \theta_0 = 0 \quad (\text{IV-47})$$

$$(k=1) \quad \theta_1 = \delta_2 X_0 = k_p + k_i \quad (\text{IV-48})$$

$$(k=2) \quad \theta_2 = \delta_2 + \delta_1 - \gamma_2 \theta_1 = k_p + 3k_i - \gamma_2 \theta_1 \quad (\text{IV-49})$$

$$(k=3) \quad \theta_3 = (\delta_2 + \delta_1 + \delta_0) - (\gamma_2 \theta_2 + \gamma_1 \theta_1) = 4k_i - (\gamma_2 \theta_2 + \gamma_1 \theta_1) \quad (\text{IV-50})$$

$$(k \geq 3) \quad \theta_k = 4k_i - (\gamma_2 \theta_{k-1} + \gamma_1 \theta_{k-2} + \gamma_0 \theta_{k-3}) \quad (\text{IV-51})$$

Equations (IV-47) through (IV-51) may be programmed on any digital machine. A program for calculating values of $\theta(kT)$ is found in Appendix E.

As an independent check on the response values obtained, the initial value and steady-state value of $\theta(kT)$ may be determined by applying the sampled-data Initial Value and Final Value Theorems to the closed-loop transfer function of Equation (IV-23).

Initial Value Theorem:

$$\lim_{t \rightarrow 0} \theta^*(t) = \lim_{z \rightarrow \infty} \theta(z) = \lim_{z \rightarrow \infty} \frac{(\delta_2 z^2 + \delta_1 z + \delta_0) X(z)}{z^3 + \gamma_2 z^2 + \gamma_1 z + \gamma_0} \quad (\text{IV-52})$$

The answer is dependent on the form of $X(z)$. For a unit step function, Equation (IV-46) may first be transformed into the z-domain, yielding

$$X(z) = \frac{z}{(z-1)} \quad (\text{IV-53})$$

Because of the nature of the feedback signal in the missile case (see Figure 1), the value of $X(z)$ should be assigned a negative sign. If the negative of Equation (IV-53) is inserted in Equation (IV-52), the initial value of $\theta^*(t)$ is seen to be zero.

$$\begin{aligned} \lim_{t \rightarrow \infty} \theta^*(t) &= \lim_{z \rightarrow 1} (1-z^{-1}) \theta(z) \\ &= \lim_{z \rightarrow 1} - \left(\frac{z-1}{z} \right) \left[\frac{(k_p + k_i)z^2 + 2k_i z - (k_p - k_i)}{z^3 + \gamma_2 z^2 + \gamma_1 z + \gamma_0} \right] X(z) \quad (\text{IV-54}) \end{aligned}$$

Again, if the theorem is applied to the case of a unit step input to the system and the negative of Equation (IV-53) is substituted into Equation (IV-54), the resulting steady-state value of $\theta^*(t)$ becomes

$$\lim_{t \rightarrow \infty} \theta^*(t) = \frac{k_p + k_1 + 2k_1 - k_p + k_1}{1 + \gamma_2 + \gamma_1 + \gamma_0} = 1 \quad . \quad (\text{IV-55})$$

The program found in Appendix E has been applied to the design example, assuming a unit step input. The result has been plotted as Figure 4.

The brief discussion found in Appendix B of other techniques that may be used to determine the system response is sufficient to convince the reader of the advantages of the cross-multiplication technique. Hence, they will not be applied to the design example.

SECTION VI. TECHNICAL SEMINAR

A technical seminar was conducted by Dr. Seltzer for selected members of the Guidance and Control Analysis Group, Guidance and Control Directorate (DRDMI-TGN). The purpose of the seminar was to develop a design expertise among members of the Group to enable them to design and evaluate discrete (i.e., digital) guidance and control systems. Both existing and newly-developed sampled-data techniques were described in detail with practical applications conducted during the course of the seminar conferences. In particular, the new techniques described in Appendices A, B, and C of this report were fully developed for the participants. The duration of the seminar was 123 contact hours.

The contents of the seminar are described in the following outline format.

- A. Introduction.
- B. The sampling process.
 1. Mathematical description of the sampling process in both the time and the frequency domains.
 2. The Sampling ("Shannon's") Theorem.
- C. The ideal sampler: the impulse sampling approximation.
 1. Motivation.
 2. Mathematical description.
 - a. Time domain.
 - b. Frequency domain.
 - (1) Fourier analysis.
 - (2) Laplace analysis.
 - (3) Complex convolution.
 - (a) Closed form.
 - (b) Series form.
- D. Comparison with carrier-modulated systems.

- E. Z-transform analysis of linear sampled-data systems.
 - 1. Introduction to, and derivation of, the z-transform.
 - 2. Evaluation of z-transforms.
 - 3. Mapping from the complex s-plane to the complex z-plane.
 - 4. Theorems of the z-transform.
 - 5. The concept of pulse transfer functions.
 - 6. Z-domain transfer function relationships between cascaded elements.
 - 7. Limitations of the z-transform method.
 - 8. Determination of the control system response between sampled instants.
 - a. Use of the submultiple method.
 - b. Use of the Modified and the Delayed z-transforms.
 - 9. Modified z-transform theorems.
- F. Data reconstruction, emphasizing zero-order and first-order holds.
- G. Sampled-data systems: Determination of outputs and other states of digital control systems.
 - 1. Block diagram manipulation and algebraic manipulation.
 - 2. Signal Flow Graphs and Mason's Gain Formula.
 - a. Conventional (B.C. Kuo) technique.
 - b. Seltzer's technique.
 - 3. A newly-developed systematic algebraic manipulation technique termed "SAM" (Systematic Algebraic Manipulation).

H. System Response.

1. Comparison of second-order response for:
 - a. Continuous system.
 - b. Sampled-data system without data holds.
 - c. Sampled-data system with zero-order hold.
2. Stability and other dynamic determinations,
 - a. Jury's Test,
 - b. Raible's Test,
 - c. Mapping from the complex s-plane to the complex w- and r-planes.
 - d. Extension of the Routh-Hurwitz Test to the w- and r-domains.
 - e. Effect of pole-zero locations on system dynamic response (in the z-domain).
 - f. The root locus method (in the z-domain) for sampled-data systems.
 - g. The Nyquist Criterion.
 - h. The Bode diagram.
 - i. The gain-phase plot (Nichols' Chart).
 - j. The parameter space.
3. Response between sampling instants,
 - a. Submultiple sampling method.
 - b. Modified z-transform method.
 - c. The newly-developed cross-multiplication method.
 - d. Hidden instabilities,

I. Conclusion.

1. Design example.
2. Comparison of classical techniques.

SECTION VII. AMERICAN INSTITUTE OF AERONAUTICS AND ASTRONAUTICS
(AIAA) ACTIVITIES

During the contract period, Dr. Seltzer has supported certain pertinent AIAA activities. This has taken the following form.

A. AIAA Aerospace Sciences Meeting

Dr. Seltzer was selected to organize the Guidance and Control (G&C) sessions at the AIAA Aerospace Sciences Meeting held in New Orleans, Louisiana, 15-17 January 1979. Also, at that meeting, Dr. Seltzer presented a paper co-authored by Dr. Harold L. Pastrick (Guidance and Control Directorate, U. S. Army Missile Research and Development Command) & Professor Michael Warren (University of Florida in Gainesville). The paper was entitled "Guidance Laws for Tactical Missiles".¹³ It includes a comparison of guidance laws applicable to short range tactical missiles. These laws are segmented into several classes and the principles underlying each class are discussed. Specific attention is given to the structure of the guidance technique and the requirements for its implementation. Evaluation and comparison of the performance of each guidance law versus the cost of implementing it are considered. An extensive bibliography of relevant literature is included. A copy of the paper is included as Appendix F.

B. AIAA Guidance and Control Conference

A paper co-authored by Dr. Pastrick and Dr. Seltzer has been accepted for delivery at the AIAA Guidance and Control Conference to be held 6-8 August 1979. The paper is entitled "Future U. S. Army Missile Guidance and Control Systems". It described the task that was recently begun by MIRADCOM to develop an advanced G&C system for Future Army Modular Missiles (see Section II of this report). The paper defines the problem and described the approach being taken as part of a seven-year program to develop a viable future G&C system. The preliminary results that have been achieved, as well as projected results, are to be presented.

SECTION VIII. SIG-D EVALUATION

On 19 January 1979, Dr. J. B. Huff, Director of the Guidance and Control Directorate appointed a team to conduct an in-depth review of the digitally-controlled SIG-D program (Appendix G). The team was placed under the leadership of Mr. Russell T. Gambill. Because of his expertise in the digital control field, Dr. Seltzer was designated to evaluate the theory and design portion of the SIG-D program. The formal review took place during 8-9 February 1979. Written reports were submitted by each of the ten team members to Mr. Gambill who combined them into an overall report entitled "SIG-D Red Team Report" dated 21 February 1979. Section II of the report entitled "Theory and Design" was prepared and submitted by Dr. Seltzer. A copy is included in Appendix G.

SECTION IX. HELLFIRE WHITE PAPER

A "white paper" was prepared by Dr. Seltzer describing how the Guidance and Control (G&C) Analysis Group's Hardware-in-the-loop (HWIL) simulation facility is used to meet that Group's HELLFIRE mission. In particular, the manner in which the G&C Analysis Group met the objective outlined in the "Low Cost Laser Seeker Evaluation Test Plan" was addressed. The paper was generated to meet the sharp criticism leveled against the HWIL facility by Mr. Art Kendell, Rockwell International - Columbus. A copy of the paper is included in Appendix H.

SECTION X. PRESENTATIONS

Several presentations were made during the course of the contract period to demonstrate progress on tasks associated with the contract.

A. Presentation to Dr. J. B. Huff and Dr. Richard Hartman.

On 10 May 1979, a presentation was made to Dr. J. B. Huff, Director of the Guidance and Control Directorate, and Dr. Richard Hartman, Director of the Research Directorate, and members of their organizations. The purpose of the briefing, held at Dr. Huff's request, was to assess the program status of the research on the Future U. S. Army Modular Missile "Advanced Guidance and Control" and to describe the program plans. To meet this request, Dr. Seltzer organized the presentation to cover the following topics.

- a. Program objectives
- b. Program plan
- c. Initial achievements and status
- d. Projected accomplishments
- e. Program implementation.

A copy of the vu-graphs used in the presentation is included in Appendix I.

B. Presentation to Advanced Sensors Directorate.

As a result of the above presentation, Dr. Hartman set up a presentation for members of the Advanced Sensors Directorate on 13 June 1979. The purpose of the presentation was to describe the Advanced Guidance and Control program, to describe the threats that the program addresses, and to enlist the assistance of Advanced Sensors personnel in the program. The description of the program was presented by Dr. Seltzer - and the description of the threats and their analysis was made by Mr. Ray Naples. Copies of the vu-graphs used in the presentation are included in Appendix J.

SECTION XI. TRIPS IN SUPPORT OF THE CONTRACT

Several trips were made in support of the contract during the implementation of Task II.

A. Trip to Eglin Air Force Base.

On 12 October 1978, Dr. Seltzer joined Mr. Russell T. Gambill and Dr. Harold L. Pastrick at Eglin Air Force Base. Their major contact and source of technical and program information was 2nd Lt. Tom Riggs, U. S. Air Force, Air-to-Air, Systems Analysis and Simulation Branch, Air Force Armament Laboratory, Air Force Systems Command, Eglin Air Force Base, Florida. Information was exchanged between the principals mentioned in considerable detail. Continued exchanges of information were sought by the Air Force personnel present.

In addition to considerable in-house effort, Eglin Air Force Base has contracts with three universities (Alabama, Florida, and Texas) and three members of industry (OrinCon, SCI, and TASC) to study advanced digital G&C for air-to-air tactical missiles.

The Eglin personnel expressed a desire to develop a memorandum of understanding with the U. S. Army MIRACOM to formalize a joint effort in the development of advanced digital G&C systems. Dr. Seltzer was requested to write a first draft of the agreement. This was presented to Lt. Riggs during a visit to MIRADCOM on 21 March 1979. It presently is under review at Eglin.

B. Trip to the Pentagon.

On 22-23 April 1979, Dr. Seltzer visited the Director of Land Warfare, Mr. Charles Bernard, of the Office of the Under Secretary of Defense for Research and Development, and members of his staff. The purpose of the visit was to determine future target characteristics so that performance requirements might be determined more realistically. While the major portion of the discussions was classified, an abbreviated, unclassified set of performance requirements has been developed for use in this contract (see Section IV).

SECTION XII. SUMMARY

This report contains the documentation performed during the period 20 October 1978 through 7 August 1979, and referred to herein as Phase II. It is intended to meet the documentation requirements specified in Form 1423 and in the Documentation Addendum to Form 1423 found on pages 17 and 18 of the contract (Reference 5) and the requirements that comprise Task II of the Statement of Work of Technical Requirement No. T-0107 (Reference 1). The latter have been repeated (for the reader's convenience) in Section I, Part A.

Task I documentation requirements were met by the Technical Report: Phase I.³ Some of the Statement of Work requirements have been augmented subsequently by this report.

Requirement 2.1 was met by Section III, Part C of Technical Report: Phase I.

Requirement 2.2 was met by Section IV of Technical Report: Phase I and augmented by Section IV of this report.

Requirement 2.3 was met by Section V of Technical Report: Phase I.

Task II documentation requirements and Statement of Work requirements are to be met by this report.

Requirement 2.4 is met by Section V, Parts A and B and by Appendices A, B, and C.

Requirement 2.5 is met by Section V, Part C.

Requirement 2.6 was deleted.²

Requirement 2.7 is met by Appendices A through E.

Requirement 2.8 is met by Section VI.

With regard to meeting the Documentation requirements of Task I:

Paragraph 2.a. A stability analysis, summary, and implementation of the discrete control ... via parameter space, including comparisons with extant methods, is documented in Section V, Part B.

Paragraph 2.b. All simulation initializing operations are described in Appendices D and E.

Paragraph 2.c. All simulation input parameters are described in Appendices D and E.

Paragraph 2.d. Analytical results produced are documented in detail in Appendices A, B, and C.

Paragraph 2.e. Operating instructions are implicit in the formats documented in Appendices D and E.

Paragraph 2.f. Deleted.⁴

Paragraph 2.g. Summaries of computer simulation runs, results, and analyses are documented in Section V, Part C, and in Appendices D and E.

In summary, this report describes the performance results of an effort of forty-one weeks duration (Phase II). The specific Statement of Work requirements were met in detail, i.e., the parameter space technique has been fully developed for stability determination of a digital control system, and the dynamics of a missile system investigated using that technique. Also, an in-depth technical seminar describing the use of digital control techniques was presented. In addition, the Principal Investigator developed and documented an analytical design tool (termed "SAM") to enable the control system engineer to derive the closed-loop transfer function (in particular) and any selected state (in general) of a digitally-controlled system. Also, he developed and documented a means (termed "cross-multiplication") of finding the response of a digitally-controlled system. He co-authored two papers describing the work of which this contract is a part being performed by the U. S. Army MIRADCOM G&C Directorate to develop an Advanced G&C System, both of which were accepted for presentations at AIAA national conferences. He made several presentations to personnel of the G&C, Advanced Sensors, Aeroballistics, and Research Directorates describing this work in order to gain their cooperation. To gain important inputs for this work, Dr. Seltzer made trips to the Pentagon and to Eglin Air Force Base. Also, he performed an evaluation of the theory and design of the digitally-controlled SIG-D as a portion of the formal review of that system. Finally, he wrote a "white paper" describing how the G&C Analysis Group's Hardware-in-the-Loop simulation is used by that Group to meet their HELLFIRE mission. All of the foregoing was accomplished with the expenditure of approximately 1400 direct scientific man-hours (the equivalent of 175 eight-hour days) or an average of approximately 34 hours per week for Phase II). Included within this time was the preparation and conduct of 123 contact hours of an intensive technical seminar.

SECTION XIII. CONCLUSIONS

The requirements set forth in the contract have been met.

Three major analytical tools have been developed to aid the G&C system engineer to design a digital system. They are:

1. A means, termed "SAM", of determining the states of a digital system in terms of that system's transfer functions and the inputs to the system.

2. A means, termed "Cross-Multiplication", for obtaining the response of a digital system from its closed-loop transfer function.

3. A means, termed "Parameter Space", for determining the stability and dynamic characteristics of a digital system in terms of several selected system parameters.

The three design tools have been compared to extant techniques and applied to the design of a typical missile system. They appear at first blush to be superior to other classical methods. In particular, they have been developed with the aim of being easily implemented on digital calculators or computers.

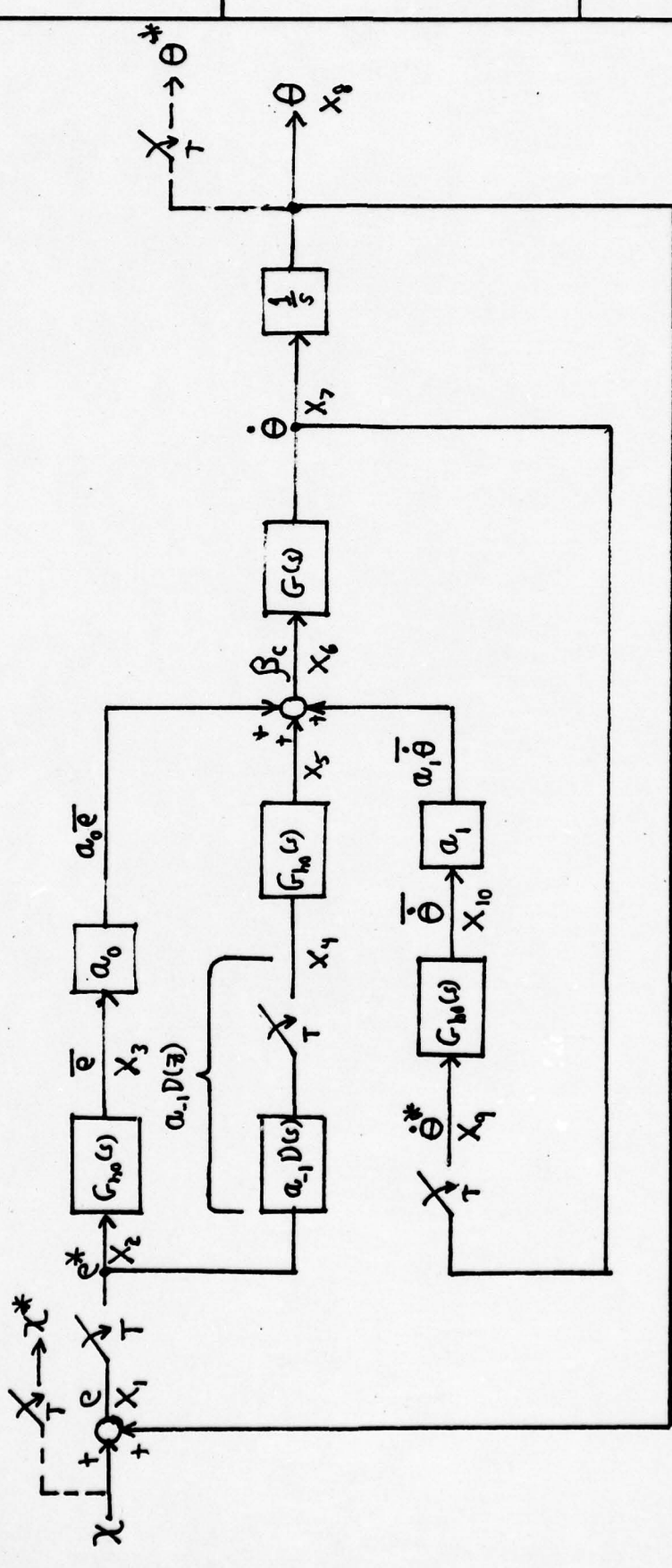
SECTION XIV. REFERENCES

- 1 U.S. Army Missile Research and Development Command Contract DAAK10-78-C-0226, dated 7 August 1978, pp. 19-20.
- 2 Amendment/Modification No. P00002, dated 31 January 1979, to contract of Reference 1.
- 3 Report ACDS-78-2, "Application of Discrete Guidance and Control Theory," Technical Report: Phase I, Applied Control Systems Dynamics Company, Huntsville, Alabama, September 1978.
- 4 Amendment/Modification No. P00001, dated 20 October 1978, to contract of Reference 1.
- 5 Contract of Reference 1, pp. 17-18.
- 6 D. D. Siljak, Nonlinear Systems, Wiley, N. Y., 1969.
- 7 D. D. Siljak, "Analysis and Synthesis of Feedback Control Systems in the Parameter Plane, Part II - Sampled-Data Systems," IEEE Transactions, Part II, Applications and Industry, Volume 83, November 1964, pp. 458-466.
- 8 S. M. Seltzer, "Sampled-Data Control System Design in the Parameter Plane," Proceedings of the Eighth Annual Allerton Conference on Circuits and System Theory, October 1970, pp. 454-463.
- 9 S. M. Seltzer, "Enhancing Simulation of Efficiency with Analytical Tools," Computers and Electrical Engineering, Volume 2, 1979, pp. 35-44.
- 10 W. Hausserrmann, "Stability Areas of Missile Control Systems," Jet Propulsion, July 1957, pp. 787-795.
- 11 S. M. Seltzer, "An Algorithm for Solving the Popov Criterion Applied to Sampled-Data Systems." Proceedings of the Third-Southeastern Symposium on System Theory, April 506, 1971, pp. 05-0 - 05-7.
- 12 B. C. Kuo, Digital Control Systems, SRL Publishing Company, Champaign, Illinois, 1977, pp. 232-236.
- 13 H. L. Pastrick, S. M. Seltzer, and M. E. Warren, AIAA Paper 75-0059 "Guidance Laws of Short Range Tactical Missiles," AIAA 17th Annual Aerospace Sciences Meeting, January 1979.

SECTION XV. FIGURES

3-0235 - 50 SHEETS - 5 SQUARES
 3-0236 - 100 SHEETS - 5 SQUARES
 3-0237 - 200 SHEETS - 5 SQUARES

GOLD KEY



TRAPEZOIDAL INTEGRATION (APPROXIMATION): $D(z) = \frac{T}{2} \frac{(z+1)}{(z-1)}$

(NOTE: $D(z)$ includes the sampler.)

$$G(s) = -\omega_2/s$$

$$G_{m0}(s) = \frac{1}{s} - \frac{-st}{s}$$

FIGURE 1. BLOCK DIAGRAM OF MISSILE

GOLD KEY
 3-0235 - 50 SHEETS - 5 SQUARES
 3-0236 - 100 SHEETS - 5 SQUARES
 3-0237 - 200 SHEETS - 5 SQUARES

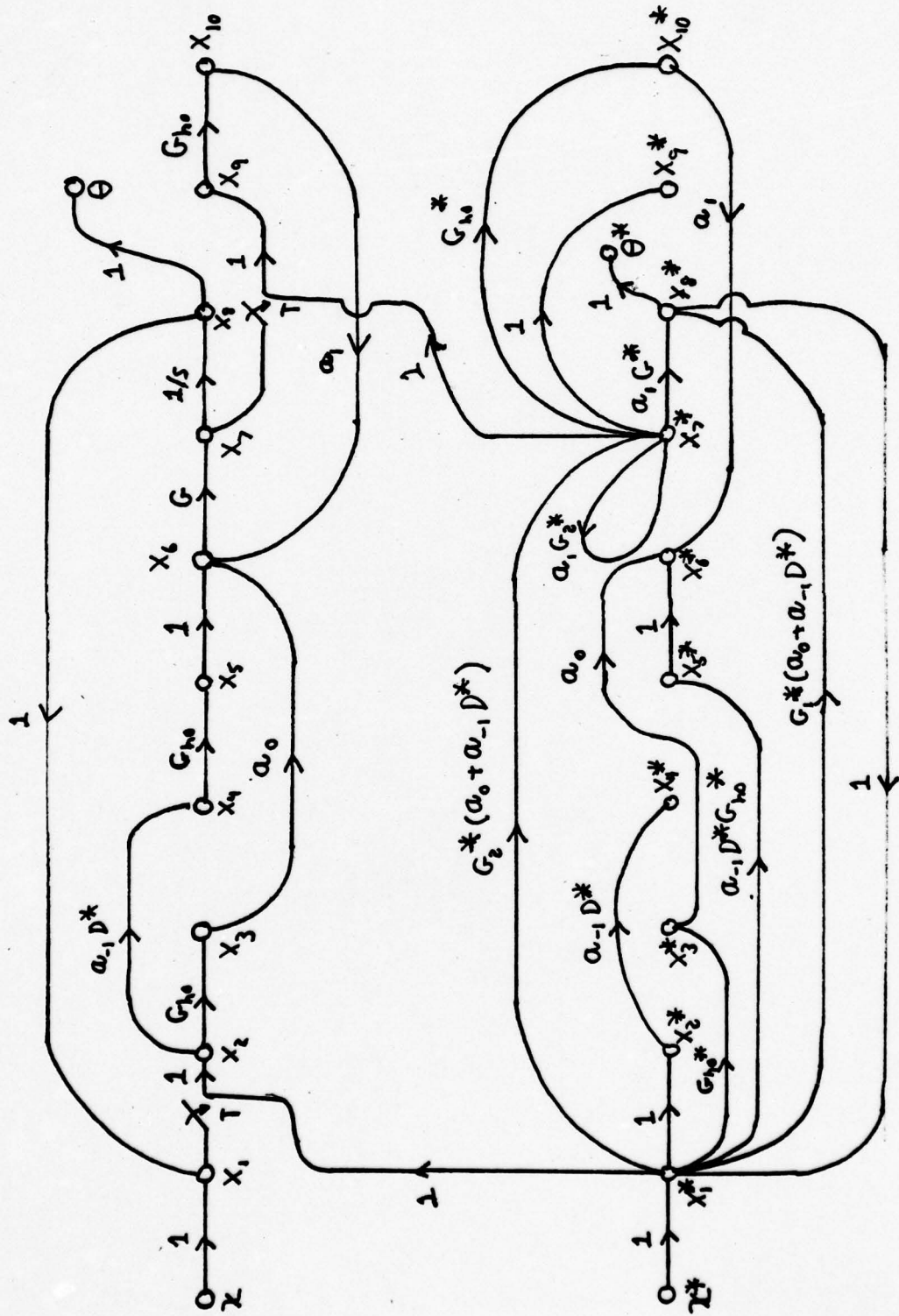


FIGURE 2. SFG OF MISSILE

3-0235 - 50 SHEETS 5 SQUARES
 3-0236 - 100 SHEETS 5 SQUARES
 3-0237 - 200 SHEETS 5 SQUARES

GOLD KEY

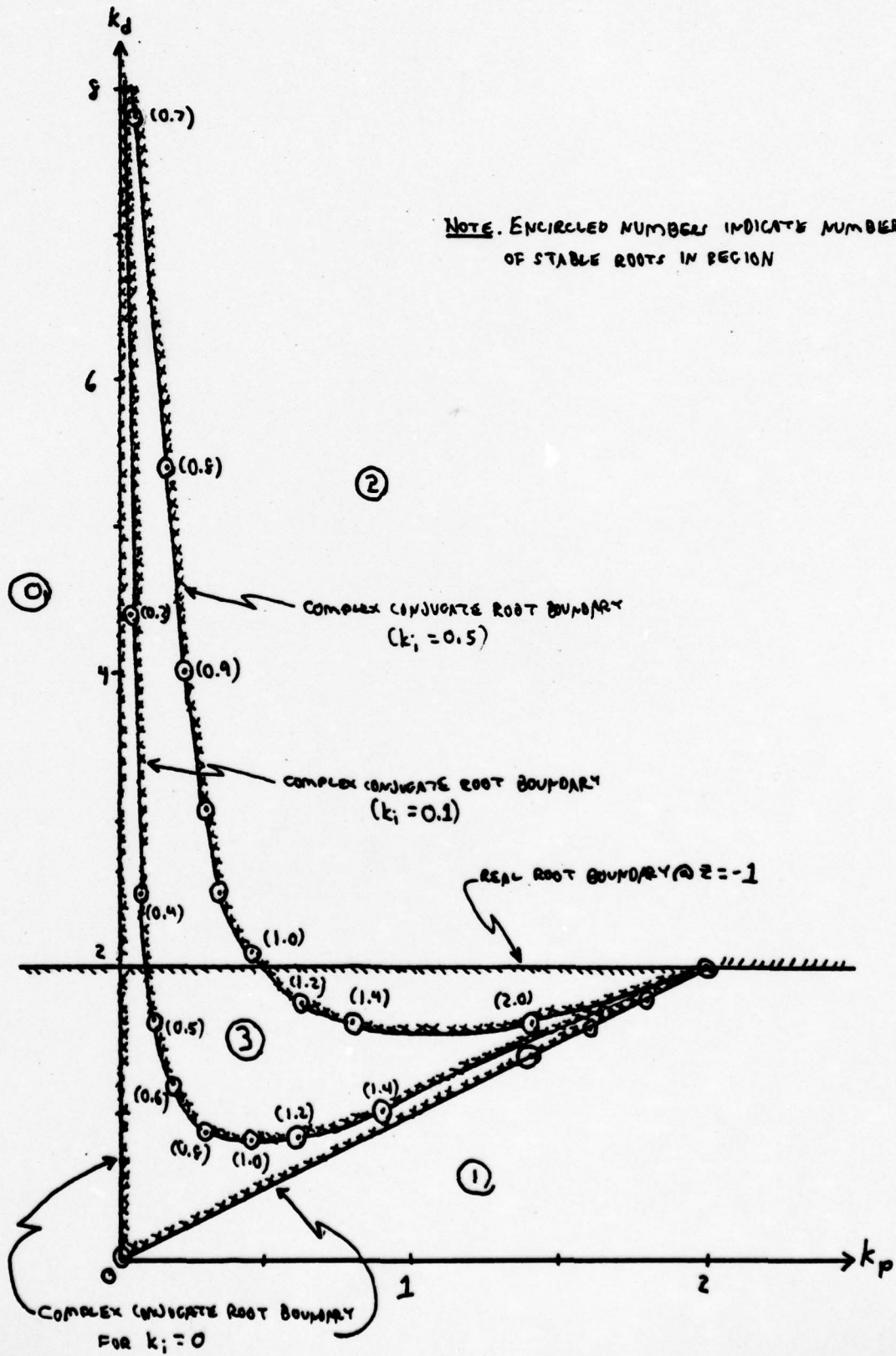


FIGURE 3. PARAMETER PLANE STABILITY MAP

GOLD KEY
 3-0235 - 50 SHEETS - 5 SQUARES
 3-0236 - 100 SHEETS - 5 SQUARES
 3-0237 - 200 SHEETS - 5 SQUARES

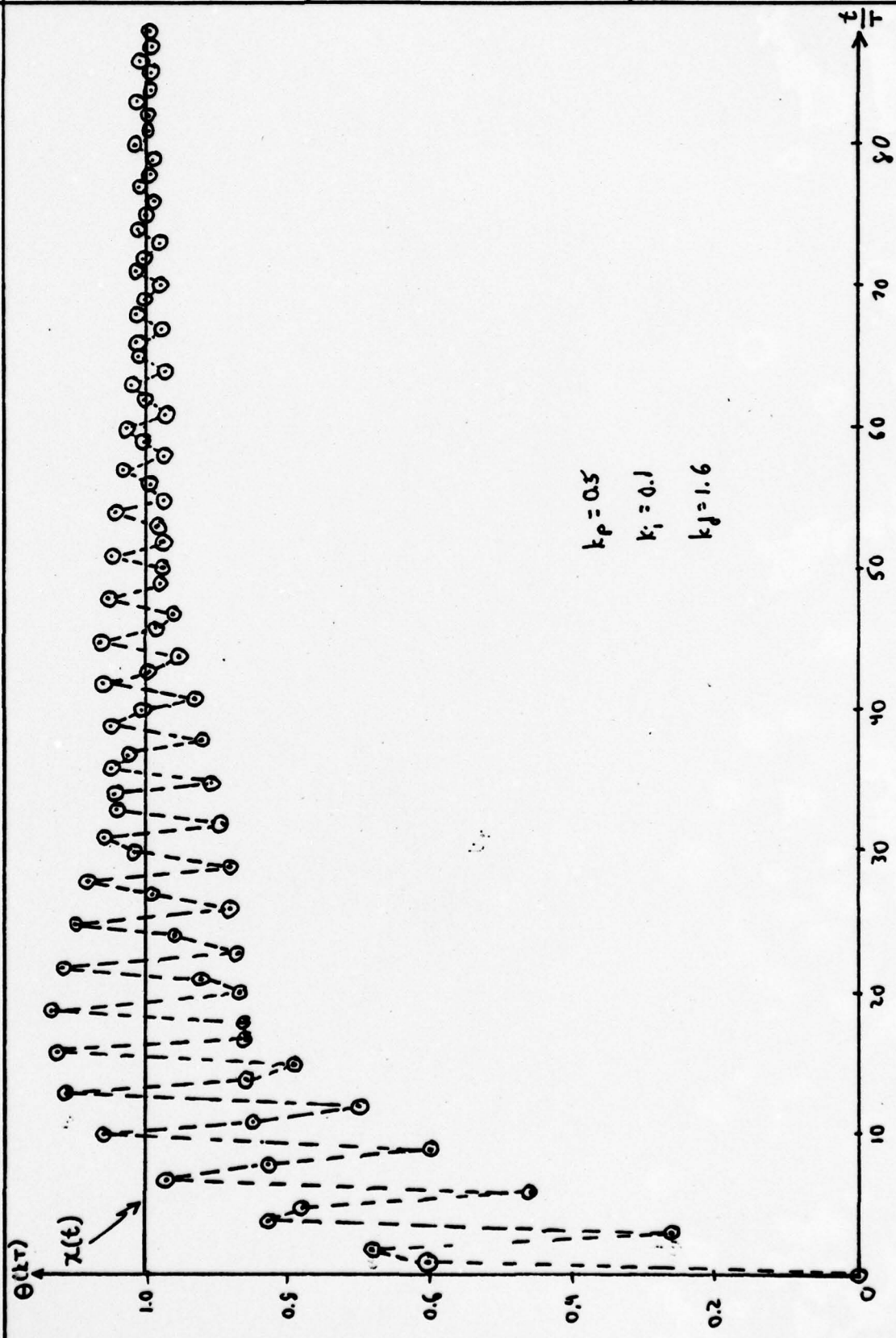


FIGURE 11. MISSILE RESPONSE $\theta(kT)$ to UNIT STEP INPUT $x(t)$

APPENDIX A: SAM: AN ALTERNATIVE TO SAMPLED-DATA SIGNAL FLOW GRAPHS



**U. S. ARMY
MISSILE
RESEARCH
AND
DEVELOPMENT
COMMAND**



Redstone Arsenal, Alabama 35809

DMR FORM 1000, 1 APR 77

TECHNICAL REPORT T-79-49

**SAM: AN ALTERNATIVE TO SAMPLED-DATA
SIGNAL FLOW GRAPHS**

S. M. Seltzer
Guidance and Control Directorate

10 MAY 1979

Approved for public release; distribution unlimited.

Unclassified

SECURITY CLASSIFICATION OF THIS PAGE (When Data Entered)

REPORT DOCUMENTATION PAGE		READ INSTRUCTIONS BEFORE COMPLETING FORM
1. REPORT NUMBER TR-T-79-49	2. GOVT ACCESSION NO.	3. RECIPIENT'S CATALOG NUMBER
4. TITLE (and Subtitle) SAM: AN ALTERNATIVE TO SAMPLED-DATA SIGNAL FLOW GRAPHS		5. TYPE OF REPORT & PERIOD COVERED Technical Report
		6. PERFORMING ORG. REPORT NUMBER
7. AUTHOR(s) S.M. Seltzer		8. CONTRACT OR GRANT NUMBER(s)
9. PERFORMING ORGANIZATION NAME AND ADDRESS Commander US Army Missile Research and Development Command ATTN: DRDMI-TG Redstone Arsenal, Alabama 35809		10. PROGRAM ELEMENT, PROJECT, TASK AREA & WORK UNIT NUMBERS
11. CONTROLLING OFFICE NAME AND ADDRESS Commander US Army Missile Research and Development Command ATTN: DRDMI-TI Redstone Arsenal, Alabama 35809		12. REPORT DATE 10 May 1979
14. MONITORING AGENCY NAME & ADDRESS (if different from Controlling Office)		13. NUMBER OF PAGES 38
		15. SECURITY CLASS. (of this report) Unclassified
15a. DECLASSIFICATION/DOWNGRADING SCHEDULE		
16. DISTRIBUTION STATEMENT (of this Report) Approved for public release; distribution unlimited.		
17. DISTRIBUTION STATEMENT (of the abstract entered in Block 20, if different from Report)		
18. SUPPLEMENTARY NOTES		
19. KEY WORDS (Continue on reverse side if necessary and identify by block number) Sampled-Data SAM Digital Guidance and Control Signal Flow Graphs		
20. ABSTRACT (Continue on reverse side if necessary and identify by block number) This report describes an alternative to the use of Signal Flow Graphs and Mason's Gain Rule for the analysis of complicated digital control systems. The technique is analytical in nature and makes use of a systematic manipulation of algebraic equations describing the system to be analyzed. The technique is modified to be amendable to a new signal flow graph method for the analyst who prefers using signal flow graphs. Both the analytical technique and the modified signal flow graph technique are applied to examples and compared to a standard signal flow graph technique to display their		

DISPOSITION INSTRUCTIONS

DESTROY THIS REPORT WHEN IT IS NO LONGER NEEDED. DO NOT RETURN IT TO THE ORIGINATOR.

DISCLAIMER

THE FINDINGS IN THIS REPORT ARE NOT TO BE CONSTRUED AS AN OFFICIAL DEPARTMENT OF THE ARMY POSITION UNLESS SO DESIGNATED BY OTHER AUTHORIZED DOCUMENTS.

TRADE NAMES

USE OF TRADE NAMES OR MANUFACTURERS IN THIS REPORT DOES NOT CONSTITUTE AN OFFICIAL ENDORSEMENT OR APPROVAL OF THE USE OF SUCH COMMERCIAL HARDWARE OR SOFTWARE.

CONTENTS

Section	Page
1. Introduction	5
2. Systematic Analytical Approach (SAM)	5
3. Modified Signal Flow Graph Technique	12
4. The Sampled Signal Flow Graph Method	21
5. Application To Z- and Modified Z-Transforms ...	31
6. Comparison of Methods	32
7. Conclusions	33
Appendix A - Review of Mason's Gain Rule	35

ILLUSTRATIONS

Figure	Page
1. Block Diagram for Example No. 1	7
2. Block Diagram for Example No. 2	9
3. Equivalent SFG for Example No. 1	13
4. Sampled SFG for Example No. 1	13
5. Composite SFG for Example No. 1	14
6. Equivalent SFG for Example No. 2.	15
7. Sampled SFG for Example No. 2 (Modified SFG Method)	16
8. Composite SFG for Example No. 2 (Modified SFG Method)	16
9. Sampled SFG for Example No. 2 (Standard SFG Method)	28
10. Composite SFG for Example No. 2 (Standard SFG Method)	30

1. INTRODUCTION

This report describes an alternative to the use of Signal Flow Graphs (SFG) and Mason's Gain Rule (Formula) for analysis of complicated sampled-data control systems. Usually in such systems, block diagram algebraic manipulation may become unwieldy, particularly when such systems include multiple loops and samplers. The Systematic Analysis Method (SAM) may be applied to such systems, as well as to simple single-loop feedback systems. This is shown in Section 2. Also shown is how to apply SAM to make use of modified z-transforms (Section 5).

The advantages of using SAM are that the cumbersome application of Mason's Gain Formula can be avoided. Further, the entire method of drawing Signal Flow Graphs may be circumvented. Since only the equations describing the system are needed for SAM, even the customary block diagram is not needed.

If the analyst prefers to use one of the Signal Flow Graph methods, a modified SFG technique is also described (Section 3). It is simpler and less cumbersome to apply than the conventional SFG method, which for purposes of comparison is described in Section 4.

All three techniques are applied to two examples. This is done to better describe the application of SAM and the modified SFG and to help provide a basis for comparison (Section 6) of the three methods.

To obviate searching for such a description, Mason's Gain Rule is described in the appendix.

2. SYSTEMATIC ANALYTICAL METHOD (SAM)

SAM is implemented by performing the following four steps. If the equations resulting from the first three steps are placed in a table of three columns (one for each step), they are easily manipulated to perform the fourth and final step.

STEP NO. 1. OBTAIN "SYSTEM EQUATIONS"

The equations describing the system are written in the Laplace domain. If the system is described by block diagram, the "system equations" are written upon inspection.

STEP NO. 2. OBTAIN "MODIFIED SYSTEM EQUATIONS"

If any of the "system equations" contain terms that in themselves contain the product(s) of an unsampled system variable and an unsampled transfer function, then the unsampled variable must be replaced by an expression containing no unsampled variable(s). In complex systems, this may require a chain of several substitutions.

An "unsampled variable" is recognized as one upon which the pulse transform operation has not taken place. For example, when the pulse transform of a Laplace transform function and/or variable is taken, that operation is denoted symbolically by placing an asterisk immediately following the expression, yielding a so-called "starred quantity." For example, the pulse transform of the Laplace function $F(s)$ is denoted as $F^*(s)$. One manner of expressing $F^*(s)$ in terms of $F(s)$ is

$$F^*(s) = \frac{1}{T} \sum_{n=-\infty}^{\infty} F(s + i 2\pi n/T) \quad (1)$$

where T represents the sampling period.

STEP NO. 3. OBTAIN "PULSED SYSTEM EQUATIONS"

Pulse transforms are now taken off each side of the "modified system equations," yielding "pulsed system equations." Now all system variables, either unsampled or sampled (pulsed), may be solved for, either in the "system equations" or the "pulsed system equations."

STEP NO. 4. OBTAIN DESIRED INPUT/OUTPUT RELATIONSHIPS

All system variables, both starred and unstarred, may be found in either the "system equations" (Step No. 1) or the "pulsed system equations" (Step No. 3). The desired output(s) may be solved for by selecting the appropriate "system" or "pulsed system" equations, substituting as necessary. This will be brought forth in the examples.

EXAMPLE NO. 1

Given: The digital system of Example No. 1 is described by the block diagram of Figure 1.

To Find: The continuous-data and pulsed (sampled) outputs, $C(s)$ and $C^*(s)$, respectively, in terms of the system input $R(s)$ and the system transfer functions $G(s)$ and $H(s)$.

STEP 1. SYSTEM EQUATIONS¹

Obtain these equations directly upon inspection of Figure 1.

$$E = R - HC \quad (2)$$

$$C = G E^* \quad (3)$$

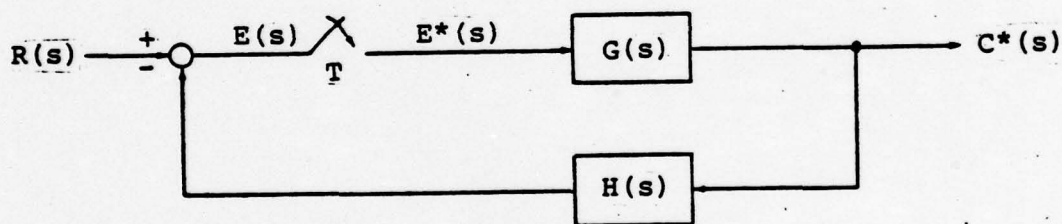


Figure 1. Block Diagram for Example No. 1.

1. Note: In the sequel, the following shorthand notation will be used:

$F \stackrel{d}{=} F(s) = \mathcal{L}\{f(t)\}$, i.e. the Laplace transform of $F(t)$,

$F^* \stackrel{d}{=} F^*(s)$,

$\overline{GH}^* \stackrel{d}{=} [G(s)H(s)]^*$

STEP 2. MODIFIED SYSTEM EQUATIONS

One sees that Equation (2) contains a product of an unsampled (i.e., unstarred) system variable, C, and an unsampled transfer function, H. Since this violates a condition stated in the description of Step No. 2, a substitute must be found for C. This is obvious in Equation (3), which is substituted into Equation (2) to yield the acceptable form,

$$E = R - HG E^*, \quad (4)$$

i.e., it contains no products of unsampled variables and unsampled transfer functions. The product of unsampled transfer functions, HG [i.e., $H(s)G(s)$], is acceptable.

STEP NO. 3. PULSED SYSTEM EQUATIONS

Take the pulse transform of each side of each of the "modified system equations," making use of the following rules:

$$[RG]^* = \overline{RG}^*, \quad (5)$$

$$[R G^*]^* = R^* G^*, \quad (6)$$

$$[R^*]^* = R^*. \quad (7)$$

$$E^* = R^* - \overline{HG}^* E^* \quad (8)$$

$$C^* = G^* E^* \quad (9)$$

The resulting equations from Step Nos. 1, 2 and 3 can be placed in a table (Table 1), while they are being developed, for systematic orderliness.

TABLE 1. SYSTEM EQUATIONS FOR EXAMPLE NO. 1

Sys. Eqs.	Mod. Sys. Eqs.	Pulsed Sys. Eqs.
$E = R - HC \quad (2)$	$E = R - HG E^* \quad (4)$	$E^* = R^* - \overline{HG}^* E^* \quad (8)$
$C = G E^* \quad (3)$	$C = G E^* \quad (3)$	$C^* = G^* E^* \quad (9)$

STEP 4. OBTAIN, C^* , C

First solve Equation (8) for E^* :

$$E^* = \left[\frac{1}{(1 + \overline{HG}^*)} \right] R^*. \quad (10)$$

Substituting this expression for E^* into Equation (9), one obtains

$$C^* = \left[\frac{G}{(1 + HG^*)} \right] R^* \quad (11)$$

"To obtain C , one substitutes...yielding"

$$C = \left[\frac{G}{(1 + HG^*)} \right] R^* \quad (12)$$

EXAMPLE NO. 2.

Given: The digital system described by the block diagram of Figure 2.

To Find: The continuous-data and pulsed (sampled) outputs, $C(s)$ and $C^*(s)$, respectively, in terms of the system input $R(s)$ and the system transfer functions.

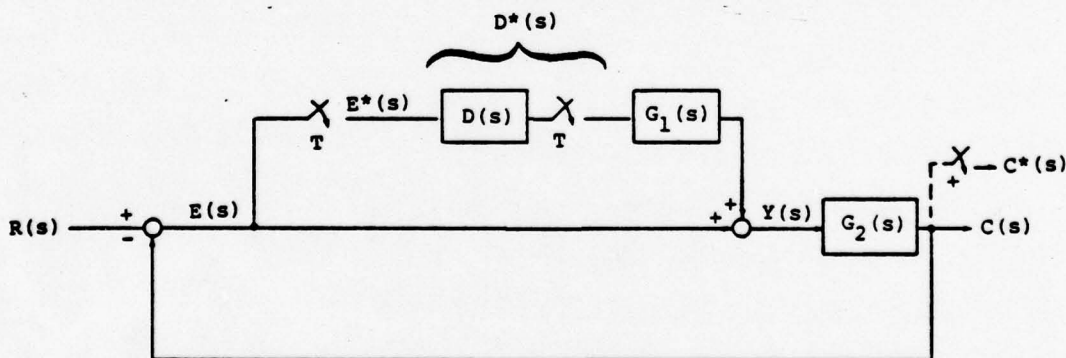


Figure 2. Block Diagram for Example No. 2.

In the interest of being systematic, the analyst may wish to assign "states" (X_j) to the various system variables. The "system equations" (Step No. 1) are written from inspection of Figure 2. In order to implement Step No. 2, the "system equations" of Step No. 1 must be checked for possible products of unsampled system variables and unsampled transfer functions. Two such products exist: G_1X_2 in Equation (15) and G_2X_3 in Equation (16). The first product is readily manipulated into

the approved form by making use of the relation between X_2 and X_1^* of Equation (14), which is substituted into Equation (15) to yield Equation (17). The product, G_2X_3 , is easily handled by substituting Equation (17) into Equation (16), then substituting Equation (13) for X_1 , and solving the resulting expression for X_4 , yielding Equation (18). This completes Step No. 2 (the second column of the array of Table 2). The third column (Step No. 3) is obtained merely by "starring" each side of each of the equations in the second column.

TABLE 2. SYSTEM EQUATIONS FOR EXAMPLE NO. 2
 Sys. Eqs. Mod. Sys. Eqs. Pulsed Sys. Eqs.

$E \equiv X_1 = R - X_4$ (13)	$X_1 = R - X_4$ (13)	$E^* = X_1^* = R^* - X_4^*$ (19)
$E^* \equiv X_2 = X_1^*$ (14)	$X_2 = X_1^*$ (14)	$E^* = X_2^* = X_1^*$ (20)
$Y \equiv X_3 = D^*G_1X_2 + X_1$ (15)	$X_3 = D^*G_1X_1^* + X_1$ (17)	$Y^* = X_3^* = D^*G_1^*X_1^* + X_1^*$ (21)
$C \equiv X_4 = G_2X_3$ (16)	$X_4 = \frac{G_2(D^*G_1X_1^* + R)}{1 + G_2}$ (18)	$C^* = X_4^* = G_3^*D^*X_1^* + R_1^*$ (22)

where

$$G_3 \triangleq \frac{G_1G_2}{1 + G_2} \quad (23)$$

and

$$R_1 \triangleq \frac{G_2R}{1 + G_2} \quad (24)$$

To find C^* , one merely substitutes Equation (19) into Equation (22):

$$\begin{aligned} C^* &= X_4^* = G_3^*D^*X_1^* + R_1^* \\ &= G_3^*D^*(R^* - X_4^*) + R_1^* \\ &= \frac{G_3^*D^*R^* + R_1^*}{1 + G_3^*D^*} \end{aligned} \quad (25)$$

In a similar manner, one finds C by substituting Equation (15) into Equation (16), substituting Equations

(14) and (13) for X_2 and X_1 , respectively, and finally substituting Equation (19) for the resulting X_1^* , i.e.

$$\begin{aligned}
 C &= X_4 = G_2 X_3 \\
 &= G_2 (D^* G_1 X_2 + X_1) \\
 &= G_2 (D^* G_1 X_1^* + R - X_4) \\
 &= \frac{G_1 G_2 D^* X_1^* + G_2 R}{1 + G_2} \\
 &= G_3 D^* X_1^* + R_1 \\
 &= G_3 D^* (R^* - X_4^*) + R_1.
 \end{aligned} \tag{26}$$

Since $X_4^* = C^*$ was just determined in Equation (25), that value is substituted into Equation (26) to yield:

$$\begin{aligned}
 C &= G_3 D^* \left[R^* - \left(\frac{G_3^* D^* R^* + R_1^*}{1 + G_3^* D^*} \right) \right] + R_1 \\
 &= G_3 D^* \left(\frac{R^* + G_3^* D^* R^* - G_3^* D^* R^* - R_1^*}{1 + G_3^* D^*} \right) + R_1 \\
 &= \left(\frac{G_3 D^*}{1 + G_3^* D^*} \right) (R^* - R_1^*) + R_1.
 \end{aligned} \tag{27}$$

An alternate form for $(R^* - R_1^*)$ may be found if desired:

$$\begin{aligned}
 R^* - R_1^* &= R^* - \left(\frac{G_2 R}{1 + G_2} \right)^* \\
 &= \left[\left(\frac{1 + G_2}{1 + G_2} \right) R \right]^* - \left(\frac{G_2 R}{1 + G_2} \right)^* \\
 &= \left(\frac{R}{1 + G_2} \right)^* + \left(\frac{G_2 R}{1 + G_2} \right)^* - \left(\frac{G_2 R}{1 + G_2} \right)^* \\
 &= \left(\frac{R}{1 + G_2} \right)^* \stackrel{d}{=} R_2^*.
 \end{aligned} \tag{28}$$

This expression for $(R^* - R_1^*)$ may be substituted into Equation (27) to yield

$$C = \frac{G_3 D^*}{1 + G_3^* D^*} R_2^* + R_1^*, \quad (29)$$

which may be slightly simpler in form than Equation (27).

3. MODIFIED SIGNAL FLOW GRAPH TECHNIQUE

If the analyst prefers to use a Signal Flow Graph (SFG) technique, the following modified SFG is proposed. It incorporates many of the features developed in SAM. As such, it appears to be simpler to implement, requiring the application of Mason's Gain Rule at only one stage of the analysis.

The first three steps are identical to those of SAM.

STEP NO. 4. CONSTRUCT EQUIVALENT SFG

The equivalent SFG is drawn directly from the information contained in the "system equations" (Step No. 1) or from the block diagram.

STEP NO. 5. CONSTRUCT SAMPLED SFG

The sampled SFG is drawn from the "pulsed system equations" (Step No. 3).

STEP NO. 6. CONSTRUCT COMPOSITE SFG

This is achieved by connecting the output nodes of the samplers in the equivalent SFG to the nodes representing those same quantities on the sampled SFG.

STEP NO. 7. OBTAIN DESIRED INPUT/OUTPUT RELATIONSHIPS

Mason's Gain Rule (Appendix A) is applied to the composite SFG to obtain desired outputs in terms of system transfer functions and inputs to the system.

Examples of the use of the modified SFG method follow. For comparative purposes, the same two examples to which SAM was applied will be used.

EXAMPLE NO. 1.

STEP NOS. 1 - 3. SYSTEM, MODIFIED SYSTEM, AND PULSED SYSTEM EQUATIONS

Repeat these steps as shown in Example No. 1 of Section 2 (SAM). They are summarized in Table 1 and are Equations (2), (3); (4), (3); and (8), (9), respectively.

STEP NO. 4. CONSTRUCT EQUIVALENT SFG

The equivalent SFG is constructed directly from the "system equations" of Step No. 1, Equations (2) and (3). The resulting SFG is shown as Figure 3.

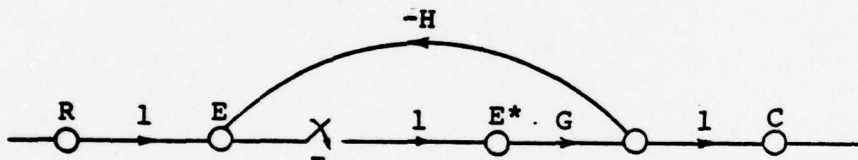
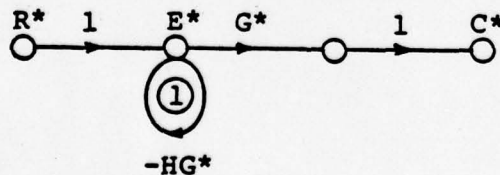


Figure 3. Equivalent SFG for Example No. 1.

STEP NO. 5. CONSTRUCT SAMPLED SFG

The sampled SFG is constructed directly from the "pulsed system equations" of Step No. 3, Equations (8) and (9). The resulting SFG is shown as Figure 4.



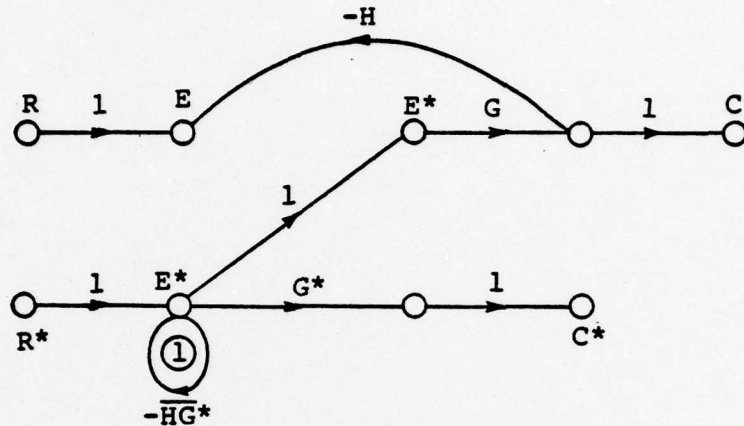
Note: Encircled number refers to identification of loop.

Figure 4. Sampled SFG for Example No. 1.

STEP NO. 6. CONSTRUCT COMPOSITE SFG

The composite SFG is constructed by joining the two SFG's of Figures 4 and 5 in the prescribed manner. In

this example a single line connecting the E*'s of the two SFG's is required (Figure 5).



Note: Encircled number refers to identification of loop.
Figure 5. Composite SFG for Example No. 1.

STEP NO. 7. OBTAIN C^* , C

Looking at Figure 5, one sees that there are two inputs to the system, R and R^* . Applying Mason's Gain Rule (appendix), one finds only one possible forward path from R^* to C^* and none from R ; hence, $k = 1$. The gain along that forward path, M_k , is seen to be

$$M_k = M_1 = G^* . \quad (30)$$

There is a single loop whose gain is

$$K_1 = - \overline{HG}^* . \quad (31)$$

The value of Δ is found to be

$$\Delta = 1 - K_1 = 1 + \overline{HG}^* . \quad (32)$$

Since the single forward path touches the single loop of this system,

$$\Delta_k = \Delta_1 = 1 . \quad (33)$$

The gain, M , between C^* and the input R^* is then

$$M = \frac{C^*}{R^*} = \frac{M_k \Delta_k}{\Delta} = \frac{G^*}{1 + \overline{HG}^*} . \quad (34)$$

Solving Equation (34) for C^* we obtain the same result as Equation (11).

In solving for C , we find that only input R^* has a forward path to C . In this case the gain along that path is seen to be G (Figure 5), i.e.

$$M_1 = G. \quad (35)$$

The value of Δ remains the same as that shown in Equation (32), as does the value of K_1 remain as shown in Equation (31). The single forward path touches the single loop of the system, so Equation (33) still applies. The gain, M , between C and the input R^* is then

$$M = \frac{C}{R^*} = \frac{M_1 \Delta_1}{\Delta} = \frac{G}{1 + HG} \quad (36)$$

Solving Equation (36) for C one obtains the same result as Equation (12).

EXAMPLE NO. 2

STEP NOS. 1 - 3

Repeat these steps as shown in Example No. 2 of Section 2 (SAM). They are summarized in Table 2.

STEP NO. 4. EQUIVALENT SFG

Construct the equation SFG directly from "system equations" (13) through (16) (Figure 6).

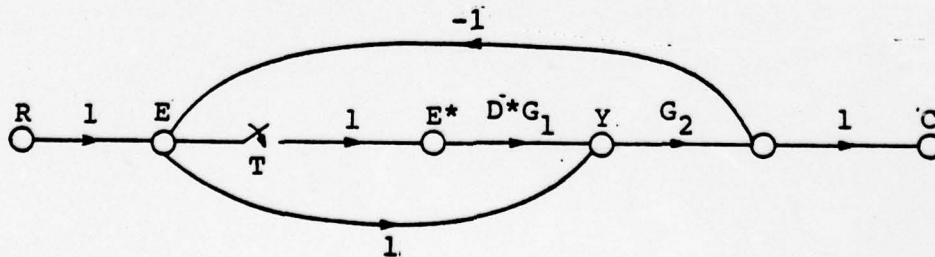


Figure 6. Equivalent SFG for Example No. 2.

STEP NO. 5. SAMPLED SFG

Construct the sampled SFG directly from "pulsed system equations" (19) - (22) (Figure 7).

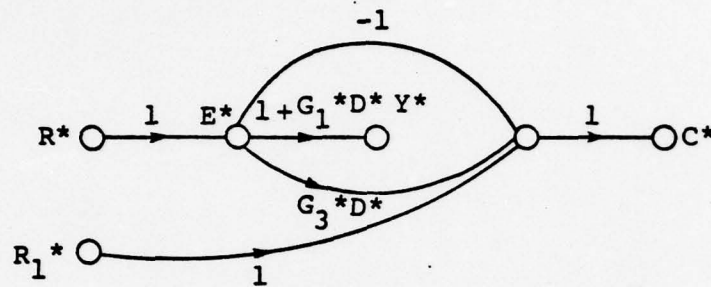
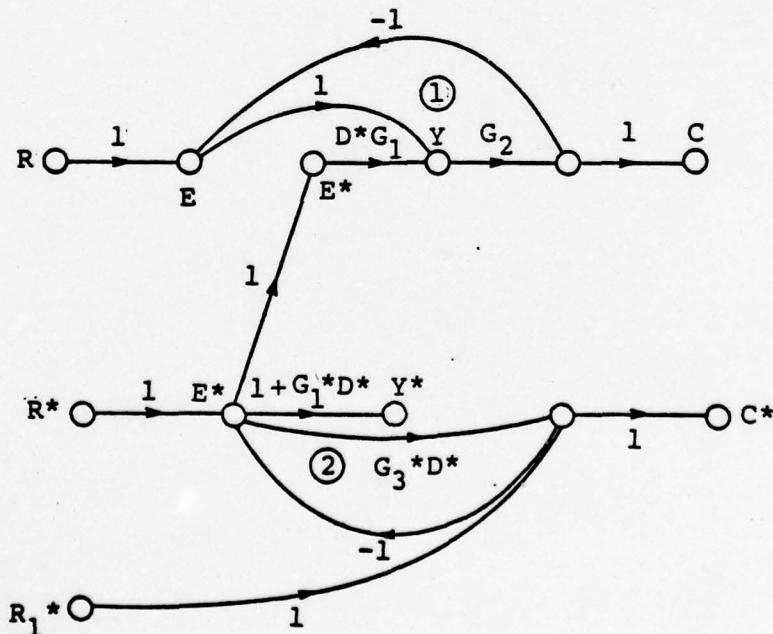


Figure 7. Sampled SFG for Example No. 2 (modified SFG method).

STEP NO. 6. COMPOSITE SFG

The composite SFG is obtained by joining the two SFG's of Figures 6 and 7 with a line connecting the E^* 's (X_2 's) of the two SFG's (Figure 8).



Note: Encircled numbers refer to identification of loops.

Figure 8. Composite SFG for Example No. 2 (modified SFG method).

STEP NO. 7. OBTAIN C^* , C

From Figure 8 one sees that there are three inputs to the system: R , R^* , and R_1^* . Applying Mason's Gain Rule, one finds two forward paths to C^* , one from R^* and one from R_1^* ; hence, $k = 2$.

There are two loop gains, denoted herein as K_1 and K_2 . The loops are designated by encircled numbers on Figure 8, and their gains are

$$K_1 = -G_2, \quad (37)$$

$$K_2 = -G_3^* D^*. \quad (38)$$

It is observed that the loops are nontouching (necessary information for formulating Δ). Δ is thus found to be

$$\begin{aligned} \Delta &= 1 - (K_1 + K_2) + K_1 K_2 \\ &= 1 - (-G_2 - G_3^* D^*) + G_2 G_3^* D^* \\ &= (1 + G_2) (1 + G_3^* D^*). \end{aligned} \quad (39)$$

The forward path from R^* to C^* may be designated as $k = 1$. Since it is touched by Loop 2 but not by Loop 1, the value of Δ_1 is

$$\begin{aligned} \Delta_1 &= 1 - K_1 \\ &= 1 + G_2. \end{aligned} \quad (40)$$

The forward path from R_1^* to C^* may be designated as $k = 2$. Since it is touched by Loop 2 but not by Loop 1,

$$\Delta_2 = \Delta_1. \quad (41)$$

The gain along the first forward path ($k = 1$) is, from Figure 8,

$$M_1 = G_3^* D^*. \quad (42)$$

The gain along the second forward path ($k = 2$) is

$$M_2 = 1. \quad (43)$$

The gain M_1 between R^* and C^* is

$$\begin{aligned}
 M^1 &\triangleq \frac{C^{1*}}{R^*} = \frac{M_1 \Delta_1}{\Delta} \\
 &= \frac{(G_3^* D^*) (1 + G_2)}{(1 + G_2) (1 + G_3^* D^*)} \\
 &= \frac{G_3^* D^*}{1 + G_3^* D^*} \cdot \qquad (44)
 \end{aligned}$$

The gain M^2 between R_1^* and C^* is

$$\begin{aligned}
 M^2 &\triangleq \frac{C^{2*}}{R_1^*} = \frac{M_2 \Delta_2}{\Delta} \\
 &= \frac{(1) (1 + G_2)}{(1 + G_2) (1 + G_3^* D^*)} \\
 &= \frac{1}{1 + G_3^* D^*} \cdot \qquad (45)
 \end{aligned}$$

Solving Equations (44) and (45) each for C^{1*} and C^{2*} , respectively,

where

$$C^* = C^{1*} + C^{2*}, \qquad (46)$$

one finally obtains

$$\begin{aligned}
 C^* &= M^1 R^* + M^2 R_1^* \\
 &= \left[\frac{G_3^* D^*}{1 + G_3^* D^*} \right] R^* + \left(\frac{1}{1 + G_3^* D^*} \right) R_1^* \\
 &= \frac{G_3^* D^* R^* + R_1^*}{1 + G_3^* D^*}, \qquad (47)
 \end{aligned}$$

which is seen to be identical with the earlier SAM result of Equation (25).

To obtain C, one must first observe from Figure 8 that all three inputs to the system can find their way to the node representing C. The two loop gains, K_1 and K_2 , are the same for finding C^* , as is Δ . The forward path from input R^* to C, designated as $k = 1$, has a gain M_1 of

$$M_1 = D^* G_1 G_2. \quad (48)$$

The gain along the path between R_1^* and C, designated as $k = 2$, has a gain M_2 of

$$M_2 = -D^* G_1 G_2. \quad (49)$$

Finally, the gain along the path between R and C, designated as $k = 3$, has a gain M_3 of

$$M_3 = G_2. \quad (50)$$

The $k = 1$ and $k = 2$ paths touch both loops, so the values of Δ_1 and Δ_2 are both unity. The $k = 3$ path only touches Loop 1, so the values of Δ_3 is

$$\Delta_3 = 1 - K_2 = 1 + G_3^* D^*. \quad (51)$$

The gain M^1 between R^* and C is

$$\begin{aligned} M^1 \text{ d. } \frac{C^1}{R^*} &= \frac{M_1 \Delta_1}{\Delta} \\ &= \frac{D^* G_1 G_2}{(1 + G_2) (1 + G_3^* D^*)} \end{aligned} \quad (52)$$

The gain M^2 between R_1^* and C is

$$\begin{aligned} M^2 \text{ d. } \frac{C^2}{R_1^*} &= \frac{M_2 \Delta_2}{\Delta} \\ &= \frac{-D^* G_1 G_2}{(1 + G_2) (1 + G_3^* D^*)}. \end{aligned} \quad (53)$$

The gain M^3 between R and C is

$$\begin{aligned}
 M^3 &= \frac{C^3}{R} = \frac{M_3 \Delta_3}{\Delta} \\
 &= \frac{G_2 (1 + G_3^* D^*)}{(1 + G_2) (1 + G_3^* D^*)} \\
 &= \frac{G_2}{1 + G_2} .
 \end{aligned} \tag{54}$$

Solving Equations (52) through (54) for C^1 , C^2 , and C^3 , respectively,

where

$$C = C^1 + C^2 + C^3 , \tag{55}$$

one obtains

$$\begin{aligned}
 C &= M^1 R^* + M^2 R_1^* + M^3 R \\
 &= \frac{D^* G_1 G_2 R^*}{(1 + G_2) (1 + G_3^* D^*)} - \frac{D^* G_1 G_2 R_1^*}{(1 + G_2) (1 + G_3^* D^*)} + \frac{G_2 R}{1 + G_2} \\
 &= \frac{D^* G_3}{(1 + G_3^* D^*)} (R^* - R_1^*) + R_1 .
 \end{aligned} \tag{56}$$

Equation (28) may be used in an attempt to simplify the above result, yielding

$$C = \frac{D^* G_3}{(1 + G_3^* D^*)} R_2^* + R_1 . \tag{57}$$

This is equivalent to Equation (29) obtained using SAM.

4. THE SAMPLED SIGNAL FLOW GRAPH METHOD

The standard Signal Flow Graph method in use is the "Sampled Signal Flow Graph Method."² So that the SAM and modified SFG methods exposed in Section 2 and 3, respectively, of this report may be compared to this standard method, it is described briefly in this section. The same two examples that have been used previously in this report are used in this section to better permit comparison of the various methods. The other popularly used SFG method, "The Direct Signal Flow Graph Method," will not be described herein.³

STEP NO. 1. CONSTRUCT EQUIVALENT SFG

This is equivalent to Step No. 4 of the modified SFG procedure of Section 3.

STEP NO. 2. CONSTRUCT SAMPLED SFG

Write system equations for all noninput nodes of SFG, applying Mason's Gain Rule. A "noninput node" is defined as a node that is not an input node, where an "input" is defined as a system input or the output of a sampler.

Take the pulse transform of each side of each of the system equations.

Using equations noted in the paragraph above, draw the sampled SFG for the system.

STEP NO. 3. OBTAIN RELATION BETWEEN SAMPLED INPUTS/OUTPUTS

This is achieved by applying Mason's Gain Rule to the SFG.

STEP NO. 4. OBTAIN RELATION BETWEEN INPUTS/ CONTINUOUS-DATA OUTPUTS

Connect the SFG's of Steps No. 1 and No. 2 to yield a composite SFG.

Apply Mason's Gain Rule to SFG.

2. B. C. Kuo, Digital Control Systems, SRL Publishing Company, Champaign, Illinois, 1977, pp. 100-105.

3. Ibid, pp. 106-115.

EXAMPLE NO. 1.

See Section 2 and Figure 1 for a description of the example.

STEP NO. 1. EQUIVALENT SFG

From the block diagram describing the system (Figure 1), construct an equivalent SFG. This is the same as Figure 3.

STEP NO. 2. SAMPLED SFG

Write system equations, applying Mason's Gain Rule to equivalent SFG (Figure 3).

$$E = R - G H E^* \quad (58)$$

$$C = G E^* \quad (59)$$

Take the pulse transform of each side of the system equations.

$$E^* = R^* - \overline{GH}^* E^* \quad (60)$$

$$C^* = G^* E^* \quad (61)$$

Draw sampled SFG from pulsed system equations (Figure 4).

STEP NO. 3.

Obtain C^* , E^* from sampled SFG (Figure 4), applying Mason's Gain Rule. There is one path from R^* to E^* ; $k = 1$.

$$M_1 = 1 \quad (62)$$

$$1 \text{ loop: } K_1 = -\overline{GH}^* \quad (63)$$

$$\Delta = 1 - K_1 = 1 + \overline{GH}^* \quad (64)$$

The forward path touches the loop:

$$\Delta_1 = 1, \quad (65)$$

$$M^1 \stackrel{d.}{=} \frac{E^*}{R^*} = \frac{M_1 \Delta_1}{\Delta} = \frac{1}{1 + \overline{GH}^*} \quad (66)$$

Solving Equation (66) for E^* leads to

$$E^* = \frac{R^*}{1 + \overline{GH}^*} \quad (67)$$

There is one path from R^* to C^* , $k = 2$.

$$M_2 = G^* \quad (68)$$

$$\Delta_2 = \Delta_1 \quad (69)$$

$$M^2 = \frac{C^*}{R^*} = \frac{M_2 \Delta_2}{\Delta} = \frac{G^*}{1 + \overline{GH}^*} \quad (70)$$

Solving Equation (70) for C^* leads to

$$C^* = \frac{G^*}{1 + \overline{GH}^*} R^* \quad (71)$$

STEP NO. 4. OBTAIN, C, E

Connect SFG's of Figures 3 and 4 to form composite SFG (Figure 5).

Apply Mason's Gain Rule to Figure 5. There is one path from R^* to C , none from R : $k = 1$.

$$M_1 = G \quad (72)$$

$$K_1 = -\overline{GH}^* \quad (73)$$

$$\Delta_1 = 1 \quad (74)$$

$$M^1 \stackrel{d.}{=} \frac{C}{R^*} = \frac{M_1 \Delta_1}{\Delta} = \frac{G}{1 + \overline{GH}^*} \quad (75)$$

Solving Equation (75) for C leads to

$$C = \frac{G}{1 + \overline{GH}^*} R^* \quad (76)$$

There is one path from R^* to E ($k = 2$), and one path from R ($k = 3$).

$$M_2 = -GH \quad (77)$$

$$M_3 = 1 \quad (78)$$

$$\Delta_2 = 1 \quad (79)$$

$$\Delta_3 = 1 - K_1 = 1 + \overline{GH}^* \quad (80)$$

$$M^2 \stackrel{d.}{=} \frac{E^2}{R^*} = \frac{M_2 \Delta_2}{\Delta} = \frac{-GH}{1 + \overline{GH}^*} \quad (81)$$

$$M^3 \stackrel{d.}{=} \frac{E^3}{R} = \frac{M_3 \Delta_3}{\Delta} = \frac{1 + \overline{GH}^*}{1 + \overline{GH}^*} = 1 \quad (82)$$

Solving Equations (81) and (82) for E^2 and E^3 , respectively, and using the relationship,

$$E = E^2 + E^3, \quad (83)$$

one obtains

$$E = R - \frac{GH}{1 + \overline{GH}^*} R^* \quad (84)$$

In this elementary example, it is seen that the SFG's and algebraic relationships are identical to those obtained with the modified SFG method of Section 3. Such will not be the case with Example 2.

EXAMPLE NO. 2

See Section 2 and Figure 2 for the description of the digital control system. It is desired to find C and C^* in terms of system input R and the system transfer functions.

STEP NO. 1. EQUIVALENT SFG

This may be drawn directly from the system equations summarized in column 1 of Table 2. It is shown as Figure 6.

STEP NO. 2. SAMPLED SFG

Write system equations, applying Mason's Gain Rule to SFG of Figure 6. There is one path from R to E ($k = 1$), one path from R to Y ($k = 2$), and one path from R to C ($k = 3$). There is one path from E* to Y ($k = 4$), one path to C ($k = 5$), and one path to E.

Using the techniques that are by now well established in this report,

$$M_1 = 1, \quad (85)$$

$$M_2 = 1, \quad (86)$$

$$M_3 = G_2, \quad (87)$$

$$M_4 = D^*G_1, \quad (88)$$

$$M_5 = D^*G_1 G_2, \quad (89)$$

$$M_6 = -D^*G_1 G_2, \quad (90)$$

$$K_1 = -G_2, \quad (91)$$

$$\Delta = 1 - K_1 = 1 + G_2, \quad (92)$$

$$\Delta_k = 1, \quad (93)$$

$$M^1 \triangleq \frac{E^1}{R} = \frac{M_1 \Delta_1}{\Delta} = \frac{1}{1 + G_2}, \quad (94)$$

$$M^2 \triangleq \frac{Y^1}{R} = \frac{M_2 \Delta_2}{\Delta} = \frac{1}{1 + G_2}, \quad (95)$$

$$M^3 \triangleq \frac{C^1}{R} = \frac{M_3 \Delta_3}{\Delta} = \frac{G_2}{1 + G_2}, \quad (96)$$

$$M^4 \triangleq \frac{Y^2}{E^*} = \frac{M_4 \Delta_4}{\Delta} = \frac{D^*G_1}{1 + G_2}, \quad (97)$$

$$M^5 \triangleq \frac{C^2}{E^*} = \frac{M_5 \Delta_5}{\Delta} = \frac{D^* G_1 G_2}{1 + G_2}, \quad (98)$$

$$M^6 \triangleq \frac{E^2}{E^*} = \frac{M_6 \Delta_6}{\Delta} = \frac{-D^* G_2 G_2}{1 + G_2}. \quad (99)$$

One solves Equations (94) and (99) for E^1 and E^2 , respectively, and using the expression,

$$E = E^1 + E^2, \quad (100)$$

one obtains E:

$$\begin{aligned} E &= M^1 R + M^6 E^* \\ &= \frac{R}{1 + G_2} - \frac{D^* G_1 G_2}{1 + G_2} E^* \\ &= R_2 - D^* G_3 E^*. \end{aligned} \quad (101)$$

One solves Equations (95) and (97) for Y^1 and Y^2 , and using the expression,

$$Y = Y^1 + Y^2, \quad (102)$$

one obtains Y:

$$\begin{aligned} Y &= M^2 R + M^4 E^* \\ &= R_2 + \frac{D^* G_1}{1 + G_2} E^*. \end{aligned} \quad (103)$$

C^1 Similarly, one solves Equations (96) and (99) for C^1 and C^2 , and using the expression,

$$C = C^1 + C^2, \quad (104)$$

one obtains C:

$$\begin{aligned} C &= M^3 R + M^5 E^* \\ &= \frac{G_2 R}{1 + G_2} + \frac{D^* G_1 G_2}{1 + G_2} E^* \\ &= R_1 + D^* G_3 E^*. \end{aligned} \quad (105)$$

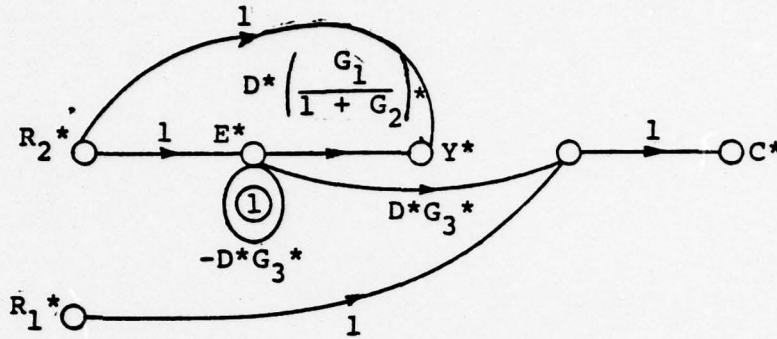
Take the pulse transforms of each side of the Equations (101), (103), and (105).

$$E^* = R_2^* - D^* G_3 E^* \quad (106)$$

$$Y^* = R_2^* + \left(\frac{G_1}{1 + G_2} \right)^* D^* E^* \quad (107)$$

$$\begin{aligned} C^* &= \left(\frac{G_2 R}{1 + G_2} \right)^* + \left(\frac{G_1 G_2}{1 + G_2} \right)^* D^* E^* \\ &= R_1^* + G_3^* D^* E^* \end{aligned} \quad (108)$$

Draw the sampled SFG from the pulsed Equations (106) through (108) (Figure 9). Note this is not the same as the sampled SFG that resulted from using the modified SFG method of Section 3. However, the final answers—the desired responses—will be the same, as will be seen in the sequel.



Note: Encircled numbers refer to identification of loops.

Figure 9. Sampled SFG for Example No. 2 (standard SFG method).

STEP NO. 3.

Obtain C^* from the sampled SFG (Figure 9), using Mason's Gain Rule. There are two inputs: R_1^* and R_2^* . They have two forward paths to C^* ; $k = 1$ and $k = 2$, respectively. Again using techniques that have been well established in this report:

$$M_1 = 1, \quad (109)$$

$$M_2 = D^*G_3^*, \quad (110)$$

$$K_1 = -D^*G_3^*, \quad (111)$$

$$\Delta = 1 - K_1 = 1 + D^*G_3^*, \quad (112)$$

$$\Delta_1 = \Delta, \quad (113)$$

$$\Delta_1 = 1, \quad (114)$$

$$M^1 \stackrel{d}{=} \frac{C^1}{R_1^*} = \frac{M_1 \Delta_1}{\Delta} = 1, \quad (115)$$

$$M^2 \stackrel{d}{=} \frac{C^2}{R_2^*} = \frac{M_2 \Delta_2}{\Delta} = \frac{D^*G_3^*}{1 + D^*G_3^*}. \quad (116)$$

One solves Equations (115) and (116) for C^{1*} and C^{2*} , respectively. Using the expression,

$$C^* = C^{1*} + C^{2*}, \quad (117)$$

one obtains C^* :

$$C^* = M^1 R_1^* + M^2 R_2^*. \quad (118)$$

Equation (118) may be manipulated into the same form as Equations (25) and (45), if desired, by substituting the expression [resulting from Equation (28)],

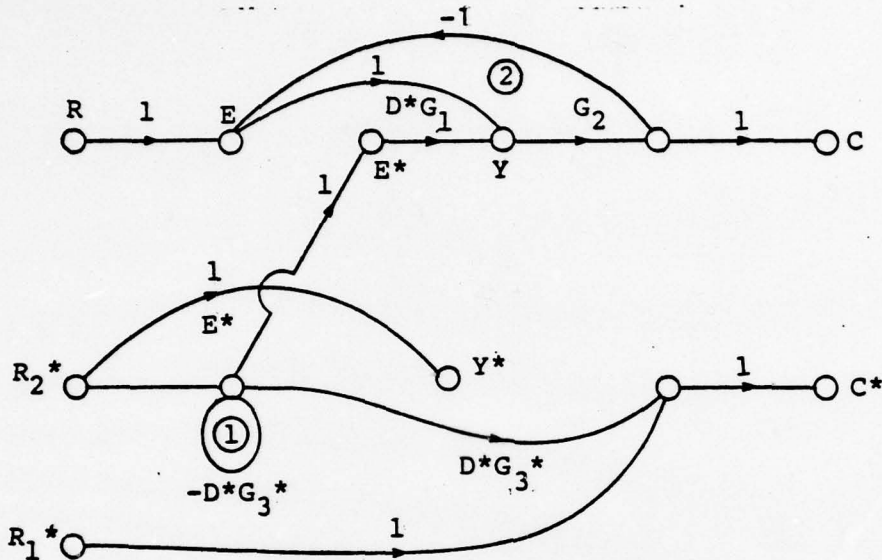
$$R^* - R_1^* = R_2^* \quad (119)$$

into Equation (118):

$$\begin{aligned} C^* &= R_1^* + \frac{D^* G_3^*}{1 + D^* G_3^*} R_2^* \\ &= \frac{R_1^* (1 + D^* G_3^*) + D^* G_3^* (R^* - R_1^*)}{1 + D^* G_3^*} \\ &= \frac{R_1^* + D^* G_3^* R^*}{1 + D^* G_3^*}. \end{aligned} \quad (120)$$

STEP NO. 4. OBTAIN C

Connect the SFG's of Figures 6 and 9 to obtain a composite SFG (Figure 10).



Note: Encircled numbers refer to identification of loops.

Figure 10. Composite SFG for Example No. 2
(standard SFG method).

Apply Mason's Gain Rule to Figure 10 to obtain C. There are three inputs to the composite system: R, R_1^* , and R_2^* . There is one forward path from R to C ($k = 1$), no forward paths from R_1^* , and one from R_2^* ($k = 2$).

$$M_1 = G_2 \quad (121)$$

$$M_2 = D^*G_1G_2 \quad (122)$$

There are now two loops (see Figure 10): (123)

$$K_1 = -D^*G_3^*,$$

$$K_2 = -G_2,$$

$$\begin{aligned} \Delta &= 1 - (K_1 + K_2) + K_1K_2 \\ &= 1 - (-D^*G_3^* - G_2) + (-D^*G_3^*)(-G_2) \\ &= 1 + D^*G_3^* + G_2 + G_2G_3^*D^* \\ &= (1 + D^*G_3^*)(1 + G_2), \end{aligned} \quad (125)$$

$$\Delta_1 = 1 - K_1 = 1 + D^*G_3^*, \quad (126)$$

$$\Delta_2 = 1, \quad (127)$$

$$M^1 \triangleq \frac{C^1}{R} = \frac{M_1 \Delta_1}{\Delta} = \frac{G_2(1 + D^*G_3^*)}{(1 + D^*G_3^*)(1 + G_2)} = \frac{G_2}{1 + G_2}, \quad (128)$$

$$\begin{aligned} M^2 \triangleq \frac{C^2}{R_2^*} &= \frac{M_2 \Delta_2}{\Delta} \\ &= \frac{D^*G_1 G_2}{(1 + D^*G_3^*)(1 + G_2)}. \end{aligned} \quad (129)$$

Using the expression,

$$C = C^1 + C^2, \quad (130)$$

and solving Equations (128) and (129) for C^1 and C^2 , respectively, one may obtain

$$\begin{aligned} C &= \frac{G_2 R}{1 + G_2} + \frac{D^*G_1 G_2 R_2^*}{(1 + D^*G_3^*)(1 + G_2)} \\ &= R_1 + \frac{G_3 D^* R_2^*}{1 + D^*G_3^*}. \end{aligned} \quad (131)$$

It is noted that the values of C^* and C just obtained are the same as those obtained using the SAM and modified SFG techniques.

5. APPLICATION TO Z- AND MODIFIED Z-TRANSFORMS

In the SAM and SFG techniques for obtaining sampled-data outputs of a system, that form has been indicated as C^* or $C^*(s)$. The z-transform of $C^*(s)$ is merely written as $C(z)$. Hence, anywhere an expression $C^*(s)$ is found, it may be replaced by $C(z)$ if it is desired to work in the z-domain rather than the s-domain.

If it is desired to find an output expression in modified z-transform, that is denoted by the symbol $C(z,m)$. This form may readily be obtained from the expression for a sampled output, such as C^* or $C^*(s)$, by noting that such outputs appear to be equal to the product of an unstarred quantity and a starred quantity. Let $A(s)$ represent the unstarred quantity, and let $B^*(s)$ represent the starred quantity. Then variable $C^*(s)$ may be written as

$$C^* = C^*(s) = A(s) B^*(s). \quad (132)$$

If one recognizes that $A(s)$ or $B^*(s)$ may be equal to unity, Equation (132) will always hold.

The modified z-transform may always be obtained from Equation (132) by performing the following transformation:

$$C(z,m) = A(z,m) B(z), \quad (133)$$

where $A(z,m)$ represents the modified z-transform of the quantity $A(s)$, and $B(z)$ represents the ordinary z-transform of the quantity $B(s)$. This technique appears to be an attractive alternative to obtaining modified z-transforms through SFG techniques (which may of course be done).

6. COMPARISON OF METHODS

The Systematic Analysis Method (SAM) can be used to determine the states of a digital system in terms of that system's transfer functions and the inputs to the system. This can also be done by the application of other methods, such as SFG techniques. The usual advertised advantages of the latter, when they are compared to block diagram or algebraic manipulation, is that they are particularly amenable to the analysis of complicated systems.

It has been demonstrated in this report that SAM can handle digital system analysis as capably as can SFG methods. It has the advantage of not requiring the cumbersome Mason's Gain Rule. Hence, it avoids the oft-committed errors associated with SFG analysis, such as overlooked closed loops, nonobvious forward paths, etc. As with SFG's, a block diagram is not needed; the system equations are sufficient. Finally, it has been shown that SAM is easy to implement. It appears to take less lengthy analytical manipulation.

If the analyst prefers using SFG's to either block diagrams or algebraic manipulation, a modified SFG technique based on SAM techniques is proposed. As such, it is systematic. While the SFG's produced by this technique are usually different from those produced by standard SFG techniques, they yield the same results. Mason's Gain Rule is only applied at one stage of the analysis in the modified SFG technique, as opposed to the standard SFG technique which requires several applications of Mason's Gain Rule.

7. CONCLUSIONS

An alternative to the Signal Flow Graph technique has been presented and compared to a standard and a modified SFG. The alternative, termed Systematic Analytical Method or SAM, is claimed herein to be simpler and more straightforward to implement than the SFG methods. Not only does it appear to be quicker to use in system analysis, but it obviates the cumbersome use of Mason's Gain Rule.

For the analyst who desires to use SFG techniques, a modified SFG technique is presented. It is systematic and reduces the number of required applications of Mason's Gain Rule.

APPENDIX A - REVIEW OF MASON'S GAIN RULE

M: The gain (transfer function) between two nodes on a Signal Flow Graph (SFG).

k: The number of forward paths leading from all system inputs to a particular selected output.

M_k : The gain along the k^{th} forward path.

$$\begin{aligned} \Delta_1 &= \sum (\text{all individual loop gains}) \\ &+ \sum (\text{gain products of all possible combinations of two nontouching loops}) \\ &- \sum (\text{gain products of all possible combinations of three nontouching loops}) \\ &+ \dots \end{aligned}$$

Δ_k = Value of Δ for that part of the graph not touching the k^{th} forward path.

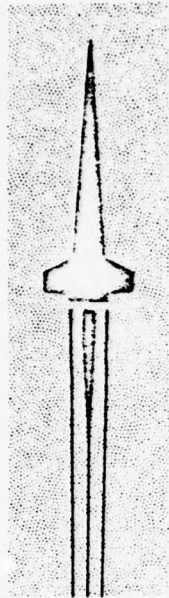
$$M = \sum_k \frac{M_k \Delta_k}{\Delta} .$$

DISTRIBUTION

	No. of Copies
Defense Documentation Center Cameron Station Alexandria, Virginia 22314	12
IIT Research Institute ATTN: GACIAC 10 West 35th Street Chicago, Illinois 60616	1
US Army Materiel Systems Analysis Activity ATTN: DRXSY-MP Aberdeen Proving Ground, Maryland 21005	1
Commander US Army Missile Research and Development Command ATTN: DRSMI-LP, Mr. Voigt DRDMI-T, Dr. Kobler	1
-TBD	1
-TI (Reference Copy)	3
-TI (Record Set)	1
-E, Director	1
-X, Technical Director	1
-TR, Director	1
Redstone Arsenal, Alabama 35809	
Control Dynamics Company 701 Corlett Drive Suite 2 ATTN: S. M. Seltzer Huntsville, Alabama 35802	30
Commander US Army Research Office ATTN: DRXRQ-PH, Dr. R. Lontz P.O. Box 12211 Research Triangle Park, North Carolina 27709	5
US Army Research and Standardization Group (Europe) ATTN: DRXSN-E-RX, Dr. Alfred K. Medoluha Box 65 FPO New York 90510	1

	No. of Copies
Commander US Army Materiel Development and Readiness Command ATTN: Dr. James Bender Dr. Gordon Bushy 5001 Eisenhower Avenue Alexandria, Virginia 22333	 1 1
Headquarters Department of the Army Office of the DCS for Research, Development and Acquisition ATTN: DAMA-ARZ Room 3A474, The Pentagon Washington, DC 20310	 1
OUSDR&E ATTN: Mr. Leonard R. Weishberg Room 3D1079, The Pentagon Washington, DC 20301	 1
Director Defense Advanced Research Projects Agency 1400 Wilson Boulevard Arlington, Virginia 22209	 1
OUSDR&E ATTN: Dr. G. Garota Deputy Asst. for Research (Research in Advanced Technology) Room 301067, The Pentagon Washington, DC 20301	 1

APPENDIX B. DETERMINATION OF DIGITAL CONTROL SYSTEM RESPONSE BY
CROSS-MULTIPLICATION



**U. S. ARMY
MISSILE
RESEARCH
AND
DEVELOPMENT
COMMAND**



Redstone Arsenal, Alabama 35809

TECHNICAL REPORT T-79-58

**DETERMINATION OF DIGITAL CONTROL
SYSTEM RESPONSE BY
CROSS-MULTIPLICATION**

S.M. Seltzer
Guidance and Control Directorate
US Army Missile Research and Development Command
Redstone Arsenal, Alabama 35809

29 May 1979

Approved for Public Release; Distribution Unlimited.

Unclassified

SECURITY CLASSIFICATION OF THIS PAGE (When Data Entered)

REPORT DOCUMENTATION PAGE		READ INSTRUCTIONS BEFORE COMPLETING FORM
1. REPORT NUMBER TR-T-79-58	2. GOVT ACCESSION NO.	3. RECIPIENT'S CATALOG NUMBER
4. TITLE (and Subtitle) Determination of Digital Control System Response By Cross-Multiplication		5. TYPE OF REPORT & PERIOD COVERED Technical Report
		6. PERFORMING ORG. REPORT NUMBER
7. AUTHOR(s) S.M. Seltzer		8. CONTRACT OR GRANT NUMBER(s)
9. PERFORMING ORGANIZATION NAME AND ADDRESS Commander US Army Missile Research and Development Command ATTN: DRDMI-TG Redstone Arsenal, Alabama 35809		10. PROGRAM ELEMENT, PROJECT, TASK AREA & WORK UNIT NUMBERS
11. CONTROLLING OFFICE NAME AND ADDRESS Commander US Army Missile Research and Development Command ATTN: DRDMI-TI Redstone Arsenal, Alabama 35809		12. REPORT DATE 29 May 1979
		13. NUMBER OF PAGES 23
14. MONITORING AGENCY NAME & ADDRESS (if different from Controlling Office)		15. SECURITY CLASS. (of this report) Unclassified
		15a. DECLASSIFICATION/DOWNGRADING SCHEDULE
16. DISTRIBUTION STATEMENT (of this Report) Approved for public release; distribution unlimited.		
17. DISTRIBUTION STATEMENT (of the abstract entered in Block 20, if different from Report)		
18. SUPPLEMENTARY NOTES		
19. KEY WORDS (Continue on reverse side if necessary and identify by block number)		
20. ABSTRACT (Continue on reverse side if necessary and identify by block number) This report describes the Cross-Multiplication technique for obtaining the response of a digital control system from its closed-loop transfer function. When the latter is expressed in the complex z-domain, the response is obtained at the sampling instants. If it is desired to know the response between the sampling instants, the submultiple method may be adapted to the cross-multiplication technique. When the transfer function is expressed in the modified z-transform domain, the response is obtained at any point within each sampling instant. The three approaches are described and applied to an example.		

Unclassified

DISPOSITION INSTRUCTIONS

DESTROY THIS REPORT WHEN IT IS NO LONGER NEEDED. DO NOT RETURN IT TO THE ORIGINATOR.

DISCLAIMER

THE FINDINGS IN THIS REPORT ARE NOT TO BE CONSTRUED AS AN OFFICIAL DEPARTMENT OF THE ARMY POSITION UNLESS SO DESIGNATED BY OTHER AUTHORIZED DOCUMENTS.

TRADE NAMES

USE OF TRADE NAMES OR MANUFACTURERS IN THIS REPORT DOES NOT CONSTITUTE AN OFFICIAL ENDORSEMENT OR APPROVAL OF THE USE OF SUCH COMMERCIAL HARDWARE OR SOFTWARE.

CONTENTS

Section	Page
1. Introduction	3
2. Response at Sampling Instants	3
3. Response Between Sampling Instants Using the Submultiple Method	8
4. Response Between Sampling Instants Using the Modified Z-Transform Method ..	14
5. Conclusions	20

1. INTRODUCTION

This report describes a technique for obtaining the response of a digital control system. It is assumed that the closed-loop transfer function is available in the z- or, modified z-transform domain. The numerator and denominator of each side of the transfer function are cross-multiplied. The Real Translation Theorem is then applied to the result, yielding a difference equation in the time-domain. ¹This may be solved for the system response in terms of the reference (or other) input(s) to the system as well as in terms of system state initial conditions.

Two different modifications to the basic technique are described / one using the submultiple method and one using the modified z-transform technique. These are applied when it is desired to determine intra-sampling responses of the system. All three techniques are applied to a single example. A summary of the techniques and their application is provided at the conclusion of the report.

2. RESPONSE AT SAMPLING INSTANTS

It is assumed that a given digital or sampled-data system can be described by a closed-loop transfer function that relates the controlled output of the system to the reference input. If there is more than one input, the technique can also be applied to the resulting sum of closed-loop transfer functions relating the controlled output to each of the inputs. Although the report refers only to a single controlled output, the technique can be applied to find any system state if it is related to the inputs to the system in the z-domain. These relationships may be derived by using any of the standard techniques (such as signal flow graphs) or by the newly developed SAM (Systematic Analytical Method) technique².

It is assumed that the state whose response is desired is denoted in the z-domain as $C(z)$, where

$$C(z) \stackrel{d}{=} z \{c(t)\} . \quad (1)$$

-
1. B.C. Kuo, *Analysis and Synthesis of Sampled-Data Control Systems*, Prentice-Hall, New Jersey, 1963.
 2. S.M. Seltzer, *S.A.M: An Alternative to Sampled-Data Signal Flow Graphs*, US Army Missile Research and Development Command, Redstone Arsenal, Alabama, Technical Report T-79-49, May 1979.

The script z denotes the operation of taking the z -transform further assume that there is only one input into the system: $R(z)$, where

$$R(z) \stackrel{\text{d.}}{=} z \{r(t)\} . \quad (2)$$

The relationship between $C(z)$ and $R(z)$ usually can be expressed as a closed-loop transfer function (or several such transfer functions) which is a ratio of two polynomials in z , i.e.,

$$\frac{C(z)}{R(z)} = \frac{\sum_{j=0}^M a_j z^j}{\sum_{k=0}^N b_k z^k} , \quad (3)$$

where coefficients a_j and b_k represent the system parameters. The procedure for finding the response at sampling instants — by the cross-multiplication method — consists of three steps: Step 1. Cross-multiply the numerators with the denominators of Equation (3), yielding the expression,

$$\sum_{k=0}^N b_k z^k C(z) = \sum_{j=0}^M a_j z^j R(z) \quad (4a)$$

$$\begin{aligned} & b_0 C(z) + b_1 z C(z) + \dots + b_k z^k C(z) + \dots + b_N z^N C(z) \\ & = a_0 R(z) + a_1 z R(z) + \dots + a_j z^j R(z) + \dots + a_M z^M R(z) . \end{aligned} \quad (4b)$$

AD-A074 782

CONTROL DYNAMICS CO HUNTSVILLE AL*
APPLICATION OF DISCRETE GUIDANCE AND CONTROL THEORY.(U)
AUG 79 S M SELTZER
CDC-79-2

F/G 17/7

DAAK40-78-C-0226

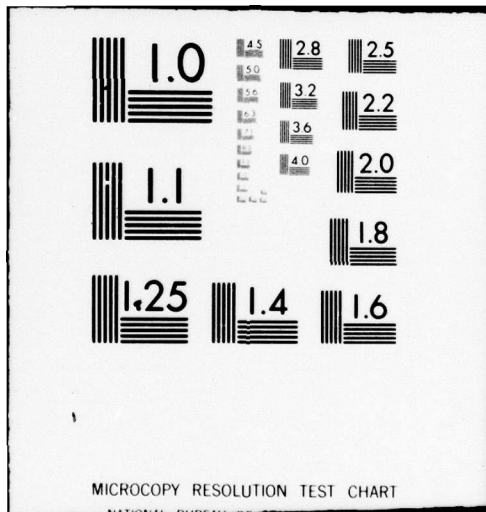
NL

UNCLASSIFIED

2 of 3

ADA
074782





Step 2. Each side of Equation (4a) or (4b) is divided by $b_N z^N$. The resulting equation is then solved for the $C(z)$ term that is not multiplied by a non-zero power of z , Equation i.e.,

$$\begin{aligned}
 C(z) = & \frac{a_0}{b_N} z^{-N} R(z) + \frac{a_1}{b_N} z^{1-N} R(z) + \dots + \frac{a_j}{b_N} z^{j-N} R(z) + \dots \\
 & + \frac{a_M}{b_N} z^{M-N} R(z) - \frac{b_0}{b_N} z^{-N} C(z) - \frac{b_1}{b_N} z^{1-N} C(z) - \dots \\
 & - \frac{b_k}{b_N} z^{k-N} C(z) - \dots - \frac{b_{N-1}}{b_N} z^{-1} C(z) . \quad (5)
 \end{aligned}$$

Step 3. Apply the Real Translation Theorem to Equation (5), recalling that

$$\mathcal{Z}^{-1} \{C(z)\} = c^*(t) \triangleq \sum_{n=0}^{\infty} c(nT) \delta(t-nT) \quad (6a)$$

and

$$\mathcal{Z}\{c(t-kT)\} = z^{-k} C(z). \quad (6b)$$

The asterisk is used to indicate a variable that has been sampled, and $\delta(t-nT)$ denotes a Dirac function occurring at the instant $t=nT$. The resulting value of $c(nT)$ at each sampling instant, nT , then becomes

$$\begin{aligned}
 c(nT) = & \frac{a_0}{b_N} r[(n-N)T] + \frac{a_1}{b_N} r[(n-N+1)T] + \dots \\
 & + \frac{a_j}{b_N} r[(n-N+j)T] + \dots + \frac{a_M}{b_N} r[(n-N+M)T] \\
 & - \frac{b_0}{b_N} c[(n-N)T] - \frac{b_1}{b_N} c[(n-N+1)T] - \dots \\
 & - \frac{b_k}{b_N} c[(n-N+k)T] - \dots + \frac{b_{n-1}}{b_N} c[(n-1)T], \quad (7)
 \end{aligned}$$

where $j, k, M, N,$ and n are integers.

The advantages of the form of Equation (7) are three-fold:

- The value of $c(nT)$, for any $t=nT$, may be obtained for any form of $r(t)$, whether or not it is "z-transformable."
- The expression for $c(nT)$ does not have to be recalculated every time the form of $r(t)$ changes, as is the case when the response is determined by the partial fraction, power series, or inversion formula methods¹.
- The form of the expression for $c(nT)$ permits the inclusion of initial conditions, such as $c(0)$, if they exist.

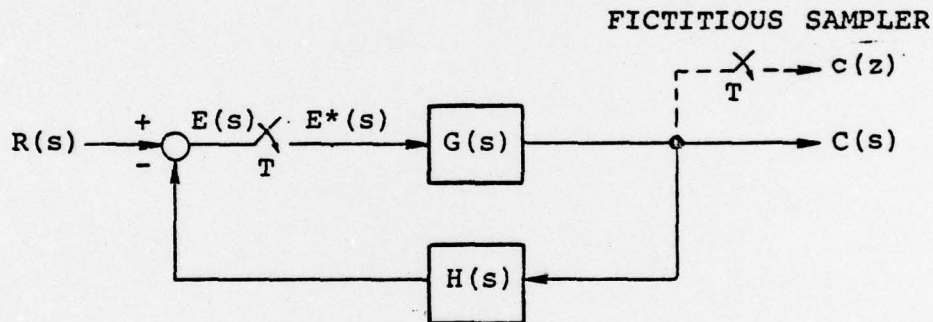


Figure 1. Closed-loop sampled-data system.

Example 1. Given the closed-loop sampled-data system of Figure 1,¹ the closed-loop transfer function easily is found to be:

$$\frac{C(z)}{R(z)} = \frac{G(z)}{1 + HG(z)} \quad (8)$$

If $G(s)$ and $H(s)$ are given to be

$$G(s) = 1/s(s + 1)$$

and

$$H(s) = 1, \quad (9)$$

respectively, their z-transforms are

$$G(z) = \frac{z(1 - e^{-T})}{(z-1)(z - e^{-T})} \quad (10)$$

and

$$HG(z) = G(z) \quad (11)$$

If one substitutes the expressions of Equations (10) and (11) into Equation (8), one obtains the closed-loop transfer function,

$$\frac{C(z)}{R(z)} = \frac{(1 - e^{-T})z}{z^2 - 2e^{-T}z + e^{-T}} \quad (12)$$

One may now apply the three steps prescribed for the cross-multiplication procedure, obtaining:

Step 1:

$$z^2C(z) - 2e^{-T}zC(z) + e^{-T}C(z) = (1 - e^{-T})zR(z) \quad (13)$$

Step 2:

$$C(z) = (1 - e^{-T})z^{-1}R(z) + 2e^{-T}z^{-1}C(z) - e^{-T}z^{-2}C(z) \quad (14)$$

Step 3:

$$c(nT) = (1 - e^{-T})r[(n-1)T] + 2e^{-T}c[(n-1)T] - e^{-T}c[(n-2)T] \quad (15)$$

If, as in pp. 145-147 of Kuo's book, $r(t)$ is assumed to be a unit step input, the system is assumed to be initially at rest, and the sampling period T is assumed to be 1 second, application of

Equation (15) readily yields the following values for $c(nT)$:

$c(T) = 0.6321$, the value of $c^*(t)$ at 1 sec.

$c(2T) = 1.0972$ the value of $c^*(t)$ at 2 sec.

$c(3T) = 1.2067$, the value of $c^*(t)$ at 3 sec.

$c(nT) = 0.6321 + 0.736 c[(n-1)T] - 0.368[c(n-2)T]$, the value of $c^*(t)$ at $t = n$ sec.

These values correspond to those obtained by more tedious means in pages 145-147 of Kuo's book.

3. RESPONSE BETWEEN SAMPLING INSTANTS USING THE SUBMULTIPLE METHOD

If it is desired to find the intra-sampling response of the same type digital system described in Section 2, it may be accomplished by applying the submultiple method found in pages 83-86 of Kuo's book. Briefly, let $c\left(\frac{mT}{n}\right)$ represent the value of the response $c(t)$ at the instant, $t = \left(\frac{mT}{n}\right)$, where $n-1$ represents the number of intrasampling responses desired (n is an integer with value greater than unity). If m is an integer, the sampling period within which the submultiples are to be determined is denoted as mT . The z -transform of $c\left(\frac{mT}{n}\right)$ may be found from the ordinary z -transform in the following manner. In essence, $c\left(\frac{mT}{n}\right)$ is the output of a fictitious sampler which samples n times as fast as the real sampler. The z -transform of that output is defined as

$$z \left\{ c\left(\frac{nT}{m}\right) \right\} \stackrel{d}{=} C(z)_n = C(z) \left| \begin{array}{l} z \rightarrow z_n \\ T \rightarrow T_n \end{array} \right. \quad (16)$$

where

$$z_n = z^{1/n} \quad (17a)$$

and

$$T_n = T/n. \quad (17b)$$

Now the closed-loop expression of Equation (3) may be altered to read

$$\frac{C(z)_n}{R(z)} = \frac{\sum_{j=0}^M a_j z_n^j}{\sum_{k=0}^N b_k z_n^k} \quad (18)$$

The submultiple modification to the basic method also consists of three steps.

Step 1. Cross-multiply the numerators and denominators of Equation (18), yielding the expression,

$$\sum_{k=0}^N b_k z_n^k C(z)_n = \sum_{j=0}^M a_j z_n^j R(z) \quad (19a)$$

or

$$\begin{aligned} & b_0 C(z)_n + b_1 z_n C(z)_n + \dots + b_k z_n^k C(z)_n + \dots + b_N z_n^N C(z)_n \\ & = a_0 R(z) + a_1 z_n R(z) + \dots + a_j z_n^j R(z) + \dots + a_M z_n^M R(z). \end{aligned} \quad (19b)$$

Step 2. Each side of Equation (19a) or (19b) is divided by $b_N z_n^N$. The resulting equation is then solved for the $C(z)_n$ term that is not multiplied by a non-zero power of z_n , i.e.,

$$\begin{aligned} C(z)_n &= \frac{a_0}{b_N} z_n^{-N} R(z) + \frac{a_1}{b_N} z_n^{-(N-1)} R(z) + \dots \\ &+ \frac{a_j}{b_N} z_n^{-(N-j)} R(z) + \dots \\ &+ \frac{a_M}{b_N} z_n^{-(N-M)} R(z) - \frac{b_0}{b_N} z_n^{-N} C(z)_n \\ &- \frac{b_1}{b_N} z_n^{-(N-1)} C(z)_n - \dots \\ &- \frac{b_k}{b_N} z_n^{-(N-k)} C(z)_n - \dots - \frac{b_{N-1}}{b_N} z_n^{-1} C(z)_n. \end{aligned} \quad (20)$$

Step 3. Similar to the procedure of Section 2, the value of $c(t)$ at the n^{th} submultiple of the sampling instant mT is:

$$\begin{aligned}
 c\left(\frac{mT}{n}\right) &= \frac{a_0}{b_N} r\left[\frac{(m-N)T}{n}\right] + \frac{a_1}{b_N} r\left[\frac{(m-N+1)T}{n}\right] + \dots \\
 &+ \frac{a_j}{b_N} r\left[\frac{(m-N+j)T}{n}\right] \\
 &+ \dots + \frac{a_n}{b_N} r\left[\frac{(m-N+M)T}{n}\right] - \frac{b_1}{b_N} c\left[\frac{(m-N+1)T}{n}\right] + \dots \\
 &- \frac{b_k}{b_N} c\left[\frac{(m-N+k)T}{n}\right] - \dots - \frac{b_{N-1}}{b_N} c\left[\frac{(m+1)T}{n}\right]. \quad (21)
 \end{aligned}$$

where all values of $r[\cdot]$ are equal to zero except for those values of r at integral multiples of T , i.e.,

$$r(\ell T) = \begin{cases} 0 & \text{not integers} \\ r(t) \Big|_{t=\ell T} & \text{for } \ell = 0, 1, 2, \dots \text{ (integers)} \end{cases} \quad (22)$$

and j, k, M, m, N, n are integers.

Example 2. The same sampled-data system is used in this example as in Example 1. It may be shown, for the example at hand, that

$$C(z)_n = G(z)_n E(z), \quad (23)$$

where $G(z)_n$ is found in the same manner as demonstrated in Equation (16). From Figure 1 it is seen that

$$E(z) = \frac{R(z)}{1 + HG(z)}. \quad (24)$$

Substitution of Equation (24) into Equation (23) leads to

$$\frac{C(z)_n}{R(z)} = \frac{G(z)_n}{1 + HG(z)}. \quad (25)$$

Replacing z by z_n and T by T_n in Equation (10) leads to the expression,

$$G(z)_n = \frac{z_n (1 - e^{-T_n})}{(z_n - 1) (z_n - e^{-T_n})} \quad (26)$$

If one substitutes Equations (17) into Equation (11) and substitutes the resulting equation and Equation (26) into Equation (25), one obtains the closed-loop expression,

$$\frac{C(z)_n}{R(z)} = \frac{z_n (1 - e^{-T_n}) (z - 1) (z - e^{-T})}{(z_n - 1) (z_n - e^{-T_n}) (z_n^{2n} - 2e^{-T} z_n^n + e^{-T})} \quad (27)$$

The denominator of this expression is of course (when equated to zero) the characteristic equation. It may be expanded into the following polynomial in z_n :

$$\begin{aligned} D(z_n) = & z_n^{2n+2} - (1 + e^{-T_n}) z_n^{2n+1} + e^{-T_n} z_n^{2n} \\ & - 2e^{-T} z_n^{n+2} + 2e^{-T} (1 + e^{-T_n}) z_n^{n+1} - 2e^{-(T+T_n)} z_n^n \\ & + e^{-T} z_n^2 - e^{-T} (1 + e^{-T_n}) z_n + e^{-(T+T_n)}. \end{aligned} \quad (28)$$

Similarly, the numerator of Equation (27) may be expressed as the polynomial,

$$N(z_n) = (1 - e^{-T_n}) \left[z_n^{2n+1} - (1 + e^{-T}) z_n^{n+1} + e^{-T} z_n \right]. \quad (29)$$

Step 1. If Equations (28) and (29) are substituted into Equation (27) and the resulting numerators and denominators cross-multiplied, one obtains the equivalent of Equation (19b):

$$\begin{aligned}
 & z_n^{2n+2} C(z)_n - (1 + e^{-Tn}) z_n^{2n+1} C(z)_n + e^{-Tn} z_n^{2n} C(z)_n \\
 & - 2e^{-T} z_n^{n+2} C(z)_n + 2e^{-T} (1 + e^{-Tn}) z_n^{n+1} C(z)_n \\
 & - 2e^{-T+Tn} z_n^n C(z)_n \\
 & + e^{-T} z_n^2 C(z)_n - e^{-T} (1 + e^{-Tn}) z_n C(z)_n + e^{-(T+Tn)} C(z)_n \\
 & = (1 - e^{-Tn}) [z_n^{2n+1} R(z) - (1 + e^{-T}) z_n^{n+1} R(z) \\
 & + e^{-T} z_n R(z)].
 \end{aligned} \tag{30}$$

Step 2. If one applies the procedure of Step 2 to Equation (30) one obtains

$$\begin{aligned}
 C(z)_n &= (1 - e^{-Tn}) [z_n^{-1} R(z) - (1 + e^{-T}) z_n^{-(n+1)} R(z) \\
 & + e^{-T} z_n^{-(2N+1)} R(z)] + (1 + e^{-Tn}) z_n^{-1} C(z)_n \\
 & - e^{-Tn} z_n^{-2} C(z)_n + 2e^{-T} z_n^{-n} C(z)_n \\
 & - 2e^{-T} (1 + e^{-Tn}) z_n^{-(n+1)} C(z)_n + 2e^{-(T+Tn)} z_n \\
 & -(n+2) C(z)_n - e^{-T} z_n^{-2n} C(z)_n \\
 & + e^{-T} (1 + e^{-Tn}) z_n^{-(2n+1)} C(z)_n \\
 & - e^{-(T+Tn)} z_n^{-(2N+2)} C(z)_n.
 \end{aligned} \tag{31}$$

Step 3. Finally, one may apply the procedure of Step 3 to obtain the time-domain difference equation that yields the value of $c^*(t)$ at the instant of time, $t = \frac{mT}{n}$, where m is any desired integer.

$$\begin{aligned}
 c \frac{mT}{n} = & (1 - e^{-Tn}) \left\{ r \left[\frac{(m-1)T}{n} \right] - (1 + e^{-T}) r \left[\frac{(m-n+1)T}{n} \right] \right. \\
 & \left. + e^{-T} r \left[\frac{(m-2n-1)T}{n} \right] \right\} \\
 & + (1 + e^{-Tn}) c \left[\frac{(m-1)T}{n} \right] - e^{-Tn} c \left[\frac{(m-2)T}{n} \right] \\
 & + 2e^{-T} c \left[\frac{(m-n)T}{n} \right] \\
 & - 2e^{-T} (1 + e^{-Tn}) c \left[\frac{(m-n-1)T}{n} \right] + 2e^{-(T+Tn)} c \left[\frac{(m-n-2)T}{n} \right] \\
 & - e^{-T} c \left[\frac{(m-2n)T}{n} \right] + e^{-T} (1 + e^{-Tn}) c \left[\frac{(m-2n-1)T}{n} \right] \\
 & - e^{-(T+Tn)} c \left[\frac{(m-2n-2)T}{n} \right]. \tag{32}
 \end{aligned}$$

Again, as in Kuo's book and in Example 1, it is assumed the system is at rest initially, and the sampling period T is one second. One may desire to know two intra-sampling values of the output $c^*(t)$. In that case, $n = 2 + 1 = 3$. If one substitutes these numerical values into Equation (32), one obtains the equation,

$$\begin{aligned}
 c\left(\frac{m}{3}\right) = & 0.2835r\left(\frac{m-1}{3}\right) - 0.4866 r\left(\frac{m-4}{3}\right) \\
 & + 0.1043r\left(\frac{m-7}{3}\right) + 1.7165 c\left(\frac{m-1}{3}\right) \\
 & - 0.7165c\left(\frac{m-2}{3}\right) + 0.5272c\left(\frac{m-3}{3}\right) - 1.2630c\left(\frac{m-4}{3}\right) \\
 & + 0.5272c\left(\frac{m-5}{3}\right) \\
 & - 0.3679c\left(\frac{m-6}{3}\right) + 0.6315c\left(\frac{m-7}{3}\right) - 0.2636c\left(\frac{m-8}{3}\right). \tag{33}
 \end{aligned}$$

It is worthwhile to pause a moment and consider the power of the difference equation just obtained. First, the output $c\left(\frac{m}{3}\right)$ can be obtained for any deterministic reference input $r(t)$. It only need be specified at the sampling instants. Second, initial conditions or instantaneous changes can be accommodated readily by the equation. Third, difference equations are particularly amenable to programming on desktop calculators or digital computers. These three advantages are not enjoyed by all methods found in the standard textbooks for determining the state(s) of a sampled-data system. The submultiple method does suffer from the drawback of having to specify beforehand the number $n-1$ of the intrasampling instants for which it is desired to know a given state, such as $c(t)$ in this case.

In the case at hand, a brief demonstration of the calculation of $c(t)$ at instants $t=0, T/3, 2T/3, T, \dots$, is provided below. A unit step input is assumed so that the results may be compared to those of Kuo in pages 195-198 of his book. The symbol $c\left(\frac{m}{3}\right)$ denotes the value of $c(t)$ at $t = \left(\frac{m}{3}\right)$ sec.

$$m=0: c(0) = 0$$

$$m=1: c(1/3) = 0.2835 r(0) + 1.7165 c(0) = 0.2835$$

$$m=2: c(2/3) = 0.2835 r(1/3) + 1.7165 c(1/3) = 0.4866$$

$$m=3: c(1) = 0.2835 r(2/3) + 1.7165 c(2/3) - 0.7165 c(1/3) = 0.6321$$

$$m=4: c(4/3) = 0.2835 r(1) - 0.4866 r(0) + 1.7165 c(1) - 0.7165 c(2/3) + 0.5272 c(1/3) = 0.8407$$

$$m=5: c(5/3) = 0.2835 r(4/3) - 0.4866 r(1/3) + 1.7165 c(4/3) - 0.7165 c(1) + 0.5272 c(2/3) - 1.2630 c(1/3) = 0.9901$$

$$m=6: c(2) = 1.0972$$

$$m=7: c(7/3) = 1.1464$$

$$m=8: c(8/3) = 1.1816$$

$$m=9: c(3) = 1.2067$$

4. RESPONSE BETWEEN SAMPLING INSTANTS USING MODIFIED Z-TRANSFORM METHOD

If it is desired to find the intra-sampling response of the same type of digital system described in Section 2, it also may be accomplished by applying the modified z-transform method. In this method it is necessary first to determine the modified z-transform equivalent of the closed-loop transfer function of Equation (3). The reader's mind will be refreshed (as needed).

Let $c(t)$ denote the response of a digital system and $c^*(t)$ its sampled output. The value of $c(t)$ at the instant of time, $t=(n-\Delta)T$, is the value of $c(t)$ that has been delayed by an increment of time ΔT . The latter is represented symbolically as $c(t-\Delta T)$. If the relation,

$$m = 1 - \Delta, \quad 0 \leq m \leq 1, \quad (34)$$

is used, the value of $c(t)$ delayed by an amount ΔT after the sampling instant, $t=nT$, may be denoted as $c[(n-1+m)T]$. The z-transform of $c[(n-1+m)T]$ is termed the modified z-transform (\mathcal{Z}_m) of $c(t)$, i.e.,

$$\begin{aligned} \mathcal{Z}\{c(t-T)\} &= \mathcal{Z}\{c[(n-1+m)T]\} = \\ \mathcal{Z}_m\{c(t)\} &\stackrel{d}{=} C(z, m) = C(z, \Delta) \Big|_{\Delta = 1-m}. \end{aligned} \quad (35)$$

It also may be shown that

$$C(z, m) = z^{-1} \mathcal{Z}\{c(t+mT)\} = z^{-1} \sum_{k=0}^{\infty} c[(m+k)T] z^{-k}. \quad (36)$$

Alternately, $C(z, m)$ may be derived through its complex convolution definition:

$$\begin{aligned} C(z, m) &= \mathcal{Z}\{c(t-\Delta T) * \sigma_T(t)\} \Big|_{z=\ell^{Ts}} \\ &= [\mathcal{Z}\{c(t-\Delta T)\} * \mathcal{Z}\{\sigma_T(t)\}] \Big|_{z=\ell^{Ts}} \\ &= \frac{1}{z\pi i} \int_{c-i\infty}^{c+i\infty} C(\xi) C^{-\Delta T \xi} [1 - e^{-T(s-\xi)}]^{-1} d\xi \Big|_{z=\ell^{Ts}}, \end{aligned} \quad (37)$$

where $\sigma_T(t)$ represents a train of impulses each with a unit area, the star symbol ($*$) denotes the complex convolution operation, \mathcal{Z} denotes the operation of taking the Laplace transform, c denotes the abscissa of convergence (a positive real number), and ξ represents a dummy complex variable.

Equations (35) - (37) represent two methods of determining analytically the modified z-transform (it is recommended that one look it up in a modified z-transform table, if one is

available). The above relationships may also be used to determine the modified z-transform of the transfer function, $G(z, m)$.

For the purpose of exposition, assume the modified z-transform equivalent of the closed-loop transfer function is known and is

$$\frac{C(z, m)}{R(z)} = \frac{\sum_{j=0}^M a_j z^j}{\sum_{k=0}^N b_k z^k}, \quad (38)$$

where a_j and b_j may be functions of m . The cross-multiplication technique is similar to those two previously described.

Step 1. Cross-multiply the numerators and denominators of Equation (38), yielding the expression,

$$\sum_{k=0}^N b_k z^k C(z, m) = \sum_{j=0}^M a_j z^j R(z) \quad (39a)$$

$$\begin{aligned} & b_0 C(z, m) + b_1 z C(z, m) + b_2 z^2 C(z, m) + \dots + b_k z^k C(z, m) \\ & + \dots + b_N z^N C(z, m) = a_0 R(z) + a_1 z R(z) + \dots + a_j z^j R(z) \\ & + \dots + a_M z^M R(z). \end{aligned} \quad (39b)$$

Step 2. Each side of Equation (39a) or (39b) is divided by $b_N z^N$. The resulting equation is then solved for the $C(z, m)$ term that is not multiplied by a non-zero of z , i.e.,

$$\begin{aligned} C(z, m) = & \frac{a_0}{b_N} z^{-N} R(z) + \frac{a_1}{b_N} z^{-(N-1)} R(z) + \dots + \frac{a_j}{b_N} z \\ & -(N-j) R(z) + \dots + \frac{a_M}{b_N} z^{-(N-M)} R(z) - \left[\frac{b_0}{b_N} z^{-N} C(z, m) \right] \end{aligned}$$

$$\begin{aligned}
& + \frac{b_1}{b_N} z^{-(N-1)} C(z, m) + \dots + \frac{b_k}{b_N} z^{-(N-k)} C(z, m) + \dots \\
& + \left. \frac{b_{N-1}}{b_N} z^{-1} C(z, m) \right] \quad (40)
\end{aligned}$$

Step 3. The inverse z-transform of each term of Equation (40) is determined, using the inverse of Equation (39b),

$$\begin{aligned}
C[(n-1)T, m] & \equiv C[(n-1+m)T] = \frac{a_0}{b_N} r[(n-N)T] + \frac{a_1}{b_N} r[(n-N+1)T] + \\
& \dots + \frac{a_j}{b_N} r[(n-N+j)T] + \dots + \frac{a_n}{b_N} r[(n-N+m)T] \\
& - \left\{ \frac{b_0}{b_N} C[(n-1+m-N)T] + \frac{b_1}{b_N} C[(n+m-N)T] + \dots \right. \\
& \left. + \frac{b_k}{b_N} C[(n-1+m-N+k)T] + \dots + \frac{b_{N-1}}{b_N} C[(n-2+m)T] \right\} \quad (41)
\end{aligned}$$

where j, k, m, M, N are integers.

Example 3. Again, the same sampled-data system is used in this example as in Examples 1 and 2. The modified z-transform method will be applied. A fictitious time delay, e^{-1-mT} , is placed following the forward loop gain, $G(s)$, and a fictitious time advance (of the same magnitude as the time delay) is placed just before the feedback loop gain $H(s)$. The closed-loop transfer function that results from these two addition elements being added is

$$\frac{C(z, m)}{R(z)} = \frac{G(z, m)}{1 + HG(z)} \quad (42)$$

Using Equation (9) for $G(s)$, one may obtain $G(z, m)$:

$$\begin{aligned}
G(z, m) & = \mathcal{Z}_m \{G(s)\} = \mathcal{Z}_m \left\{ \frac{1}{s(s+1)} \right\} \quad (43) \\
& = \frac{(1-e^{-mT})z + (e^{-mT}-e^{-T})}{(z-1)(z-e^{-T})}
\end{aligned}$$

The value for $HG(z)$ is given in Equation (9) - (10) which, with Equation (43), may be substituted into Equation (42) to yield

$$\begin{aligned} \frac{C(z, m)}{R(z)} &= \frac{(1-e^{-mT})z + (e^{-mT}-e^{-T})}{(z-2)(z-e^{-T}) \left[1 + \frac{(1-e^{-T})z}{(z-1)(z-e^{-T})} \right]} \\ &= \frac{(1-e^{-mT})z + (e^{-mT}-e^{-T})}{z^2 - 2e^{-T}z + e^{-T}}. \end{aligned} \quad (44)$$

It may be observed that Equation (44) is in the same form as Equation (38). Hence the operations denoted as Steps 1, 2, and 3 (above) may be applied.

Step 1. The numerators and denominators of Equation (44) are cross-multiplied, yielding

$$\begin{aligned} z^2 C(z, m) - 2e^{-T} z C(z, m) + e^{-T} C(z, m) \\ = (1-e^{-mT})z R(z) + (e^{-mT}-e^{-T})z^{-2}R(z). \end{aligned} \quad (45)$$

Step 2. Each term of Equation (45) is divided by z^2 , and the resulting equation is rearranged to solve for $C(z, m)$:

$$\begin{aligned} C(z, m) &= (1-e^{-mT})z^{-1}R(z) + (e^{-mT}-e^{-T})z^{-2}R(z) \\ &+ 2e^{-T}z^{-1}C(z, m) - e^{-T}z^{-2}C(z, m). \end{aligned} \quad (46)$$

Step 3. Equation (46) is now transformed into the time domain, resulting in the following difference equation:

$$\begin{aligned} c[(n-1+m)T] &= (1-e^{-mT}) r[(n-1)T] + (e^{-mT}-e^{-T}) r[(m-2)T] \\ &+ 2e^{-T} c[(n-2+m)T] - e^{-T} c[(n-3+m)T]. \end{aligned} \quad (47)$$

During the n^{th} sampling period, i.e., $(n-1)T \leq t \leq nT$, where n is an integer, one lets m assume values between zero and one to find the intrasampling values of $c(t)$. For instance if it is desired to verify the values obtained in Example 2, let $m=1/3$ and $2/3$ and vary the integer n incrementally, starting at $n=0$. Again, for simplicity, let $T = 1$ second

$$n = 0: \quad c(m-1) = 0$$

$$n = 1: \quad c(m) = (1-e^{-m}) r(0) = 1-e^{-m}$$

$$m = 0 \text{ (check case): } c(0) = 0$$

$$m = 1/3: c(1/3) = 1 - 0.7165 = 0.2835$$

$$m = 2/3: c(2/3) = 0.4866$$

$$m = 1: c(1) = 0.6321$$

$$n = 2: \quad c(1+m) = (1-e^{-m}) r(1) + (e^{-m}-e^{-1}) r(0)$$

$$+ 2e^{-1} c(m)$$

$$m = 0 \text{ (check case): } c(1) = 0.6321$$

$$m = 1/3: c(4/3) = (1-e^{-1/3}) + (e^{-1/3}-e^{-1})$$

$$+ 2e^{-1} c(1/3)$$

$$= 0.8407$$

$$m = 2/3: c(5/3) = (1-e^{-2/3}) + (e^{-2/3}-e^{-1})$$

$$+ 2e^{-1} c(2/3)$$

$$= 0.9901$$

$$m = 1: c(2) = (1-e^{-1}) + (e^{-1}-e^{-1}) + 2e^{-1}$$

$$c(1) = 1.0972$$

$$n = 3: c(2+m) = (1-e^{-m}) r(2) + (e^{-m}-e^{-1}) r(1) \\ + 2e^{-1} c(1+m) - e^{-1} c(m)$$

$$m = 0 \text{ (check case): } c(2) = (1-e^{-0}) \\ + (e^{-0}-e^{-1}) \\ + 2e^{-1} c(1) - e^{-1} c(0) \\ = 1.0972$$

$$m = 1/3: c(7/3) = 1-e^{-1/3} + e^{-1/3}-e^{-1} \\ + 2e^{-1} c(4/3) - e^{-1} c(1/3) \\ = 1.1464$$

$$m = 2/3: c(8/3) = 1-e^{-2/3} + e^{-2/3}-e^{-1} \\ + 2e^{-1} c(5/3) - e^{-1} c(2/3) \\ = 1.1816$$

$$m = 1: c(3) = 1-e^{-1} + e^{-1}-e^{-1} + 2e^{-1} c(2) \\ - e^{-1} c(1) \\ = 1.2067$$

etc.

5. CONCLUSIONS

Several analytical techniques for obtaining the response of a digital control system have been described. They are based on a single principle: cross-multiplication followed by applications of the real translation theorems. Each is applied to a single example. As a starting point for application of each of the techniques, it is required that the dynamics of the digital control system be described in the z- or modified z-domain.

The advantages of the three techniques over extant classical methods are:

- The response may be obtained for any deterministic reference input into the system as long as its value is known at the sampling instants. It need not be described by a differential equation, and the z-transform for a specific reference input need not be determined before obtaining an expression for the response.
- Initial conditions and instantaneous changes can be accommodated readily by the equations obtained through use of the cross-multiplication methods.
- The difference equations obtained are particularly amenable to programming on a desktop calculator or digital computer.
- A detailed knowledge of the theory underlying digital or sampled-data control systems is not required (although it certainly is helpful) by the analyst in order to apply the recipes described herein.

DISTRIBUTION

	No. of Copies		No. of Copies
Commander Defense Documentation Center ATTN: DDC-TCA Cameron Station Alexandria, Virginia 22314	12	Headquarter, Department of the Army, Office of the DSC for Research, Development and Acquisition ATTN: DAMA-ARZ Room 3A474, The Pentagon Washington, DC 20310	1
Commander US Army Missile Research and Development Command Redstone Arsenal, Alabama 35809 ATTN: DRDMI-X, Technical Director	1	OUSTR&E ATTN: Mr. Leonard R. Weisberg Room 3D1079, The Pentagon Washington, DC 20301	1
-T, Director	1		
-E, Director	1	Director	
-TR, Director	1	Defense Advanced Research	
-TBD	1	Projects Agency	
-TI (Reference copy)	1	1400 Wilson Boulevard	
-TI (Record Set)	1	Arlington, Virginia 22209	1
DRSMI-LP, Mr. Voigt	1		
Commander US Army Research Office ATTN: DRXRQ-PH, Dr. R. Lontz P.O. Box 12211 Research Triangle Park, North Carolina 27709	5	OUSTR&E ATTN: Dr. G. Gamota Deputy Associate for Research (Research in Advanced Technology) Room 3D1057, The Pentagon Washington, DC 20301	1
US Army Research and Standardization Group (Europe) ATTN: DRXSN-E-RX, Dr. Alfred K. Medoloha Box 65 FPO New York 90510	1	US Army Materiel Systems Analysis Activity ATTN: DRXSY-MP Aberdeen Proving Ground, Maryland 21005	2
Commander US Army Material Development and Readiness Command ATTN: Dr. James Bender Dr. Gordon Bushy 5001 Eisenhower Avenue Alexandria, Virginia 22333	1	IIT Research Institute ATTN: GACIAC 10 West 35th Street Chicago, Illinois 60616	1
	1	Control Dynamics Company ATTN: S.M. Seltzer 701 Corlett Drive, Suite 2 Huntsville, Alabama 35802	30

APPENDIX C. SAMPLED-DATA ANALYSIS IN PARAMETER SPACE

TECHNICAL REPORT TR-79-64

SAMPLED-DATA ANALYSIS ~~IN THE~~ ^l PARAMETER ~~PERIOD~~ ^{SPACE} *e*

S.M. Seltzer
Guidance and Control Directorate
US Army Missile Research and Development Command
Redstone Arsenal, AL 35899.

June 1979

ABSTRACT

This report describes a technique for determining the stability and dynamic characteristics of a digital control system in terms of several selected system parameters. The method requires that the system characteristic equation be available in the z -domain. An example is provided to further elucidate the technique.

It is this capability that makes the method more powerful than most design techniques (which describe stability in terms of only one variable parameter K or gain).

CONTENTS

	Page
SECTION I. INTRODUCTION	4
SECTION II. ANALYTICAL PRELIMINARIES	7
SECTION III. STABILITY DETERMINATION	9
SECTION IV. SYSTEM DYNAMICS	13
SECTION V. <i>EXAMPLE</i>	15
SECTION VI. CONCLUSIONS	23
SECTION VII. REFERENCES	24
APPENDIX. DERIVATION OF RECURSIVE RELATIONS	25

SECTION I. INTRODUCTION

The parameter space method provides an analytical tool developed for use in control system analysis and synthesis. Although not necessary, its application is facilitated by augmenting the analytical results with graphical portrayals in a selected multi-parameter space.

The method requires that the control system be described by a characteristic equation which, for sampled-data or digital systems, ~~is expressed~~ may be expressed in the z-domain. The technique is based on the analysis and synthesis methods for linear and nonlinear control system design which are

amply described in Siljak's excellent monograph on the subject.¹

Reference 2 describes

the application of the technique to the analysis and synthesis of linear sampled-data control systems.

ations of Once the system characteristic equation has been obtained, the parameter plane method enables the designer to evaluate graphically the roots of the equation. Hence, he may design the control system in terms of the chosen performance criteria; e.g. absolute stability, damping ratio, and settling time. He is able to see the effect on the characteristic equation roots of changing two adjustable parameters. Siljak further simplified the design procedure by introducing Chebyshev functions into the equations, thereby putting them in a form particularly amenable to their solution by a digital computer.

The extended method

permits

The method has been extended to portray the effect of varying the sampling period.^{3,4}

Thus one can see the effect of the choice of values assigned to the sampling period on absolute and relative stability. Also, the recursive formulas shown therein are simpler in form than the Chebyshev functions of Ref. 2.

The resulting formulation is deliberately cast in a form that makes it particularly amenable to solution by a digital computer or a desk calculator, again emphasizing the interplay between analysis and computing machines.

When portrayed graphically, the results show the dynamic relation between the selected parameters and the characteristic equation roots, as a function of the independent argument.

$\omega_n T$. Hence one can deduce readily the dynamic effect upon the system of various combinations of values of the selected parameters defining the parameter space.

The history of the continuous-time domain version of the parameter plane technique is well-described with suitable references in Ref. 1. Briefly summarizing that history, in 1870 A.A. Vishnegradsky of developed and the Leningrad School of Theoretical and Applied Mechanics used the first version of the parameter plane technique to portray system stability and transient characteristics of a third order system on a two-parameter plane. In 1949 Professor Yu I. Neimark of the Russian School of Automatic Control generalized Vishnegradsky's approach to permit the decomposition of a two-parameter domain (D) describing an nth order system into stable and unstable regions.

The technique was called D-decomposition. During the period 1959-1966 Professor D. Mitrovic, founder of a Belgrade group of automatic control, extended the method to enable the analyst to relate the system's variable parameters to the system response, using the last two coefficients of an nth order characteristic equation. Beginning in 1964, Professor D.D. Siljak, then a student of Mitrovic's at the University of Belgrade, generalized the method and called it the Parameter Plane method. His method permitted the analyst to select an arbitrary pair of characteristic equation coefficients (or parameters appearing within the coefficients) and portray both graphically and analytically the dependence of the system response upon the selected parameters. The method was subsequently extended by Siljak and others to encompass a host of related problems.

In 1967 Professor J. George modified the D-decomposition method to enable the portrayal of the absolute stability region in a multi-parameter space (George also showed how to portray contours of relative stability, as did Siljak). All of the foregoing work is carefully and completely referenced within Ref. 1. In 1966 and subsequently, Soltzer has applied the parameter

space method to: the design of missile, aircraft, and satellite controllers, including systems containing one or two nonlinearities; the analysis of the dynamic effects of the nonlinear "Solid Friction" (Dahl) model for systems with ball bearings, such as control moment gyroscopes and reaction wheels; and the specification by the system designer of the dynamic structural flexibility constraints to the structural designer. Most of this work has appeared in the technical journals of the IEEE, the AIAA, the International Journal of Control, and the journal, Computers & Electrical Engineering. A portion

of the history that has not been reported upon ^(previously) (with one exception to be noted) is the control system work conducted by the German rocket scientists in the early 1940's at Peenemunde. There, Dr. W. Haeussermann and others applied the D-decomposition technique to the design of the V-2 Rocket, following Dr. Haeussermann's earlier (pre-World War II) application to the control of ^{an} underwater torpedo. This work was not published in the open literature because of national security constraints. When the group came to the United States to work with the Army Ballistic Missile Agency (first at Ft. Bliss, Texas, then at Redstone Arsenal, Huntsville, Alabama), Dr. Haeussermann and his associates continued to apply the method to US Army missiles (and later to NASA space vehicles). Again, national (this time, another nation!) security precluded publication in the open literature until 1957. ⁵

In 1964 Professor Siljak ^{published} made the first application of the parameter plane technique to sampled-data systems. ² As mentioned above, this was extended in Ref. 3-4. In 1971 Seltzer presented an algorithm for systematically solving the Popov Criterion applied to sampled-data systems. Applications of these sampled-data parameter space techniques are found in Ref. 3, 4, and 6.

SECTION II. ANALYTICAL PRELIMINARIES

The technique requires that the control system be described by a characteristic equation in which is transformed into the z -domain. Two adjustable parameters (k_0, k_1) are selected, and the characteristic equation (CE) is recast in terms of them; i.e.

$$CE = \sum_{j=0}^n \gamma_j z^j = 0, \quad (1)$$

$$\gamma_j = \gamma_j(d_j, k_0, k_1) \quad (2)$$

$$z = e^{T_s} = r e^{i\theta}, \quad (3)$$

$$r = r(\zeta, \omega_n, T) = e^{-\zeta \omega_n T}, \quad (4)$$

$$\theta = \theta(\zeta, \omega_n, T) = \cos^{-1} \left(\frac{\zeta}{\sqrt{1-\zeta^2}} \right) = \cos^{-1} \omega T \quad (5)$$

where ζ , ω_n , and T represent the damping ratio, natural frequency, and sampling period, respectively. To transform the characteristic equation from an n th order polynomial

into an algebraic equation, z^j may be defined as in terms of its

The symbol d_j represents all system parameters other than k_0, k_1 .

real and imaginary parts, R_j and I_j :

$$z^j = R_j + i I_j. \quad (6)$$

It readily follows from Eq. (3) that the values of R_j and I_j are

$$R_j = r^j \cos j\theta \quad (7R)$$

and

$$I_j = r^j \sin j\theta. \quad (7I)$$

While Eqs. (7) are satisfactory for determining the values of R_j and I_j , a set of recursive formulas can be derived that are particularly amenable to implementation on a desktop calculator or digital computer.

They are shown below as Eqs. (8) and are derived in the Appendix:

$$X_{j+1} = 2r \cos \theta X_j - r^2 X_{j-1}, \quad (8)$$

where X_j may be either R_j or I_j . Only two values of X_j (i.e. two

are needed to obtain iteratively, one at a time, all other values of R_j, I_j .

values of R_j and I_j . These are obtained from the definition of z in Eq. (3) when $j=0$, the value of z^j is unity and, from Eq. (6),

$$z^0 = R_0 + i I_0 \quad (9)$$

or

$$1 = R_0 \quad (10R)$$

$$0 = I_0 \quad (10I)$$

When $j=1$, the value of z^j is, in Euler form,

$$\begin{aligned} z^1 = z &= r \cos \theta + i r \sin \theta \\ &= R_1 + i I_1 \end{aligned} \quad (11)$$

Hence,

$$R_1 = rB \quad (12R)$$

and

$$I_1 = r\sqrt{1-B^2} \quad (12I)$$

It will turn out to be useful in the sequel to observe from Eq. (9) that the radical, $\sqrt{1-B^2}$, appears as a factor in each value of I_j .

Solely for simplicity, it may be factored out by defining a new term,

I_j' as

$$I_j' = I_j / \sqrt{1-B^2} \quad (13)$$

If Equation (6) is substituted into Equation (1) and the real and imaginary parts of the resulting equation are separated, two simultaneous algebraic equations are obtained.

These two equations contain the adjustable parameters, or variables,

k_0, k_1 . Hence, it may be observed that the two equations may be solved explicitly for k_0 and k_1 as functions of the other system parameters (d_j) and, in particular, as functions of the independent argument, $\omega_n T$.

It is this latter observation that forms the basis of the parameter space method for determining stability regions and dynamic response in terms of selected system parameters.

It may be observed that R_j and I_j are functions of r and B or of $\omega_n T, \omega_n$, and T . Eq. (1)

SECTION III. STABILITY DETERMINATION

The method involves the definition of stability boundaries on a multi-parameter (to include k_0, k_1) space. These boundaries are found from the pair of simultaneous algebraic equations that result from the following operations on the system characteristic equation written in terms of the complex variable, z . Equation (6) is substituted into characteristic equation (1), and the resulting real and imaginary parts are separated and equated to zero. The two resulting algebraic equations may be solved for any two parameters within them.

There may be as many as four stability boundaries for any system described by characteristic equation (1), although it is not necessary for all four to exist.

1. One stability boundary separates the stable complex conjugate pairs of roots from the unstable ones. It consists of a map of the unit circle from the complex z -plane onto a selected (such as k_0, k_1) parameter space.

Initially, one may

Consider the oft-occurring case where the coefficients δ_j of the powers of z in the characteristic equation are linear combinations of k_0, k_1 , i.e.

$$\delta_j = a_j k_0 + b_j k_1 + c_j, \quad (14)$$

where a_j, b_j, c_j represent all system parameters other than k_0, k_1 .

In this case the two simultaneous equations resulting from the real and imaginary, respectively, parts of the characteristic equation assume the form,

$$\text{Re}\{C.E.\} = A_1 a + B_1 b - C_1 = 0, \quad (15R)$$

$$\text{Im}\{C.E.\} = A_2 a + B_2 b - C_2 = 0, \quad (15I)$$

Cramer's

and may be solved for k_0 and k_1 readily by applying Cramer's Rule, yielding

$$k_0 = \frac{B_1 C_2 - B_2 C_1}{J}, \quad (16)$$

$$k_1 = \frac{A_2 C_1 - A_1 C_2}{J}, \quad (17)$$

$$J = A_1 B_2 - A_2 B_1 \quad (18)$$

$$\begin{aligned} A_1 &= \sum_{j=0}^n a_j R_j, & B_1 &= \sum_{j=0}^n b_j R_j, & C_1 &= \sum_{j=0}^n c_j R_j, \\ A_2 &= \sum_{j=0}^n a_j I_j, & B_2 &= \sum_{j=0}^n b_j I_j, & C_2 &= \sum_{j=0}^n c_j I_j, \end{aligned} \quad (19)$$

where J represents the Jacobian associated with the pair of algebraic equations.

To find the stability boundary in question, one merely sets \mathcal{J} equal to zero in the definitions of R_j and I_j used in obtaining k_0 and k_1 in Eqs. (16) - (17). The result is a boundary in the $k_0 - k_1$ parameter plane that is defined in terms of system parameters d_j

[in the general case -- see Eq. (2)] ~~of the special case of Eq. (14)~~ ^{a_j, b_j, c_j} and the independent argument, $\omega_n T$. The independent argument is varied in value between zero and ∞ , thereby defining the boundary in terms of k_0 and k_1 . If the coefficients a_j , b_j , and c_j contain exponential terms with T appearing in the exponents, then each exponent may be replaced by its power series and truncated according to the accuracy that is desired. If the two parameters k_0 and k_1 do not appear linearly as expressed in Eq. (14), they ~~still~~ may be solved for ~~by~~ by substituting Eq. (6) into the characteristic equation (1) and separating the result into the real and imaginary parts. This still results in two simultaneous algebraic equations which may be solved for the two variables, k_0 and k_1 , although not as readily as expressed in Eqs. (16) - (17).

π (assuming that the system being designed possesses low-pass filter characteristics)

2. The next two stability boundaries are those separating the stable real roots from the unstable ones. These comprise a mapping of the $z=1$ and $z=-1$ points from the z -plane onto the selected parameter space. These are found readily by substituting $z=1$ and $z=-1$, respectively, into the characteristic equation (1). Each of the two resulting equations results in a definition of the two real root boundaries in the selected parameter space.

3. The fourth boundary is a mapping of the conditions that cause the two simultaneous algebraic equations (used to define the complex conjugate root boundary) to become dependent. In the case where k_0 and k_1 appear linearly as in Eq. (14), this case is found by determining the conditions that cause the Jacobian of Eq. (13) to become identically equal to zero.

For a linear sampled-data control system to be stable, it is necessary that all roots of the characteristic equation lie within the unit circle on the z -plane. If the system is low-pass in nature, the stable region is bounded by the semi-circle defined by the upper half of the unit circle (part 1, above) and the singularities associated with $z = \pm 1$ (part 2, above) and $J=0$ (part 3, above). The mapping of these boundaries onto the parameter space will bound the stable region, if one exists. That region is determined by applying a shading criterion or using a test point. If the Jacobian is greater than zero, then the stable region (if it exists) lies to the left of the complex conjugate root boundary as $\omega_m T$ increases.

the left side of the line is double cross-hatched to indicate a boundary associated with double, or complex conjugate, roots. (If the Jacobian is less than zero, the stable region lies to the right.) Single cross-hatching is used on the two contours associated with the real roots. The side of the contour on which to place the cross-hatching is determined by the

requirement that cross-hatching be continuous, or on the same side, of the contours as the intersections corresponding to $z = +1$ and $z = -1$ are approached along either the complex root or real root stability boundary. In the unusual (but physically possible)

singular case when $J=0$, the shading of ~~the~~ resulting boundary is determined in a similar ~~(but unspecified)~~ manner, i.e. the side on which to shade the boundary is determined by the physical requirement that the number of stable roots must never become less than zero as one moves across a stability boundary. This $J=0$ case may arise for a particular frequency, ω , or for a particular combination of system parameters. The latter situation is included in the work reported upon in Ref. 7.

SECTION IV. SYSTEM DYNAMICS

Once the stable region, if it exists, has been determined in the selected parameter space, the dynamic or transient characteristics of the system can be specified in terms of the locations of the roots of the characteristic equation (pole placement). For the ~~complex~~ complex conjugate roots, these locations are defined in terms of damping ratio (ζ) and system natural frequency (ω_n). Contours of constant ζ are determined as functions of ω_n and T in precisely the same manner that the complex conjugate stability boundary was determined except that ζ is not set equal to zero.

The real root locations corresponding to values of z when θ equals 0° and 180° (may also be plotted on the parameter plane by setting z equal to a positive or negative real constant, substituting that value into Equation (1), and solving for k_1 as a function of k_0 . Each resulting contour corresponds to a location of a real root in the z -domain. When $z = +\alpha$

$$\sum_{j=0}^n \gamma_j \alpha^j = 0, \quad (20)$$

and when $z = -\alpha$,

$$\sum_{j=0}^{n/2} \gamma_{2j} \alpha^{2j} - \sum_{j=0}^{(n-2)/2} \gamma_{(2j+1)} \alpha^{(2j+1)} = 0, \quad n \text{ even} \quad (21)$$

$$\sum_{j=0}^{(n-1)/2} (\gamma_{2j} \alpha^{2j} - \gamma_{(2j+1)} \alpha^{(2j+1)}) = 0, \quad n \text{ odd} \quad (22)$$

where α is a positive real number.

Values of α corresponding to desired real root locations may be substituted into Eqs. (20) - (22) to obtain parameter space contours corresponding to these locations. Now the dynamic effect of any chosen design point in the parameter space may be specified in terms of ζ , ω_n , α , and T .

(The analytical technique developed permits the designer to observe the effect of simultaneously changing three control parameters and the sampling period. Most existing conventional techniques permit the observation of the effect of changing only one control parameter and don't show the effect of various sampling periods. If the designer is clever,

(The true associated stability boundaries may be found by setting α equal to ∞)

sometimes the system parameters may be manipulated within the equations defining the stability and dynamic contours so that more than two parameters (such as k_0 , k_1) may be used to define a parameter space. An example of a three-parameter space is provided ~~herein~~ in the sequel.

¶ Sometimes it is specified that the settling time of the system be less than a prescribed value. This corresponds to requiring that the real part of the roots of the characteristic equation be less than a prescribed negative real constant. A boundary corresponding to this requirement can be drawn on the parameter plane by mapping a circle of constant radius (for a chosen values of ζ , ξ , and T) from the s -plane onto the parameter plane. Relations exist for estimating the maximum overshoot and peak time of transient response when it is valid to assume a second order system. However, a simple estimate can sometimes be made by merely looking at the difference equation representing the system response, estimating when the overshoot will occur, and plotting a corresponding line on the parameter plane. This procedure is brought out in the example. Steady state response may be found from the open loop transfer function and the assumed forcing functions in the conventional manner.

The third order characteristic equation is Eq. (1) with $n=3$, where the coefficients of z^j are in the form of Eq. (14), i.e.

$$\gamma_0 = (a - b + 2c - 1), \quad (28)$$

$$\gamma_1 = (-2a + 2c + 3), \quad (29)$$

$$\gamma_2 = (a + b - 3), \quad (30)$$

$$\gamma_3 = 1. \quad (31)$$

Modified gains a, b, c are defined as

$$a \equiv K_R T / J_V, \quad (32)$$

$$b \equiv K_P T^2 / 2J_V, \quad (33)$$

$$c \equiv K_I T^3 / 4J_V. \quad (34)$$

The stability boundaries are presented in terms of a, b, c , and $\omega_n T$ by observing that the roots (in this case three) of a characteristic equation representing a stable linear sampled-data control system must all lie within the unit circle in the z -plane.

It is assumed that the system possesses low-pass filter characteristics so that only the primary strip (corresponding to $0 \leq \theta \leq \pi$) need be considered. The stable Region

may be defined by mapping its three boundaries from the z -plane onto the

a, b, c parameter space by first considering parameters a, b to be k_0, k_1 in Eq.

(14).

The boundary at $z = +1$ is found by substituting that value for z into the C.E., yielding the stability boundary

$$c = 0 \quad (35)$$

The boundary at $z = -1$ is found by substituting that value for z into the C.E., yielding

$$a = 2. \quad (36)$$

The complex conjugate root stability boundary may be found by setting z equal to $\cos \omega_n T + j \sin \omega_n T$ in the C.E. However, at this point

it is convenient

to use the recursive formulas of Eq. (8) and transform the C.E.

into two algebraic equations by separating the real and imaginary parts. If they are solved for a and b and the associated Jacobian J , one obtains as the complex conjugate root stability boundary,

$$a = [(1 + B)/(1 - B)] c + (1 - B), \quad (37)$$

$$b = c + (1 - B), \quad (38)$$

and

Examination of Eq. (39) reveals that the stability boundary associated with the singular case $J=0$ only occurs when $B=1$, which is the already considered $z=1$ case.

← Now the stability boundaries of Eqs. (35), (36), and (37)-(38) can be plotted on a three-dimensional plot with axes a , b , c . A sketch of these boundaries is shown in Fig. 2. The stability region is

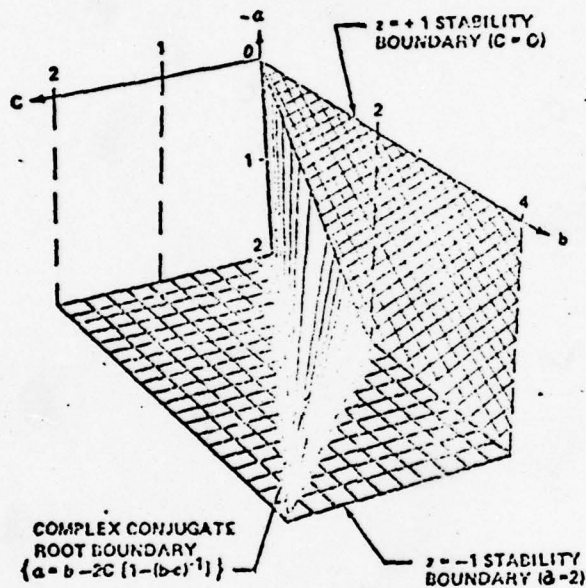


Fig. 2. Stability Boundaries in 3-Dimensions

found by applying the "cross-hatching" rules or by using one or more test points (known to be stable, to lie on a stability boundary, or to be unstable). If $J > 0$ the stable region (if it

exists) lies to the left of the complex conjugate root stability boundary of Eqs. (37)-(38), as 0 (or $u_n T$) increases; the left side of the line is double cross-hatched to indicate a boundary associated with double, or complex conjugate, roots. If $J < 0$, as in this case, the stable region lies to the right and the right side of the line is double cross-hatched. Single cross-hatching is used on the contours of Eqs. (35)-(36) associated with single root boundaries. The side of the contour on which to place the cross-hatching is determined by the requirement that cross-hatching be continuous, or on the same side, of the contours as the intersections corresponding to $z = +1$ ($C = 0$) and $z = -1$ ($a = 2$) are approached along either the complex root or real root stability boundary. Using this criterion, the stable region is found to be bounded by the $c = 0$ plane, the $a = 2$ plane, and the curve specified by Eqs. (37)-(38). The latter may be solved for a as a function of b , resulting in the simple expression

$$a = b - 2c(1 - (b - c)^{-1}) \quad (40)$$

The limiting values for a and b may be found by letting θ approach 0 and π . For the case of $\theta \rightarrow 0$, represent B by the series expansion

$$B = \cos \theta = 1 - (\theta^2/2!) + (\theta^4/4!) - (\theta^6/6!) + \dots \quad (41)$$

Then, using Eqs. (22), (23), and (26), one obtains

$$\lim_{\theta \rightarrow 0} b = c \quad (42)$$

$$\lim_{\theta \rightarrow 0} a = \lim_{\theta \rightarrow 0} c \left[\frac{(4/\theta^2) - (2/3) + (\theta^2/36) - \dots}{(\theta^2/2!) - (\theta^4/4!) + \dots} \right] \quad (43)$$

For $c = 0$, Eq. (27) still holds (recognize $K_1 = 0$ is really the case one is interested in). Then, using Eqs. (19c) and (22), one obtains

$$\begin{aligned} \lim_{\theta \rightarrow 0} a &= \lim_{\theta \rightarrow 0} \frac{(K_1 \theta^3 / 4J \omega^3) [2 - (\theta^2/2!) + (\theta^4/4!) - \dots]}{(\theta^2/2!) - (\theta^4/4!) + \dots} \\ &= \lim_{\theta \rightarrow 0} (K_1 \theta / 2J \omega^3) [2 - (2\theta^2/6) + (\theta^4/72) - \dots] = 0 \quad (44) \end{aligned}$$

For the limiting case of $\theta \rightarrow \pi$:

$$\lim_{\theta \rightarrow \pi} a = \lim_{\theta \rightarrow \pi} \left\{ \frac{[(1+B)c/(1-B)] + (j-B)}{1} \right\} = 2 \quad (45)$$

and

$$\lim_{\theta \rightarrow \pi} b = \lim_{\theta \rightarrow \pi} (c + 1 - B) = c + 2 \quad (46)$$

The results of the foregoing are sketched graphically in two dimensions on Fig. 3, for the cases where $c = 0$ and when $c \neq 0$.

¶ The design technique employs the pole placement approach. It is based on the premise that the dynamic behavior of the system is closely related to the location of the roots of its associated characteristic equation. The method shows both analytically and graphically the direct

correlation between these roots and the control gains and sample period of the controller. The design technique then involves the specification of the characteristic equation root locations and the subsequent determination of the control system gains and sample period needed to attain these locations. The control system designer then must determine the system response resulting from using these numerical values and assess its adequacy. If it is not adequate, he usually relies on his experience to re-locate the roots to improve the response in the manner desired for his particular system (i.e., faster settling time, lower peak overshoot, etc.). It is assumed that one wishes the pair of complex conjugate poles of the C.E. to dominate the dynamic response of the system. This response will then be modified by locating the third (real) root.

First consider the pair of complex conjugate roots. One may use Eqs. (17)-(18), substituting a, b for k_0, k_1 , respectively, [also using Eqs. (28)-(31)].

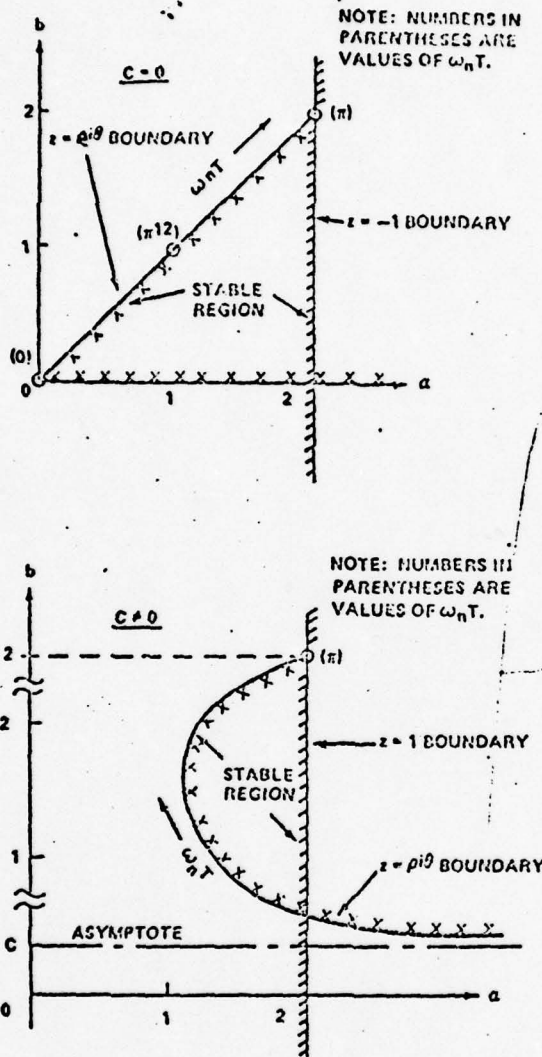


Fig. 3. Stability Boundaries in 2-Dimensions

Upon examining the nature of the equations for a, b, one sees that they are functions of r, B, and c, or (finally) functions of ζ, θ, c .

← For each value of ζ , b versus a may be determined analytically and plotted graphically as a function of θ for a given value of c. This may be repeated for a number of values of c. Now the value of θ may be selected (for selected values of c) that best meets whatever design criteria one chooses. In effect, selecting θ and c will also choose the real root location. This may be shown by designating the real root of the C.E. as z_R , where

$$z_R = \delta = e^{-\zeta \omega_n T} \quad (47)$$

and ζ represents the damping factor. One may substitute Eq. (47) into C.E. (1) and solve for b, obtaining

$$b = [(1-\delta)/(1+\delta)]a + [2/(1-\delta)]c - [(1-\delta)^2/(1+\delta)] \quad (48)$$

One sees that Eq. (48) yields a straight line contour of b vs. a for a given value of c and a given value of δ . Thus, for a given value of c , where the δ -contour of Eq. (48) crosses the ζ -contour of Eq. (37), one obtains a value of θ for the given value of c and those specified values of ζ and δ . From Eq. (48), c may be determined as a function of the characteristic equation root locations:

$$c = (\alpha^2 + \beta^2 - 2\alpha + 1)(1 - \delta)/4, \quad (49)$$

where α and β are the real and imaginary parts, respectively, of the pair of complex conjugate roots of characteristic equation (4). For a specified location (α, β) of the pair of complex conjugate roots, a value for c is established by setting a value for δ (location of the real root).

An additional constraint is imposed by Shannon's Sampling Theorem:

$$\omega < \omega_s/2, \quad (50)$$

where ω is defined in Eq. (5) and $\omega_s/2\pi$ is the sampling frequency,

$$\omega_s = 2\pi/T. \quad (51)$$

From Eqs. (50) - (51), this constraint may be restated as

$$\theta < \pi. \quad (52)$$

The stable region portrayed in Figs. 2-3 may be shown for several selected values of c on Fig. 4 using Eqs. (8) and (98). As c increases

in value, the stable region shrinks in size and the ζ contours lie further to the right. When $c = 0.6$, the $\zeta = 1/2$ contour lies entirely to the right (and outside) of the stable region. Finally when $c > 2$, the stable region disappears entirely (for a geometric explanation, see Fig. 2).

The application of the foregoing technique will now be summarized.

1. Based on desired system response characteristics, tentatively select locations for the three roots of the characteristic equation. Although the zeros of the system characteristic equation also affect the dynamics, placement of the poles will dominantly affect the dynamics.

a. A root location criteria might be to select numerical values for ζ and ω_n .

b. Then qualitatively determine how much integral gain is desired for the types of disturbance inputs expected. This gives an indication of the value of c to use.

c. Determine computer design constraints. One might be to select as large a value of T as possible to minimize on-board memory capacity requirements.

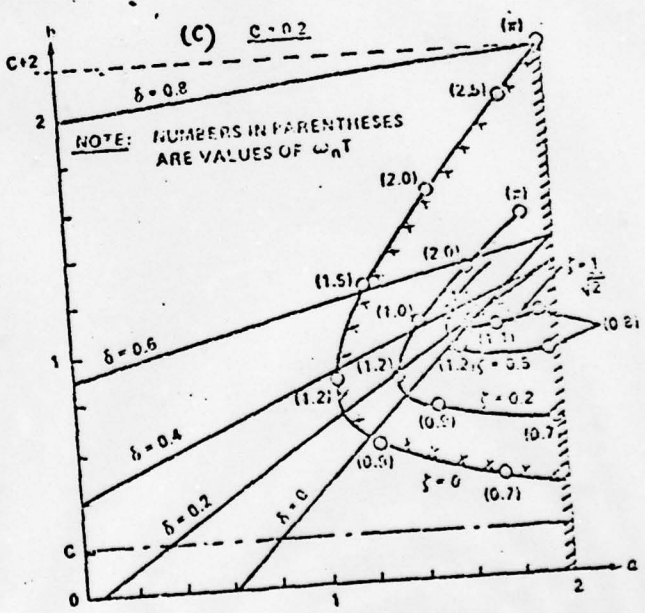
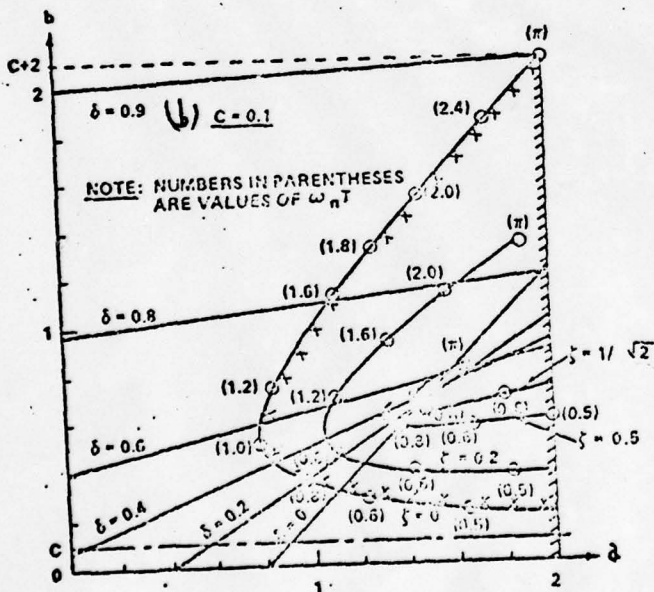
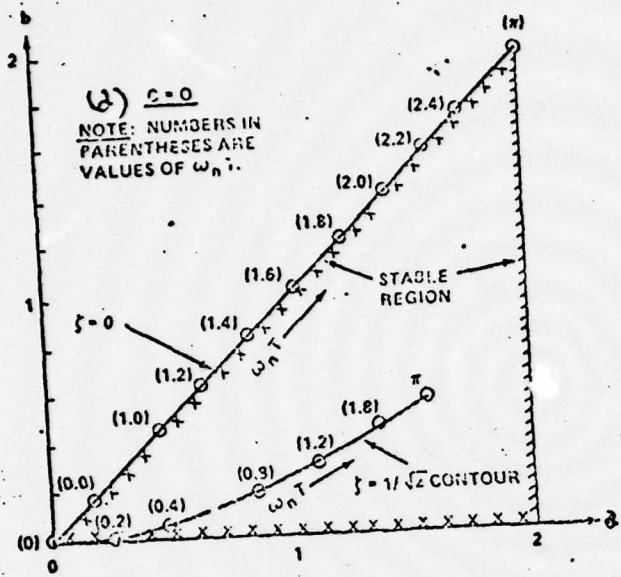


Fig. 4. Parameter Plane Plots Portraying Root Locations ($c=0, 0.1, 0.2$)

2. Using the value of c tentatively established in paragraph 1b above, plot the stability boundaries in the b vs. a parameter plane, using Eqs. (36)-(38). Then plot the desired ζ -contour (as a function of argument $\omega_n T$) on the b vs. a parameter plane, using Eqs. (17)-(19).
3. Using various values of δ , plot δ -contours on the same plot, using Eq. (48).
4. Find an intersection of a δ -contour which gives a desired value for $\omega_n T$ (and hence T , since ω_n has already been specified) and δ . In

general, if $\delta \rightarrow 0$, its effect on the system dynamics is small compared to the effect of the pair of complex conjugate poles (placed by $\omega_n T$, c).

5. Check the response of the system using the values of a , b , c , and $\omega_n T$ (and hence K_D , K_I , K_P , and T) associated with the selected intersection. If it is unsatisfactory, reiterate the above procedure, selecting another value of c .

If the design procedure were merely to specify the three root locations (such as in terms of α , β , δ or ζ , $\omega_n T$, δ), iteration would not be required. Unfortunately, in design practice one must exercise engineering judgement in selecting the three root locations, giving rise to iterative design procedures such as the one outlined above. However, another possibility does exist. If the real root is placed near the origin of the z -plane ($\delta \rightarrow 0$), and if the pair of complex conjugate roots are located near the unit circle in the z -plane (i.e., specifying ζ and $\omega_n T$), the latter two roots will dominate the system response. Then the already developed tools for specifying the system response (such as determining explicitly the maximum overshoot and the settling time) of second-order systems may be applied handily. The foregoing procedure

may be amplified through the application of realistic numerical values for the system parameters. Assume that a spacecraft similar to the Space

Telescope is to have a digital on-board controller. ~~They~~ further assume that it is desired to have a controller natural frequency (ω_n) of six rad/s, and that the moment of inertia (J_y) about the single axis ~~coincident in part to the Space Telescope YZ axis~~ is 4.30×10^4 kg-m². Assume that integral control is desired to drive to zero the effect of constant input disturbances. This means a non-zero value of c is desired. If a value of ζ of $1/\sqrt{2}$ is selected, and if the value of δ is desired to be kept as close to zero as possible, it is implied from Fig. 4c that, for $\delta > 0$, no intersections of the ζ -contour occur when $c > 0.2$. Hence, a value of $c = 0.1$ is chosen. The smallest value of δ whose corresponding δ -line intersects the ζ -contour, with a reasonable factor of safety, is $\delta = 0.4$. The value of $\omega_n T = 1.2$ is on the ζ -contour at the intersection, yielding a value of 0.20s for T . Corresponding values of a and b are 1.41 and 0.68, respectively. This gives a set of gain values of 1.14×10^4 N-m/rad, 1.67×10^4 N-m/rad-s, and 2.35×10^4 N-m-s/rad for K_D , K_I , and K_P , respectively. If response studies show that a larger value of integral gain is deemed necessary, a larger value of c (and consequently a smaller value of ζ) would be selected.

SECTION VI. CONCLUSIONS

An analytical method for portraying stability regions in a selected parameter space has been shown for a digital system. The method requires that the system characteristic equation be available and expressed in the complex z -domain. It also is possible ~~to~~ ^{apply pole placement} obtain desired dynamic characteristics using this modified parameter space technique. The advantage of the technique over existing classical sampled-data methods is that the stability and dynamic response characteristics are expressed in terms of several (rather than merely one) selected parameters. Also, the sampling period, T , need not be expressed numerically before the design technique begins, giving the system designer one more degree of freedom.

SECTION VII. REFERENCES

1. Siljak, D. D.: Nonlinear Systems, Wiley, N.Y., 1968.
2. Siljak, D. D.: Analysis and Synthesis of Feedback Control Systems in the Parameter Plane. Part II - Sampled-Data Systems. IEEE Trans., Part II Applications and Industry, Vol. 83, November 1964, pp. 458-466.
3. S. M. Seltzer, Sampled-data control system design in the parameter plane. Proc. 8th Ann. Allerton Conf. Circuits and System Theory, pp. 458-466, 1970.
4. Seltzer, S. M., "Enhancing Simulation Efficiency with Analytical Tools," Computers and Electrical Engineering, Vol. 2, pp. 35-44, 1975.
5. Moossermann, W., "Stability Areas of Missile Control Systems," Jet Propulsion, July 1957, pp. 787-795.
6. Seltzer, S. M., "An Algorithm for Solving the Popov Criterion Applied to Sampled Data Systems," Proc. Third Southeastern Symposium on System Theory, April 5-6, 1971, pp. G5-0 - G5-7.
7. Seltzer, S. M., "Passive stability of a Spinning Skylab," Journal of Spacecraft and Rockets, Vol. 9, No. 9, September 1972, pp. 651-655.
8. Kuo, B. C., Analysis and Synthesis of Sampled-Data Control Systems, Prentice-Hall, New Jersey, 1967.

APPENDIX. DERIVATION OF RECURSIVE RELATIONS

It is possible to obtain algebraic recursive relations for the real and imaginary parts of the complex variable, z , when it is raised to the j^{th} power (j is a positive integer). From Eq. (3), z is defined as the vector (or complex variable),

$$z = e^{i\theta} = r e^{i\theta} = r \cos \theta + i r \sin \theta. \quad (\text{A1})$$

The real and imaginary parts of z^j may be defined as R_j and I_j , respectively, i.e.

$$z^j = R_j + i I_j, \quad \text{and (A2)}, \quad (\text{A3})$$

If $j=1$, Eq. (A3) becomes identical with Eq. (A1) leading to

$$R_1 = rB \quad (\text{A4R})$$

and

$$I_1 = r\sqrt{1-B^2}. \quad (\text{A4I})$$

Using Eq. (5) ^{in Eq (A1)} i.e. letting $B = \cos \theta$, leads to

$$z = rB + i r\sqrt{1-B^2}. \quad (\text{A2})$$

If $j=0$, then Eq. (A3) becomes

$$z^0 = 1 = R_0 + i I_0, \quad (\text{A5})$$

or

$$R_0 = 1 \quad (\text{A6R})$$

and

$$I_0 = 0. \quad (\text{A6I})$$

If one squares the left and right hand sides of Eq. (A1), one may

$$\begin{aligned} z^2 &= r^2 e^{i2\theta} = r^2 (\cos 2\theta + i \sin 2\theta) \\ &= r^2 (\cos^2 \theta - \sin^2 \theta + i 2 \cos \theta \sin \theta) \end{aligned}$$

$$\begin{aligned}
 &= 2 r^2 \cos \theta (\cos \theta + i \sin \theta) - r^2 \\
 &= 2rBz - r^2.
 \end{aligned} \tag{A7}$$

One may now multiply each term of Eq. (A7) by z^{k-1} to yield

$$z^{k+1} = 2rBz^k - r^2z^{k-1}. \tag{A8}$$

Substitution of Eq. (A3) into Eq. (A8), letting $j = k-1, k,$ and $k+1$, leads to

$$R_{k+1} + i I_{k+1} = 2rB(R_k + i I_k) - r^2(R_{k-1} + i I_{k-1}). \tag{A9}$$

Separately equating the real and imaginary parts, respectively, of Eq. (A9) leads to the two equations,

$$R_{k+1} = 2rBR_k - r^2R_{k-1} \tag{A10R}$$

and

$$I_{k+1} = 2rBI_k - r^2I_{k-1}. \tag{A10I}$$

One may observe the identical forms of Eqs. (A10) and write them both as a single equation,

$$X_{k+1} = 2rBX_k - r^2X_{k-1}, \tag{A11}$$

where X_k may be used to represent either R_k or I_k . Of course the dummy index k may be exchanged with j , yielding Eq. (9) of the text.

If one knows the two values X_k and X_{k-1} of Eq. (A11), one may determine the third value X_{k+1} . Since two values of X_k are known, i.e. for $k=0$ and $k=1$ [see Eqs. (A4) and (A6)], as many values of X_k as are needed for the particular problem at hand can be determined recursively from Eq. (A11).

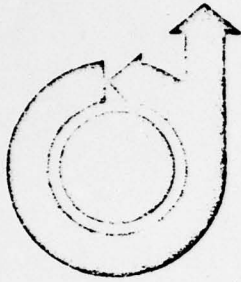
APPENDIX D. PARAMETER SPACE PROGRAM: STABILITY REGIONS

A program has been written for the Hewlett Packard 9100B Calculator to map stability boundaries for the missile system described in Section V, Part C. Since the real root boundary is known, only the complex conjugate root boundary need be plotted. This is the map of the unit circle from the complex z -domain onto the selected parameter plane. In the design example, the control gains k_p and k_d are selected for various selected numerical values of k_i (in this example, $k_i = 0, 0.1, \text{ and } 0.5$). Inputs required to start the program are the numerical value of k_i (which is entered in the d storage register) and the starting value of ωT (which is nominally zero and entered in the a storage register). The program automatically steps the value of ωT upward positively in increments of one (although this value can be altered by inserting a different number into program steps 0c through 10). The program prints out values of k_p (in the z display) and k_d (in the y display) for each printed (in the x display) increment of ωT .

APPENDIX E. SYSTEM RESPONSE PROGRAM

The purpose of this program is to compute values of the missile attitude, θ_k , at each sampling instant, $t=kT$. In this case, the response to a unit step input has been computed, using Equations (IV-47) through (IV-51). The program has been written for the Hewlett Packard 9100B Calculator. The required inputs to the program are the selected numerical values of the control gains, k_p , k_i , and k_d , and the initial conditions on θ at $t=0$, $t=T$, and $t=2T$. These latter three are calculated from Equations (IV-47) through (IV-49), respectively. The program can be easily modified to accept initial conditions other than $\theta_0=0$ and for inputs other than a unit step input. The program prints out values of $\theta(kT)$ for $t \geq 3T$ in the y display. The numerical value for k_i must be inserted in program steps 57 through 5b. Figure 4 indicates a plot of the outputs of this program for selected values of k_p , k_i , and k_d (see Figure 3 for rationale in selecting these values).

APPENDIX F. AIAA PAPER: "GUIDANCE LAWS FOR SHORT RANGE TACTICAL MISSILES"



79-0059

Guidance Laws for Short Range Tactical Missiles

H.L. Pastrick, *U.S. Army Missile Research & Development Command, Huntsville, Ala.;*
and S.M. Seltzer, *Control Dynamics Co., Huntsville, Ala.;* and M.E. Warren, *University of Florida, Gainesville, Fla.*

AD-790059

GUIDANCE LAWS FOR SHORT RANGE TACTICAL MISSILES

H. L. Pastrick*
US Army Missile Research and Development Command
Huntsville, Alabama

S. M. Seltzer**
Control Dynamics Company
Huntsville, Alabama

M. E. Warren†
University of Florida
Gainesville, Florida

Abstract

A comparison of guidance laws applicable to short range tactical missiles is made. These laws are segmented into several classes and the principles underlying each class are discussed. Specific attention is given to the structure of the guidance technique and the requirements for its implementation. Evaluation and comparison of the performance of each guidance law versus the cost of implementing it are considered. An extensive bibliography of relevant literature is included.

I. Introduction

The US Army Missile Research and Development Command (MIRADCOM) recently began a task to develop an advanced guidance and control system for further Army Modular Missiles. The intent is to "leapfrog" systems currently under development. The purpose of this paper is to describe the work that has been done within this new task and to provide an indication of future efforts that are now planned.

The reason for embarking on this task is now summarized. Present weapon systems performance may be seriously degraded in engagements against targets with predicted characteristics of the 1990s and beyond and in the battlefield environments of that time frame (see, e.g., p. 11, Aviation Week and Space Technology, March 20, 1978). It has been established that the guidance laws currently in wide use may not be adequate to combat those threats. Thus, it is projected that fundamental advances in guidance and control systems theory are required to enhance the effectiveness of future weapon systems. Additionally, missile airframe and propulsion systems may require advances commensurate with the predicted target scenarios. In particular, air defense weapons currently in Research and Development (R&D) may be seriously hampered in the combat scenarios envisioned. From an overall systems viewpoint, this task shall address the issue of creating new theory in the guidance and control area to meet the high performance threat of the future as a leading technology item. Closely associated with it and in parallel with the guidance and control effort, weapon system work shall be undertaken to modify airframe and propulsion modules to be capable of engaging the 1990s threat. General support weapons shall be viewed initially as a subset of the air defense

system. Heretofore these two classes of weapons each were developed independently. This research shall attempt to view them as potentially similar systems that utilize different modules such as propulsion, guidance, warhead, etc.

The first step in implementing this task was to conduct a literature survey to establish a technology base starting point. Constraints on length of the paper result in summarizing (alphabetically by author) the list to include only those references considered by the authors to be most relevant.

Following this survey, guidance laws were placed in five categories and defined mathematically. The implementation and predicted performance of each category was then investigated and compared in light of current and predicted hardware and software capabilities. This paper describes these results.

II. Guidance Laws

The development of guidance laws for short range tactical missiles has become a well-researched topic over the past 25 years. A summary of a detailed literature survey, how each guidance law can be implemented, and guidance law predicted performance are described within the five guidance law categories stated in the Introduction.

Line-of-Sight Guidance (Command-to-Line-of-Sight and Beam Rider)

Clemow (1960), in his book Missile Guidance, provides a detailed discussion of beam riding, while Mahapatra (1976) discusses morphological design based on beam riding. Clemow (1960) discusses command-to-line-of-sight (CLOS), while Kain and Yost (1976) use this method in their ship defense scenario, using Kalman filters to reduce beam jitter.

At the MIRADCOM, CLOS and Beam Rider (BR) concepts are each considered a subset of the line-of-sight guidance laws. They differ primarily in their mechanization. The CLOS uses a wire for the transponder link, e.g., TOW or DRAGON. BR may use an electro-optical link, e.g., SHILLELAGH, and fly in a directed beam aimed at the target. Generically they are similar and will be discussed as one.

*Research Aerospace Engineer. Member AIAA.

**Senior Scientist. Associate Fellow AIAA.

†Associate Professor, Electrical Engineering Department. Member AIAA.

The line-of-sight (LOS) guidance scheme (CLOS and BR) is one in which the missile is guided on an LOS course so as to remain on a line adjoining the target and the point of control. To fly along the LOS, the missile requires a velocity component (v_{M1}) perpendicular to the LOS that is equal to the LOS velocity described by the relation

$$v_{M1} = R_{SM} \dot{\gamma}_{ST} \quad (1)$$

where R_{SM} represents the range from the missile to the tracking station and γ_{ST} represents the LOS.

In general, the missile flies a pursuit guidance course at the initiation of the entry into the beam at launch and flies an approximately constant bearing course near impact. This is observed from the velocity equation

$$v_{M1} = \frac{R_{SM}}{R_{ST}} v_T \quad (2)$$

where the range of the tracking station to the target is given by R_{ST} and v_T represents the target velocity relative to the surface of the earth.

Figures 1 and 2 are simplified control block diagrams highlighting features of the scheme for each of the two cases. It should be noted that the projector mount dynamics in Figure 1 and the tracker mount dynamics in Figure 2 may be considerably more

complex than depicted here. Also the BR missile requires onboard autopilot compensation since the projector does not know where the missile is located once enroute. The CLOS scheme, however, does keep track of the missile and thus compensates for its position prior to transmitting the guidance signal via the wire link.

Performance of a missile flying this guidance law is generally very good. Without the man-in-the-loop guidance error, flawless guidance has been demonstrated but can be expected virtually on each shot. In the more realistic condition where the target is moving, the major error source, given that the target has been fired, the performance is expected to be better than 1 ft CEP with a 90% probability level.

Pursuit Guidance

Goodstein (1972) gave a comparison of the qualities and sensitivities of LOS, pursuit, and proportional navigation guidance for air-to-ground and air-to-air missiles. In another paper in the same report, Goodstein discusses the guidance and control system tradeoffs in missile design.

Two pursuit guidance laws are discussed herein: attitude pursuit guidance and velocity pursuit guidance. Attitude pursuit guidance tries to keep the centerline of the missile pointed at the target. In a missile which flies an angle of attack when maneuvering, the velocity vector will always lag

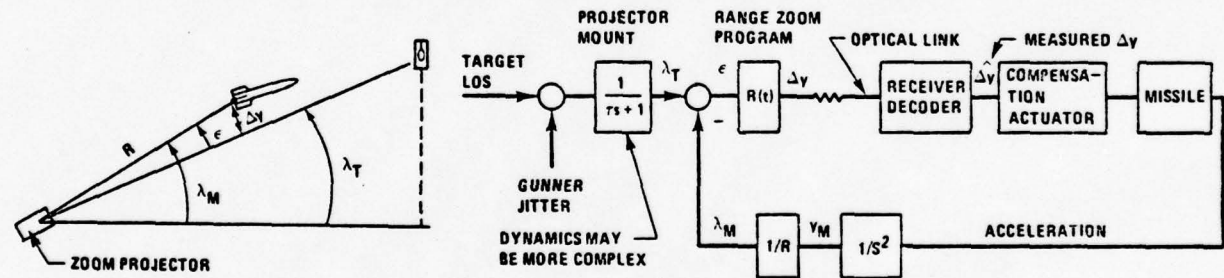


Figure 1. Beam Rider Scheme*

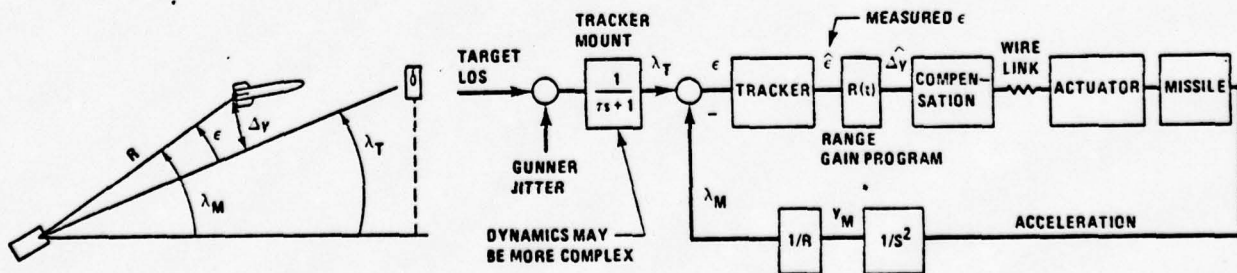


Figure 2. Command-to-Line-of-Sight Scheme*

*Implementation scheme provided by R. H. Farmer, Technology Laboratory, US Army Missile Research and Development Command.

the vehicle pointing direction. Miss distance is a strong function of the maneuver capability of the missile and can be reduced by a fast responding high-g vehicle.

Velocity pursuit guidance attempts to keep the velocity vector of the missile pointed at the target. It is mechanized in some less sophisticated missiles by mounting a target sensor on an air vane which indicates relative wind direction. The difference between this velocity vector and a true velocity vector is the primary error in the scheme. The attitude pursuit guidance mechanization decouples the angle of attack from the target seeker and improves miss distance performance by an amount proportional to the vehicle angle of attack. Figure 3 depicts two-dimensional geometry useful for describing the pursuit guidance laws.

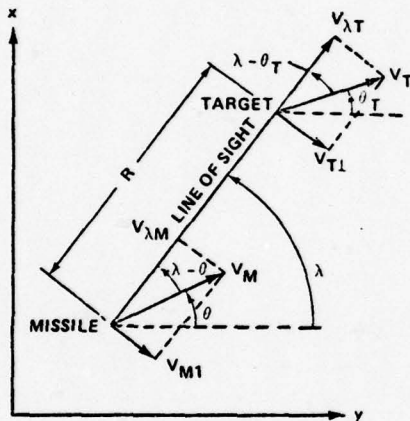


Figure 3. Pursuit Guidance Geometry

Neglecting the case of a maneuvering target, for simplicity, one notes that

$$\dot{R} = v_T - v_M \quad (3)$$

and the LOS rate is

$$\dot{\lambda} = \frac{v_T - v_M}{R} \quad (4)$$

For an ideal pursuit, $\theta = \lambda$. Since $\dot{\theta} = \dot{\lambda}$, the missile will always have to turn during the attack except for the case of a perfect head or tail chase.

Figures 4 and 5 present examples of simplified control system diagrams for the attitude and velocity pursuit guidance laws, respectively. In the former, a wide angle target sensor is required since it is typically mechanized to be body fixed. In the latter, a narrower field-of-view (FOV) sensor may be utilized as a result of the decoupling of the body from the sensor mount as previously described. In each case, K_N is the forward guidance gain, and it will differ for each as will the feedback damping gain K_R . The guidance filter in Figure 5 indicates that higher guidance gain in the velocity pursuit law requires some smoothing to inhibit noise of the target sensor optics and its associated electronics.

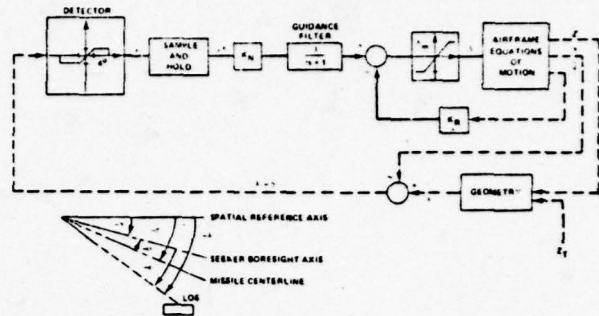


Figure 4. Attitude Pursuit Guidance

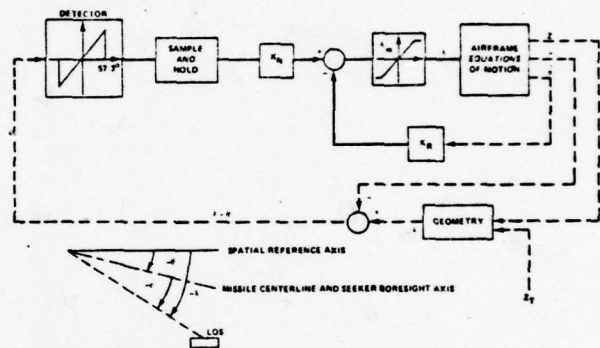


Figure 5. Velocity Pursuit Guidance

The performance to be expected from pursuit guidance is indicated in Figures 6, 7, and 8. These were obtained for a tactical weapon of the class known as close support antitank weapons. They are indicative of the quality of performance one may expect for these guidance laws. Although these are simulation results, recent experience with flight hardware has validated the simulated performance to a high degree of confidence.

The proportional navigation guidance (PNG) law performance is also indicated; therefore, it shall be described next.

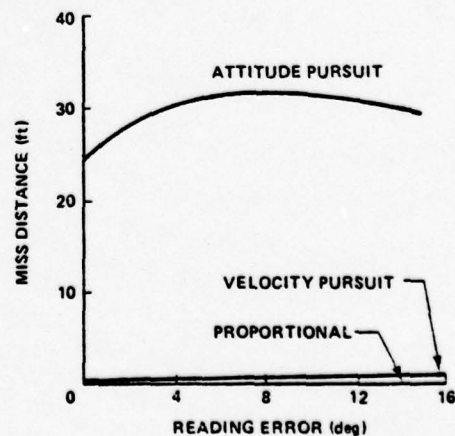


Figure 6. Performance of Classical Guidance Laws for a Given Heading Error at First Target Acquisition

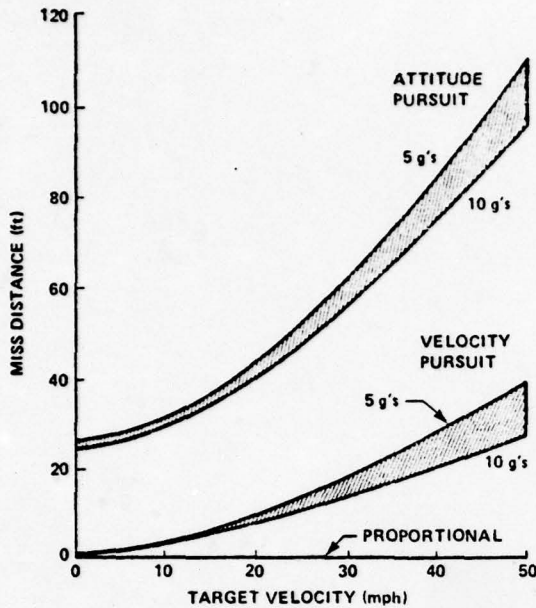


Figure 7. Performance of Classical Guidance Laws for a Given Target Velocity and as a Function of Control Authority (Units Expressed in g's)

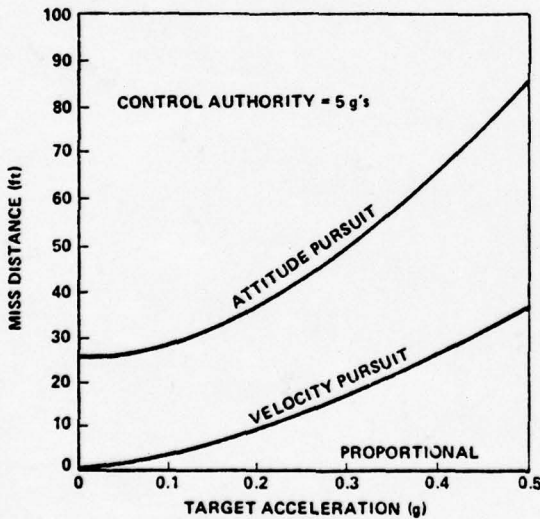


Figure 8. Performance of Classical Guidance Laws for a Given Target Acceleration Commencing 5 sec Before Impact

Proportional Navigation Guidance

Adler (1956) provided one of the seminal papers in the area, considering PNG in three dimensions. Adler provides a readable development of the theory using vector calculus, whereas most subsequent authors have considered only the planar case for simplification. Murtaugh and Criel (1966) provided another fundamental paper developing three-dimensional PNG for a satellite rendezvous problem.

Clemow (1960) gives another basic derivation of PNG, while Pitman (1972) compiled sensitivity functions and projected errors for PNG with gains of 2, 3, and 4. Calculations of terminal homing parameters were made by Rawlings (1970). In a 1971 paper, Rawlings considered the effects of saturating aerodynamic surfaces on trajectories flown with PNG. Many authors have considered augmenting PNG to account for target accelerations. Arbenz (1970) considered making the closing velocity heading rate proportional to LOS rate and developed a closed form expression for a modified PNG law. Siouris (1974) added an estimate of target acceleration to the missile acceleration command to yield an augmented PNG law. Guelman used geometric arguments to give the structure of the missile trajectory; he showed in 1971 that PNG will almost always result in an intercept for a constant velocity target in 1972. For constant target accelerations, qualitative trajectories were determined and target acquisition boundaries assessed. In 1976 Guelman considered the structure of trajectories under true proportional navigation guidance (TPNG), where the commanded acceleration is normal to the LOS rather than the missile velocity. In this work he showed that TPNG results in intercept only if the initial conditions lie in a well defined subset of the parameter space. Shinar (1976) considered PNG for a rolling missile where he considered the cross-coupling between roll and the control system. Slater and Wells (1973) studied optimal evasive tactics against a PNG missile, incorporating a lag into the missile dynamics, and generated two strategies based upon different optimality criteria. A comprehensive study of classical (PNG) and optimal control techniques for terminal homing of cruciform and bank-to-turn steering missiles was performed by Balbirnie, Sheporaitis, and Merriam (1975).

PNG is a guidance law in which the angular rate of the missile flight path is directly proportional to the angular LOS rate of change. This is shown simplistically in Figure 9 for a two-dimensional case.

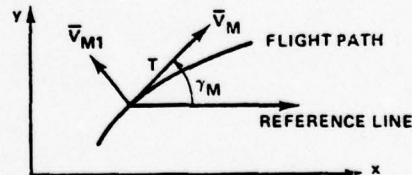


Figure 9. Geometry of Flight Path

The geometry of Figure 9 suggests

$$\dot{\gamma}_M = N \dot{\lambda} \tag{5}$$

where γ_M represents flight path angle relative to a fixed reference, λ represents the LOS relative to a fixed reference, and N is the navigation ratio. A general expression for missile acceleration may be written

$$\eta = V_M \dot{\gamma}_M \bar{R} + V_M \bar{T} \tag{6}$$

where η represents total missile acceleration; V_M , the missile speed; γ_M , the missile flight

path angle; \bar{V}_{M1} , a unit vector lateral to the missile flight path; and \bar{T} , a unit vector tangential to missile flight path. The definitions of \bar{R} and \bar{T} yield the relationship, $\bar{R} \cdot \bar{T} = 0$. One may implement proportional navigation via the relationship (in the Laplace domain)

$$\eta_M(s) = kc(s) = \frac{[k\tau s \lambda(s)]}{(1 + \tau s)} \quad (7)$$

where η_M represents the lateral acceleration in units of g's and ϵ represents the LOS error which is measured by a seeker having a time lag constant of τ sec and an error of $\tau\lambda$. The symbol k represents a guidance gain factor.

By noting that a constant bearing course is determined if missile and target are flying constant speed and neither is maneuvering, it may be concluded that the LOS at each instant of time would be parallel to the LOS at a previous instant. Laterally perturbing the collision course noted by target and missile positions X_T and X_M respectively yields Z_T and Z_M which may be integrated to yield the missile trajectory using proportional navigation:

$$\frac{\tau d^2 Z_M}{dt^2} + \frac{dZ_M}{dt} = -gk\tau\lambda + \tau \left(\frac{d^2 Z_M}{dt^2} \right)_{t=0} + \left(\frac{dZ_M}{dt} \right)_{t=0} + gk\tau(\lambda)_{t=0} \quad (8)$$

The performance and implementation of the guidance law are best appreciated in their relationship to two other guidance laws which are similar in that no requirement is established for range or range rate information. Velocity pursuit and attitude pursuit are in this category with PNG. The performance is indicated in Figures 6, 7, and 8.

Optimal Linear Guidance

Since the mid-1960's the missile guidance literature has become increasingly permeated by techniques based upon optimal control. The great success found by linear-quadratic regulator theory and its dual analog, Kalman filtering, plus the attractive and easily determined form of a feedback solution has led to almost all work in this area being based upon linear model dynamics, with quadratic costs and additive Gaussian noise (LQG). Most formulations consider terminal miss distance and running control effort only in the cost functional. Unlike the standard regulator format, a running cost on the state is generally not appropriate in this framework. The general optimization problem then becomes

$$\min_{u(\cdot)} E[J] = E \left\{ x'(t_f) S_f x(t_f) + \int_{t_0}^{t_f} u'(t) R u(t) dt \right\}$$

subject to $x(t) = A x(t) + B u(t) + G w(t) \quad (9)$

where $E(\cdot)$ designates the expected value operation, S_f and K are weighting matrices, x is the state, u is the control, and w is a white noise process. In most formulations the dynamics are assumed constant to obtain closed form solutions.

Bryson, Denham, and Dreyfus (1963); Denham and Bryson (1964); and Denham (1964) were among the first to consider optimization techniques applied to missile guidance problems. In a series of papers they formulated and solved the optimal control problem with inequality constraints, and then applied the result to the trajectory shaping of a surface-to-surface missile for range maximization.

Stallard (1968) gave a good tutorial review of classical and modern methods for homing interceptor missiles. In an earlier paper (1966), he dealt with an autopilot design. In a 1972 paper, he applied discrete optimal control to a missile system with undesirable stability characteristics, and then modified the dynamics to yield a new problem with more desirable characteristics.

An excellent review of deterministic optimal control and its applications, with an extensive bibliography, is found in an IEEE paper by Athans (1966). Another excellent review with extensive references is in a 1965 AIAA paper by Paiewonsky. Kokotovic and Rutman (1965) provided a survey of sensitivity methods drawing heavily upon Soviet literature.

Some early authors, in an attempt to justify the resulting guidance laws achieved via linear optimal control, showed that their results were an extension of PNG. Axelband and Hardy (1969, 1970) used linear optimal control to develop what they called quasi-optimum PNG. As with almost all linear optimal schemes, time-to-go is required for implementation.

Lee (1969) described several techniques in nonlinear control which extended the linear regulator theory and drew heavily upon recent dissertations at the University of Minnesota.

Deyst and Price (1973) used linear dynamics with a planar engagement to develop optimal control laws where the target acceleration was a first-order Markov process, and found that the saturation of control surfaces was an important factor in modeling a maneuver limited missile.

Nazaroff (1976) formulated an LQG approach in which he assumed extremely simplified missile dynamics but included target acceleration and jerk terms. Stockum and Wiener (1976) assumed exponentially correlated target accelerations in generating an LQG guidance law. The feedback they obtained on projected miss distance and rate was analogous to time-varying PNG. They compared their guidance scheme against an augmented PNG law.

Asher and Matuszewski (1974) considered the optimal control problem where target acceleration was accounted for as an external disturbance, resulting in a tracking formulation of the regulator problem. They constrained the final miss distance to be zero but, to achieve this, needed to know the target acceleration history precisely.

Balbirnie, Sheporaitis, and Merriam (1975) gave a means to obtain weighting matrices which result in "classical type" control gains in an LQG formulation. Sheporaitis, Balbirnie, and Liebner (1976) considered a quadratic cost on the angle of attack. They used a second order Newton-Raphson scheme to solve the resulting optimization problem.

Speyer (1976) applied his linear-exponential-Gaussian (LEG) controller to a terminal guidance problem. Rather than minimizing the expectation of a quadratic form J_2 (as given previously), Speyer's LEG formulation minimizes $E\left\{\mu \exp\left(\frac{1}{2}\mu J\right)\right\}$ where μ is a scalar. The dynamical model is again linear. Speyer used a Kalman filter to obtain estimates of state variables for feedback. His controller did not enjoy a separation principle; control gains depended upon the filter state covariance. Speyer's LEG cost functional had the effect of very heavily weighing large excursions and thus reduced the tails of the terminal miss distribution.

Youngblood (1977) used very simplified linear dynamics to compute inner launch boundaries. Youngblood's report contains a description of the Fletcher-Powell functional optimization method.

Fiske developed a number of guidance and estimation schemes based upon LQG formulations with varying degrees of model complexity. The closed form solutions for the controllers are given in the report, allowing one to examine the effect of model parameters on the gains. Fiske also presents a stochastic guidance law, wherein the target acceleration is assumed to be a first order system driven by white noise. In addition, a nonlinear law, based upon nulling projected miss distance over a single control interval was given. York and Pastrick (1977) looked at the problem of minimizing the terminal miss distance and the deviation of the missile from a desired orientation at the final time. A formulation was given for a system that had finite time delay. In fact, the increase and decrease in time delay had interesting ramifications on the solution. The angle of attack assumption was investigated and, although not solved analytically in closed form, the system was derived.

For completeness, the following example summarizes a typical optimal control law formulation. The geometry of the tactical missile-target position is given in Figure 10. Assume that the angle of attack is small and thus can be neglected (this assumption will be considered later), and choose the following set of variables:

$$x = \begin{bmatrix} Y_d \\ \dot{Y}_d \\ A_L \\ \theta \end{bmatrix} \equiv \begin{bmatrix} Y_t - Y_m \\ \dot{Y}_t - \dot{Y}_m \\ A_L \\ \theta \end{bmatrix} \quad (10)$$

where Y_d is the position variable from the missile to the target projected on the ground; Y_t is the position variable of the target; Y_m is the

position variable of the missile projected on the ground; \dot{Y}_d is the derivative of Y_d , the missile to the target velocity projected on the ground; A_L is the lateral acceleration of the missile; θ is the body attitude angle of the missile; and α is the angle of attack of the missile shown in Figure 10.

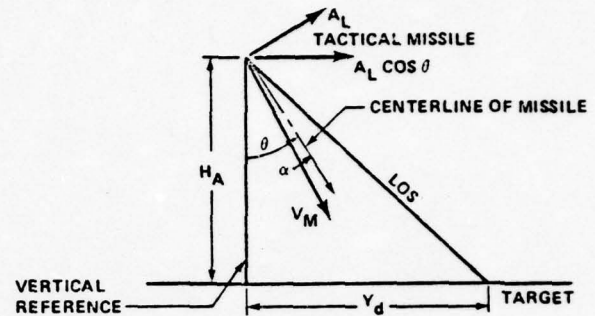


Figure 10. Geometry of Tactical Missile Target Positions

This optimal control problem will have a controller of the form

$$u = C_Y Y_d + C_{\dot{Y}} \dot{Y}_d + C_{\theta} \theta + C_{A_L} A_L \quad (11)$$

where C_Y , $C_{\dot{Y}}$, C_{θ} , and C_{A_L} are time-varying coefficients chosen to minimize the cost functional

$$J = Y_d(t_f) + \gamma \theta(t_f) + \beta \int_0^{t_f} u^2(t) dt \quad (12)$$

For the case where the angle of attack probably cannot be ignored e.g., for the larger tactical missile, the system of equations should include the angle of attack α . In addition, because it is feasible to achieve only a small angle of attack at impact, a reasonable performance index to be minimized would seem to be

$$J = C_1 Y_d^2(t_f) + C_2 \theta^2(t_f) + C_3 \alpha^2(t_f) + C_4 \int_{t_0}^{t_f} u^2(t) dt. \quad (13)$$

The performance obtainable from the optimal guidance law formulated and simulated for Equation (13) was comparable and even better than the PNG law in terms of miss distance. Additionally, it had the added feature of meeting a constraint or the impact angle which the PNG law could not achieve. In particular the impact angle was shown via simulation on an all-digital 6-DOF missile simulation to be within 1 deg of the desired impact angle and within 1 ft of the desired miss distance. Other researchers have corroborated these results.

The performance of any realistic optimal control law in a missile application is dependent on the estimation of final time or, equivalently, on

time-to-go. Typically, an estimate of the range between the target and missile, and the rate of change of this range are obtained from radar or other ranging devices; the time-to-go estimate is then calculated. This estimate works quite well as long as the range and range-rate information are accurate. In many instances, however, the data are contaminated by noise either covertly, as in the case of radar jamming devices, or by the processing electronics. This adversely impacts the estimate of time-to-go and the optimal control law, and missile performance suffers. Pastrick and York (1977) present a discussion of several aspects of the problem in the context of a realistic application and provide analytic computer algorithms for its solution, as well as a closed-form result. Another more recent attempt to estimate time-to-go was made by Fiske. He also addresses the possibility of obtaining this variable by an intensity ranging technique.

Another difficulty with optimal guidance laws is their sensitivity to initial conditions, as shown by York (1978). The primary message therein is the strong need for accurate modeling of the system and the importance of the selection of numerical quantities for the elements of the weighting matrices in the performance index.

Other Guidance Schemes

Whiting and Jobe (1972) considered using a "virtual target" approach to guidance for a short range air-to-ground missile.

Poulter and Anderson (1976) considered a nonlinear differential game framework to derive an optimal steering law for a terminal homing missile. In a prior paper, Anderson (1974) gave a method of updating a differential game solution via linearized two-point boundary value problems.

For background material, Froning and Giesecking (1973) gave a description of autopilot steering mechanisms for bank-to-turn missiles. Gido, Jaffe, and Wilson (1974) provided computer programs to produce autopilot designs using both classical (PNG) and modern (LQG) formulations. George (1974) discussed trends in IMU, guidance and control hardware.

Mahmoud (1977) described a dual level, hierarchical optimization scheme based on invariant imbedding which is used to obtain approximate solutions to many nonlinear control problems. Connor and Vlach (1977) presented a new augmented penalty function approach to optimal control problems. Their formulation is applicable to finite dimensional optimization problems with terminal constraints.

Lansing and Battin (1965) presented much background material on random processes applied to automatic control. Radbill and McCue (1970) provided background material on quasi-linearization methods in solving coupled nonlinear two-point boundary value problems.

Chin's book on missile design (1961) has a section on missile transfer functions which is very useful in assessing the contribution of aerodynamic factors and control surfaces to missile motion. Goodstein (1972) provided an overview of missile control system development and, in the same AGARD report, Acus (1972) presented a description and comparison of inertial guidance technology for tactical missiles.

III. Discussion

A survey has been made of guidance laws applied to short range tactical missiles, and they have been organized into five categories for convenience of discussion.

To better place them in relative perspective, Figure 11 presents the hardware requirements for mechanizing them. Though the concepts are reasonably self explanatory, it should be noted that the BR and CLOS concepts are configured with aft sensor and optics while the others are forward. Also, the optimal guidance scheme suggests the need for a microprocessor to handle the more complex guidance algorithms.

Guidance concept configuration comparisons depicted in the Table feature the relative cost and other items that show complexity and performance. With the exception of the microprocessor requirement

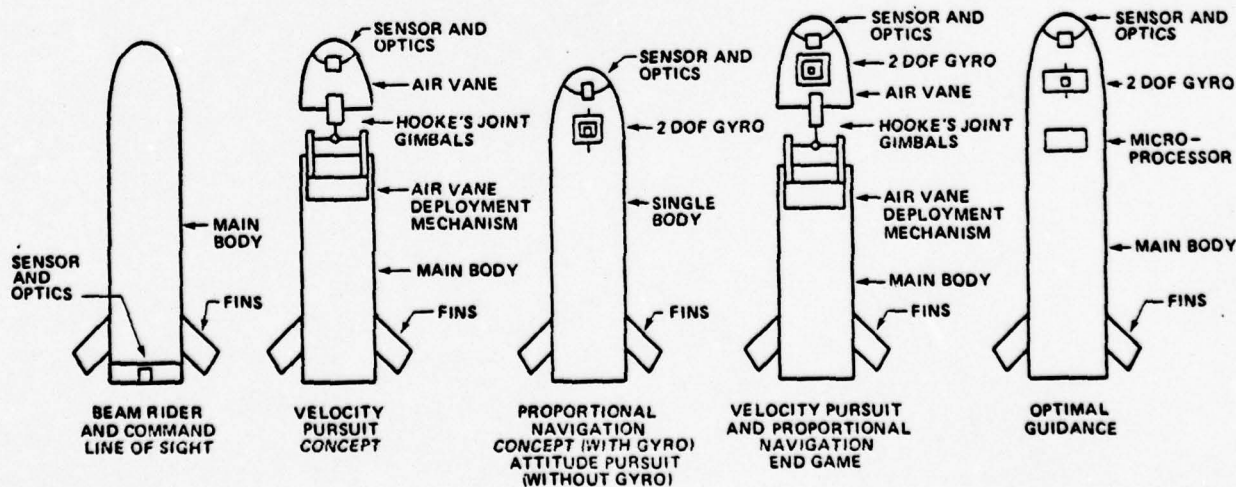


Figure 11. Instrumentation Configuration Concepts

Table. Guidance concepts configuration comparison

Guidance Concept	Accuracy (ft)	Gyroscope	Gimbal Mechanism (Sensor)	Electronics (On-Board)	Control Effort	Relative Cost (On-Board)
Attitude Pursuit	> 30	None	None	Same	High Turning Acceleration Required	1.0
Velocity Pursuit	> 20	None	Air Vane	Same		1.4
PNG	< 5	Single 2 DOF Gyro	Gyro	Same	Low Turning Acceleration Required	1.6
Beam Rider	< 2	Attitude	None	Same		0.9
CLOS	< 2	Attitude	None	Same		0.8
Optimal	<	2 DOF Gyro	Gyro	Micro-processor	High Turning	1.6

for the optimal guidance law all onboard electronics are relatively comparable. However, it is important to note that the CLOS and BR concepts have vastly more complex ground stations inherent in their mechanizations. For this reason alone, their airborne complexity is relatively low and less expensive compared to the others implying that their ground trackers are not included in that cost estimate.

Barring unforeseen breakthroughs in the fifth category (Other Guidance Schemes), comparison of performance characteristics favors PNG for defeating targets that are either stationary or moving with a constant velocity. PNG is simple, requires a state measurement that is easily attainable, and is relatively easy to implement. However, for highly maneuverable accelerating (or decelerating) targets, optimal guidance laws are superior, performance-wise, to other forms of guidance. Further, if miss distance is the only criterion of performance, PNG is favorable. If other performance criteria are important, such as impact angle at the target, then these criteria can be incorporated into the performance index and optimal guidance becomes superior.

As indicated, most linear optimal guidance laws require time-to-go to be implemented. Thus far, a means of measuring this important variable has not been devised, although considerable attention has been given to its estimation. Development of a means of measuring time-to-go is an item that will be addressed in the MIRADCOM task to develop an advanced guidance and control system for future U.S. Army modular missiles.

Because of the anticipated small size and light weight of future microcomputers, maximum use will be made of the program flexibility offered by digital implementation of guidance laws (including state estimators or observers, if utilized) and autopilots. It is planned to exploit digital characteristics in this task while remaining within the constraints imposed by the digital sampling phenomena such as quantization and finite word length. The difficulties inherent in predicting and analyzing the effects of system nonlinearities are compounded with a digital system and must be addressed in the development of any advanced guidance and control system.

IV. Conclusion

When the performance comparisons and anticipated implementation difficulties are considered, the following conclusion is reached. PNG is a strong contender but cannot cope with all expected targets of the future. Therefore, optimal guidance is the chosen candidate guidance law, even with its added complexity and current implementation difficulties. However, these may be alleviated with judicious use of the microprocessor technology now enjoying a high state of development activity. Considerable effort will have to be devoted to overcoming what appears to be its strongest shortcoming: measuring or accurately estimating the time-to-go.

Bibliography

- M. J. Abzug, "Final-Value Missile Homing Guidance," J. Spacecraft and Rockets, pp. 279-280, Feb. 1967.
- R. W. Acus, "Self-Contained Guidance Technology," AGARD Report: Guidance and Control of Tactical Missiles, May 1972.
- F. Adler, "Missile Guidance by Three-Dimensional Proportional Navigation," J. Applied Physics, pp. 500-507, 1956.
- A. Y. Adrienko and A. A. Muranov, "Statistical Synthesis of a Sampled-Data Terminal Control System for Multipurpose Object," Automation and Remote Control, pp. 14-21, May 1973.
- G. M. Anderson, "A Near Optimal Closed-Loop Solution Method for Nonsingular Zero-Sum Differential Games," J. Optimization Theory and Applications, Vol. 13, No. 3, pp. 303-318, 1974.
- G. M. Andrew, "Control and Guidance Systems with Automatic Aperiodic Sampling," J. Spacecraft and Rockets, pp. 59-60, Dec. 1970.
- J. F. Andrus, I. F. Burns and J. Z. Woo, "Study of Optimal Guidance Algorithms," AIAA Journal, pp. 2252-2257, Dec. 1970.
- K. Arbenz, "Proportional Navigation of Nonstationary Targets," IEEE Trans. Aerospace and Electronic Systems, pp. 455-457, July 1970.

- R. S. White and J. C. Mattingly, "Optimal Guidance of Finite Bandwidth System with Zero Terminal Miss," AIAA Guidance and Control Conf., pp. 110-119, 1974.
- R. S. White and J. C. Mattingly, "Optimal Guidance for Nonlinear Systems," AIAA Journal, pp. 1180-1186, March 1974.
- M. Athans, "The Status of Optimal Control Theory and Applications to Optimal Control Systems," Trans. Auto. Control, pp. 500-501, 1971.
- M. Athans, "On Optimal Allocation of Control Effort for Linear Interception and Rendezvous Problems," IEEE Trans. Aerospace and Electronic Systems, pp. 843-853, Sept. 1971.
- E. I. Axelband and F. W. Hardy, "Quality of Optimal Proportional Navigation," 2nd Hawaii Int. Conf. Sys. Sciences, pp. 417-421, 1969.
- E. I. Axelband and F. W. Hardy, "Optimal Feedback Missile Guidance," 3rd Hawaii Int. Conf. Sys. Sciences, pp. 874-877, 1970.
- E. C. Balbirnie, L. P. Sheporaitis and C. W. Merriam, "Merging Conventional and Optimal Control Techniques for Practical Missile Terminal Guidance," AIAA Guidance and Control Conf., AIAA paper 75-1127, 1975.
- G. Bashein and C. P. Neuman, "Linear Feedback Guidance for Interception and Rendezvous in a Stochastic Environment," 1st Hawaii Int. Conf. Sys. Sciences, pp. 654-657, 1968.
- S. M. Brainin and R. B. McGhee, "Optimal Biased Proportional Navigation," IEEE Trans. Auto. Control, pp. 440-442, Aug. 1968.
- A. S. Bratus, "Approximate Solution of Bellman's Equation for a Class of Optimal Terminal State Control Problems," J. Applied Math and Mechanics, Vol. 37, No. 3, pp. 396-407, 1973.
- A. E. Bryson, Jr., "Applications of Optimal Control Theory in Aerospace Engineering," 10th AIAA Minta Martin Memorial Lecture, Cambridge, Mass., 1966.
- A. E. Bryson, Jr., W. F. Denham and S. E. Dreyfus, "Optimal Programming Problems with Inequality Constraints I: Necessary Conditions for External Solutions," AIAA Journal, pp. 2544-2550, Nov. 1963.
- C. S. Chang, "A Terminal Guidance Theory Using Dynamic Programming Formulation," AIAA Journal, pp. 912-916, May 1970.
- A. A. Chikrii, "Nonlinear Problem of Evasion of Contact with Terminal Set of Complex Structure," J. Applied Math and Mechanics, Vol. 39, No. 1, pp. 3-11, 1975.
- S. S. Chin, Missile Configuration Design, McGraw-Hill, pp. 130-154, 1961.
- J. Clemow, Missile Guidance, Temple Press Unlimited, London, 1960.
- M. A. Connor and M. Vlach, "A New Augmented Penalty Function Technique for Optimal Control Problems," J. Optimization Theory and Applications, pp. 39-49, Jan. 1977.
- E. P. Connaughton, "Double Manoeuvring Terminal Control for Missile Guidance," J. Spacecraft and Rockets, pp. 11-121, Jan. 1964.
- M. I. Dandam, "Banked Maximum Acceleration Surface-to-Surface Missile with Inequality Inequality Constraints," J. Spacecraft and Rockets, pp. 78-83, Jan. 1964.
- W. F. Denham and S. E. Dreyfus, "Optimal Programming Problems with Inequality Constraints II: Solution by Steepest Descent," AIAA Journal, pp. 25-34, Jan. 1964.
- J. J. Doyst and C. E. Price, "Terminal Stochastic Guidance Laws for Tactical Missiles," Spacecraft and Rockets, pp. 301-308, May 1974.
- R. E. Dickson and V. Garber, "Optimal Rendezvous, Intercept and Injection," AIAA Journal, pp. 1402-1403, July 1969.
- P. H. Fiske, "Advanced Digital Guidance and Control Concepts for Air-to-Air Tactical Missiles," The Analytical Sciences Corporation Technical Report, Dec. 1977.
- H. D. Froning and D. L. Gieseking, "Bank to Turn Steering for Highly Maneuverable Missiles," AIAA Guidance and Control Conf., AIAA paper, 73-860, 1973.
- Y. Gemin, "Polynomial Approximations in Perturbational Navigation and Guidance Schemes," Advanced Problems and Methods for Spaceflight Optimization, edited by B. F. de Veubeke, Pergamon Press, Oxford, pp. 13-24, 1969.
- L. C. George, "Missile Guidance and Control System Design Trends," SAE National Aerospace Engineering and Manuf. Meeting, SAE paper 740873, 1974.
- J. F. Gido, R. C. Jaffe and R. G. Wilson, "Merging Conventional and Modern Control Techniques for Practical Missile Autopilot Design," AIAA Mechanics and Control of Flight Conf., AIAA paper 74-911, 1974.
- R. Goodstein, "Development of Control System Requirements," AGARD Report: Guidance and Control of Tactical Missiles, May 1972.
- R. Goodstein, "Guidance Law Applicability to Missile Closing," AGARD Report: Guidance and Control of Tactical Missiles, May 1972.
- P. C. Gregory, "General Considerations in Guidance Control Technology," AGARD Report: Guidance and Control of Tactical Missiles, May 1972.
- P. C. Gregory, P. B. Teets and B. G. Lee, "Guidance, Navigation and Control," Space/Aeronautics, pp. 61-66, July 1969.
- K. V. Grider, W. E. Jordan and M. Kim, "Suboptimal Guidance for Attitude Angle Constrained Flight Trajectories," 6th Hawaii Int. Conf. Sys. Sciences, pp. 455-457, 1973.
- M. Guelman, "A Qualitative Study of Proportional Navigation," IEEE Trans. Aerospace and Electronic Systems, pp. 337-343, July 1971.

- M. Guelman, "Proportional Navigation with a Manuevering Target," IEEE Trans. Aerospace and Electronic Systems, pp. 364-371, May 1972.
- M. Guelman, "The Closed Form Solution of True Proportional Navigation," IEEE Trans. Aerospace and Electronic Systems, pp. 472-482, July 1976.
- G. L. Harmon, K. E. Kent and W. P. Purcell, "Optimal Bang-Bang Guidance System," Western Electric Show and Convention, Part 5, paper 19.1, 1962.
- Y. C. Ho, "Optimal Terminal Maneuver and Evasion Strategy," SIAM J. Control, Vol. 4, No. 3, pp. 421-428, 1966.
- Y. C. Ho, A. E. Bryson, Jr. and S. Baron, "Differential Games and Optimal Pursuit-Evasion Strategies," IEEE Trans. Auto. Control, pp. 385-389, Oct. 1965.
- R. M. Howe, "Guidance," Chapter 19 appearing in System Engineering Handbook, ed. by R. E. Machol, W. P. Tanner, Jr. and S. N. Alexander. McGraw-Hill, NY 1965.
- S. S. Hu and M. L. Thompson, "A Direct and Analytical Solution for Space Flight Guidance Functions," AIAA Aerospace Sciences Meeting, 1966.
- L. A. Irish, "A Basic Control Equation for Rendezvous Terminal Guidance," IRE Trans. Aerospace and Navigational Electronics, pp. 106-113, Sept. 1961.
- W. H. Ito and J. E. Tushie, "P-Matrix Guidance," AIAA/ION Astrodynamics Guidance and Control Conf., Aug. 1964.
- A. Ivanov, "Radar Guidance of Missiles," IEEE International Conf., pp. 321-335, 1975.
- J. E. Kain and D. J. Yost, "Command to Line-of-Sight Guidance: A Stochastic Optimal Control Problem," AIAA Guidance and Control Conf., AIAA paper 76-1956, 1976.
- J. E. Kain and D. J. Yost, "Target Estimation in an ECM Environment," J. Spacecraft and Rockets, pp. 492-498, Aug. 1975.
- M. Kim and K. V. Grider, "Terminal Guidance for Impact Attitude Angle Constrained Flight Trajectories," IEEE Trans. Aerospace and Electronic Systems, pp. 852-859, Nov. 1973.
- P. V. Kokotovic and R. S. Rutman, "Sensitivity of Automatic Control Systems (Survey)," Automation and Remote Control, pp. 727-749, April 1965.
- J. H. Laning, Jr. and R. H. Battin, Random Processes in Automatic Control, McGraw-Hill, pp. 239-247, 1965.
- E. B. Lee, "Recent Development in the Theory of Optimal Control and Their Application," Proc. Technical Seminar on Guidance and Control, Huntsville, Alabama, Aug. 1969.
- I. Lee, "Optimal Trajectory, Guidance and Conjugate Points," Information and Control, pp. 589-606, 1965.
- M. H. Liu and K. W. Han, "Model Reduction of a Non-linear Control System," J. Spacecraft and Rockets, pp. 786-788, Dec. 1975.
- A. S. Locke, Guidance, D. Van Nostrand Co. Princeton, 1955.
- D. F. McAllister and E. E. Schiring, "Optimizing Thrust Vector Control for Short Powered Flight Maneuvers," appearing in Space Electronics Symposium, ed. by C. M. Wong, American Astronautical Society, 1965.
- B. A. McElhoe, "Minimal-Fuel Steering for Rendezvous Homing Using Proportional Navigation," American Rocket Society Journal, pp. 1614-1615, Oct. 1962.
- J. A. Meyer and J. G. Bland, "Minimum Information Terminal Homing Guidance," Nat. Elect. Conf., pp. 703-708, Oct. 1966.
- J. F. Muller, "Synthesis of a Guidance System for a Short Range Infantry Missile," J. Spacecraft and Rockets, pp. 314-317, March 1969.
- S. A. Murtaugh and H. E. Criel, "Fundamentals of Proportional Navigation," IEEE Spectrum, pp. 75-85, Dec. 1966.
- N. Nagarajin, "Discrete Optimal Control Approach to a Four Dimensional Guidance Problem Near Terminal Areas," Int. J. Control, pp. 277-288, Aug. 1974.
- G. J. Nazarov, "An Optimal Terminal Guidance Law," IEEE Trans. Auto. Control, pp. 407-408, June 1976.
- N. J. Niemi, "Investigation of a Terminal Guidance System for a Satellite Rendezvous," AIAA Journal, pp. 405-411, Feb. 1963.
- B. Paiwosky, "Optimal Control: A Review of Theory and Practice," AIAA Journal, pp. 1985-2006, Nov. 1965.
- H. L. Pastrick, "Filtering Inertial System Errors to Improve Terminal Sector Navigation," Proc. South-eastern Symp. Sys. Theory, 1974.
- H. L. Pastrick and R. J. York, "On the Determination of Unspecified t_f in a Guided Missile Optimal Control Law Application," Proc. 1977 IEEE Conference on Decision and Control, 1977.
- C. Pfeiffer, "A Successive Approximation Technique for Constructing a Near-Optimum Guidance Law," Int. Astronautical Conf., Astrodynamics, Guidance and Control, Miscellanea, pp. 285-291, 1967.
- D. L. Pitman, "Adjoint Solutions to Intercept Guidance," AGARD Report: Guidance and Control of Tactical Missiles, May 1972.
- J. E. Potter, "A Guidance-Navigation Separation Theorem," AIAA/ION Astrodynamics Guidance and Control Conf., Aug. 1964.
- R. A. Poulter and G. M. Anderson, "A Guidance Concept for Air-to-Air Missiles Based on Nonlinear Differential Game Theory," National Aerospace Electronics Conf., pp. 605-9, 1976.

D. L. Quam, "Missile Aerodynamic Sensitivity Analysis," AIAA Preprint, 1978.

J. R. Radbill and G. A. McCue, Quasilinearization and Nonlinear Problems in Fluid and Orbital Mechanics, American Elsevier, New York, pp. 1-21, 1970.

E. R. Rang, "A Comment on Closed-Loop Optimal Guidance Systems," IEEE Trans. Auto. Control, pp. 616-617, July 1966.

A. G. Rawling, "On Nonzero Miss Distance," J. Spacecraft and Rockets, pp. 81-83, Jan. 1969.

A. G. Rawling, "Prediction of Terminal Variables in Homing," J. Spacecraft and Rockets, pp. 764-766, June 1970.

A. G. Rawling, "Nonlinear ProNav and the Minimum Time to Turn," J. Spacecraft and Rockets, pp. 198-201, February 1971.

R. W. Rishel, "Optimal Terminal Guidance of An Air to Surface Missile," AIAA Guidance, Control and Flight Dynamics Conference, Aug. 1967.

D. M. Salman and W. Heine, "Reachable Sets Analysis - An Efficient Technique for Performing Interceptor/Sensor Tradeoff Studies," AIAA Guidance and Control Conf., AIAA paper 72-825, 1972.

C. E. Seal and A. R. Stubberud, "Final Value Control Systems," appearing in Advances in Control Systems Theory and Application, Vol. 8, pp. 23-52, 1971.

L. P. Sheporaitis, E. C. Balbirnie and G. A. Liebner, "Practical Optimal Steering for Missile Terminal Guidance," AIAA Guidance and Control Conf., AIAA paper 76-1917, 1976.

J. Shinar, "Divergence Range of Homing Missiles," Israel J. Technology, pp. 47-55, Vol. 14, 1976.

G. M. Siouris, "Comparison Between Proportional and Augmented Proportional Navigation," Nachrichten-technische Zeitschrift, pp. 278-280, July 1974.

G. L. Slater and W. R. Wells, "Optimal Evasive Tactics Against a ProNav Missile with Time Delay," J. Spacecraft and Rockets, pp. 309-313, May 1973.

K. Smith, "A Comparison of the Control Problems of Missiles and Manned Aircraft," J. Royal Aeronautical Society, pp. 177-185, March 1962.

J. L. Speyer, "An Adaptive Terminal Guidance Scheme Based on an Exponential Cost Criterion with Application to Homing Missile Guidance," IEEE Trans. Auto. Control, pp. 371-375, June 1976.

J. L. Speyer, "A Stochastic Differential Game with Controllable Statistical Parameters," IEEE Trans. Sys. Sciences and Cybernetics, pp. 17-20, June 1967.

D. V. Stallard, "Discrete Optical Terminal Control with Application to Missile Guidance," Joint Auto. Control Conf., pp. 499-508, 1972.

A. M. Steinberg and K. Shmueli, "On the Terminal Control Problem," J. Optimization Theory and Applications, Vol. II, pp. 313-320, March 1973.

A. R. Stubberud, "Theory of Pitch Steering for Ascent Guidance," Nat. Space Navigation Meeting, pp. 136-160, March 1967.

L. A. Stockum and F. C. Weimer, "Optimal and Sub-optimal Guidance for a Short-Range Homing Missile," IEEE Trans. Aerospace and Electronic Systems, pp. 355-360, May 1976.

A. I. Talkin, "Homing by Steepest Descent," IEEE Trans. Auto. Control, pp. 136-137, Jan. 1966.

W. Templeman, "Linearized Impulsive Guidance Laws," AIAA Journal, pp. 2148-2149, Nov. 1965.

L. Teng and P. L. Phipps, "Application of Nonlinear Filter to Short Range Missile Guidance," Proc. National Aerospace Electronics Conf., pp. 439-449, 1967.

R. Thibodeau and J. B. Sharp, "PDM Control Analysis Using the Phase Plane," J. Spacecraft and Rockets, pp. 1054-1057, Sept. 1969.

F. Tung, "An Optimal Discrete Control Strategy for Terminal Guidance," Joint Auto. Control Conf., pp. 499-507, 1965.

J. T. Wagner and D. F. McAllister, "Simplified Performance Analysis of Space and Missile Guidance," American Astronautical Society and ORSA, June 1969.

R. S. Warren, C. F. Price, A. Gelb, and W. E. VanderVelde, "Direct Statistical Evaluation of Non-linear Guidance Systems," AIAA Guidance and Control Conf., AIAA paper 73-836, 1973.

J. H. Whiting and J. W. Tube, "Virtual Target Steering - A Unique Air-to-Air Surface Missile Targeting and Guidance Technique," AIAA Guidance and Control Conf., AIAA paper 72-826, 1972.

T. W. J. Wong, "Guidance Systems for Air-to-Air Missiles," INTERAVIA, pp. 1525-1528, Nov. 1961.

J. Youngblood, "Optimal Guidance of Air-to-Air Missile," University of Alabama Report, Nov. 1977.

R. J. York and H. L. Pastrick, "Optimal Terminal Guidance with Constraints at Final Time," J. Spacecraft and Rockets, pp. 381, June 1977.

R. J. York, "Optimal Control for an Anti-Tank Weapon," Final Report, U.S. Army MIRADCOM Contract No. DAKR 70-78-M-0102, September 1978.

APPENDIX G. SIG-D EVALUATION

DISPOSITION FORM

For use of this form, see AR 340-15, the proponent agency is TAGCEN.

REFERENCE OR OFFICE SYMBOL	SUBJECT
DRDMI-TGN	Redteam of SIG-D Program

TO DISTRIBUTION FROM DRDMI-TG DATE 19 January 79 CMT 1

1. The flight tests of those SIG-D rounds to be launched at WSMR are scheduled to begin in late FY-79. To insure technical thoroughness and completeness, a team is appointed to conduct an in depth review of the program to date. The review will be conducted 8-9 February 1979.

2. The team members are:

Russ Gambill	6-1187	Chairman
Sherm Seltzer	6-5954	Theory and Design
Jim McLean	6-2797	Integration
Ray Deep	6-5216	Aerodynamics
(Gibson) Gerald Matthews	6-1847	Structures and Launcher
Niles White	6-2612	Propulsion
Vic Ruwe	6-3848	Electronics and Cables
Jim Brown	6-3643	Software
Bill Stripling	6-8331	Inertial
Bill Malcolm	6-1225	Control Actuator System
Charles Northrop	6-3556	Testing, Instrumentation and Launch Operations

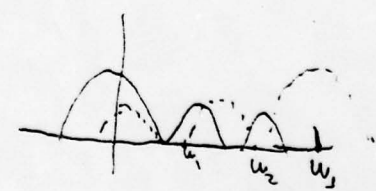
J. B. Huff
J. B. HUFF

Director
Guidance and Control Directorate
Technology Laboratory

DISTRIBUTION:

- DRDMI-EA, Mr. Northrop
- Mr. Ruwe
- TGC, Mr. Malcolm
- TGG, Mr. Brown
- TGL, Mr. Stripling
- TGN, Mr. Gambill
- Dr. Seltzer
- Mr. McLean
- TE, Mr. Deep
- TKC, Mr. White
- TL, Mr. Matthews

To



1) Anal - great way to check it
2) SOLVED
3) ANAL (orig)
4) KWIL/NYBRIO: Egg in basket - allow more t?
5) SIM DESIGN
6) ISOLATION FOR VIBRATION
7) OTHER MATH - Vib, T

2) Soln
3) Key in NW... late
4) Good sim program
5) Isolation
6) other math

II. THEORY AND DESIGN

By

Sherman M. Seltzer

1. Organization.

In an attempt to provide the reader with a logical approach to the review of the theory and design associated with the SIG-D Program, the material comprising that review is presented in the following sequence:

- a. Program objectives,
- b. Design approach,
- c. Analysis program,
- d. Simulation program,
- e. Hardware testing program,
- f. Proof of concept,
- g. Schedule,
- h. Summary and conclusions.

2. Program objectives.

As stated by Jack Clayton during the February 8-9, 1979 review, "The SIG-D Program is an exploratory development effort to investigate the technical risk areas associated with a low cost surface to surface missile utilizing a strap-down inertial navigation and guidance system." If it is intended to use SIG-D on missiles other than the particular modified LANCE upon which design has been based, certain system alterations probably will be required. As described in the presentation, SIG-D is tied closely to the characteristics of the modified Lance system on which it is carried. In particular, the bending characteristics of the modified LANCE have strong impact upon the SIG-D design. Bending filter design, computer storage capacity, the isolation system, and the selected sampling period of the computer probably all will be affected if SIG-D is used to guide a missile other than the modified LANCE.

3. Design approach.

The design approach is orderly, logical, and being implemented by apparently superb engineers. The innovative analytical techniques that have been brought to bear on the SIG-D design are outstanding. An exception to the conservative approach demonstrated throughout concerns computer memory capacity. It was stated..

that a margin of 75 words of memory still remains. I feel this is too small a margin to be entering into the hybrid and hardware-in-the-loop (HWIL) stages of (potential) design refinement. If additional memory should become required, it may be necessary to physically add an additional memory module. The possibility of decreasing memory requirements by performing a sampled-data analysis with the aim of decreasing sampling period might be considered as an alternative. Bending mode constraints then would have to be considered also.

At first I planned to recommend looking deeper into the potential problem posed by heretofore undetected sources of vibration. An example (the only one that I can think of, but there may be others) is the external cable conduit (or "tunnel"). If it were to become unbonded from the skin of the missile during the guided portion of the flight, its vibration characteristics might have an undesirable dynamic effect on the G&C system. Upon further investigation I found that this problem has been studied thoroughly. In the case of the cable conduit, the masses concerned are relatively negligible.

A design decision made at the outset of the program was to use the Ring Laser Gyroscope, presumably because of its low cost. According to Mr. Clayton, it has undergone extensive sled and missile ("UPSTAGE Program") testing, although never in the strapdown mode of operation. This should be adequate.

4. Analysis program.

As already indicated, the analysis used has been thorough and excellent in quality. Although I personally am wary of using continuous time-domain techniques to approximate sampled-data dynamic phenomena, I believe it is justified in the case at hand because of the relatively high sampling rate (the latter being set by the frequency of the highest dominant bending mode). Even the use of a continuous time-domain describing function analysis appears to have been adequate to predict the existence and characteristics of limit cycles and was stated to have been verified by simulation. This is a tribute to the engineering judgement of Ed Herbert and Dr. Paul Jacobs in particular.

Apparently the design team has searched for all dynamically significant nonlinearities and has identified only the pneumatic actuator nonlinearity. Certainly a complete HWIL simulation will show if the search results were correct (and I think they are).

If time were available, I would recommend a more conventional sampled-data analysis of a simplified (for analytical tractability) model of the system. At this late date I think a careful simulation should be adequate.

The IMU mounting plate and vibration isolation system are critically important to the performance of the G&C system. This fact has been duly recognized, and supporting analysis has been conducted. Extensive analysis (supported by hardware tests--see section 6, below) has been performed to validate the system design, using the NASA Structural Analysis (NASTRAN) program. This analysis included the identification of a number of the relatively lower longitudinal and torsional normal (free-free) bending modes. The analysis was performed for both loaded (i.e. "powered" flight) and unloaded ("post-cut-off") motor case conditions.

5. Simulation program.

Usually simulation and analysis are held to a minimum by program managers. In this instance, there appears to be an over-abundance of simulation programs, although this situation is the result of an orderly progression from all-digital simulations toward an HWIL simulation. There was some indication that agreement between the various MIRADCOM and Vought programs does not exist. The reasons for this disagreement were explained during and subsequent to the formal presentation. Of course, ultimate agreement must be sought. The hybrid and the HWIL simulations are extremely valuable design tools. It is my opinion that not enough time is allocated for their use. It is not apparent why the rush, when much valuable information should be forthcoming from the use of these two simulations.

6. Hardware testing program.

Apparently the pneumatic actuator characteristics have been confirmed by actual test. It also was stated that the isolator characteristics have been confirmed by test.

In support of the vibration analysis (see para. 4, above), vibration testing was performed on a suspended post cut-off-configuration (i.e. empty motor case) of the modified LANCE missile. There was reasonably close agreement between analytically-derived results and these test results. Apparently monetary and schedule constraints precluded a test of a simulated boost configuration (i.e. simulated propellant characteristics) as well as tests to confirm predicted torsional characteristics. In view of the previously noted agreement between analytical and test longitudinal vibrations, this is probably an acceptable risk.

7. Proof of concept.

If the time allotted to HWIL and hybrid simulations is lengthened, and if additional vibration analysis is performed, there appears no doubt that the design concept can be proven sufficiently for flight testing to begin. With a few minor exceptions, simulation results appear to agree: these exceptions should be explained. It was not shown if the several error analysis discussed were in agreement.

8. Schedule.

As already indicated, it is my opinion that the schedule is too tight to permit adequate hybrid and HWIL simulation.

9. Summary and conclusions.

The review was extremely well-conducted and presented ample evidence of a thorough, well-conceived and implemented design. The SIG-D design team is to be commended for their fine work. The following recommendations summarize the few shortcomings associated with the SIG-D theory and design.

a. Prepare a contingency plan to cope with the possibility that insufficient computer storage capacity may exist (para. 3).

b. Conduct a careful analysis of the dynamic effects of the digital phenomena as manifested in the HWIL and hybrid simulations. Be careful to discriminate between simulated on-board sampling phenomena and those sampling phenomena that arise because of the digital computer used for the simulation (para. 4).

c. Allot more time in the schedule for an orderly, indepth use of the hybrid and HWIL simulations (para. 5).

I
II
III
IV
V
VI
VII
VIII
IX
X
XI
XII
XIII
XIV
XV
XVI
XVII
XVIII
XIX
XX
XXI
XXII

APPENDIX H. HELLFIRE WHITE PAPER

DISPOSITION FORM

For use of this form, see AR 340-15, the proponent agency is TAGCEN.

REFERENCE OR OFFICE SYMBOL

DRDMI-TGN

SUBJECT

HWIL Simulation for HELLFIRE

TO DRCPM-HF

FROM DRDMI-TGN

DATE 15 Sep 78 CMT 1
Dr. Pastrick/nrr/6-5954

1. On 10 August 1978, engineers from the Guidance and Control Analysis Group were invited by personnel of the HELLFIRE Project Office to discuss the status of the group's HWIL simulation capability.
2. A paper entitled, "Utilization of Hardware-in-the-Loop Simulation for HELLFIRE Tasks," has been prepared. It describes how the Guidance and Control Analysis Group's simulation facility is used to meet that group's HELLFIRE mission, including the support of the Low Cost Laser Seeker evaluation.

1 Incl
as

Russell T. Gambill
RUSSELL T. GAMBILL
Guidance and Control Analysis
Guidance and Control Directorate
Technology Laboratory

UTILIZATION OF HARDWARE-IN-THE-LOOP SIMULATION FOR HELLFIRE TASKS

Guidance and Control Analysis Group
Guidance and Control Directorate
Technology Laboratory

1. Purpose

The purpose of this paper is to describe how the Guidance and Control (G&C) Analysis Group's Hardware-in-the-Loop (HWIL) simulation facility is used to meet that Group's HELLFIRE mission. In particular, the manner in which the G&C Analysis Group meets the objective outlined in the "Low Cost Laser Seeker Evaluation Test Plan" will be addressed.¹

It is the intent of the G&C Analysis Group to support the evaluation of the two low cost laser seekers currently under consideration for use in the HELLFIRE Modular Missile System (HMMS). This evaluation is being conducted under the direction of the Optical Guidance Technology Group, Advanced Sensors Directorate, DRDMI-TEO. That Group is responsible for determining how well each candidate seeker meets the seeker specifications. The G&C Analysis Group is responsible for comparing the two seekers in a facility that simulates the missile system and its dynamics under predicted environmental conditions. Further, the G&C Analysis Group must maintain the technical capability to monitor and spot-check the contractor's [Rockwell International, Columbus (R.I.C.)] technical development efforts and to assess his technical approach, particularly when he recommends altering it. It is the responsibility of R.I.C. to determine quantitatively how well each candidate seeker meets the seeker specifications.

2. Background

A comprehensive HWIL simulation was developed to perform guidance and control system design verification and optimization of both autopilot and seeker for a laser semi-active terminal homing weapon system.²

The facility consists of the following major components:

- a. A Xerox Sigma 5 digital computer with 64K words (32 bits) of core memory. The major tasks performed by this computer are to simulate

the missile aerodynamics, and rotational and translational dynamics, and kinematics, and to provide commands to the gimballed mirror and the laser designator.

b. Two Comcor Ci 5000 analog computers interfaced with digital computer provide a hybrid computer simulation. The analog computers simulate missile rotational dynamics and can simulate autopilot, actuator, and seeker dynamics when some or all of these items are not included within the overall HWIL simulation.

c. A laser target simulator consisting of a pulsed laser beam which is reflected onto a translucent screen by a gimballed mirror. The changing distance between the missile and the target is simulated by varying the laser spot size and the energy density.

d. The three-axis electrohydraulic gimballed Carco flight table simulates missile angular motion. The laser seeking tracker, which senses the laser spot through the translucent screen, is mounted on this table. This component provides steering signals to the actual or simulated autopilot and actuators.

The HWIL simulation was first put together in 1969 to evaluate the (then) SAM-D missile. It originally consisted of an SDS 930 digital computer interfacing with a Comcor Ci 5000. The Carco flight table also was incorporated into the simulation. In 1970-71 the facility was improved to permit the evaluation of the Terminal Homing Accuracy Demonstration (THAD), which was the predecessor of HELLFIRE. The improvement consisted of incorporating a laser terminal homing capability. By early 1971, the facility consisted of the Comcor Ci 5000, a newly incorporated Sigma 5 digital computer, the Carco flight table, and the laser simulator. In the 1971-72 time frame, the facility was used to evaluate two competing (Texas Instruments and Martin-Marietta, Orlando) proposed COPPERHEAD systems. In May 1973 it took on a true hardware-in-the-loop character. Both Texas Instruments and Martin provided 12 missiles each to be evaluated competitively for the advanced development phase of the COPPERHEAD program. Also when these two companies bid for the engineering development phase of the COPPERHEAD program, the HWIL facility was used to help evaluate the two potential contractors' technical capabilities. Finally, it was used to support the source selection evaluation board (SSEB) in evaluating the two (R.I.C. and Hughes) competing bidders.

Presently, in addition to HELLFIRE support, the COPPERHEAD program also is supported using the HWIL facility. Each produced COPPERHEAD guidance and control unit (including the seeker and the autopilot) on the Carco table and subjecting it to a standardized test at each of three roll angles, from which it is determined whether the unit is functionally operable.

3. HELLFIRE Program Support

The HWIL facility is being used to support (by performing evaluations and selected analyses) the engineering development phase of the HELLFIRE program. It is also intended to use the facility to evaluate and compare the two (R.I.C. and Martin) competing seeker systems. Rockwell will evaluate the two competing laser seekers by measuring their characteristics and simulating their in-flight operation on their own HWIL facility. The G&C Analysis Group will evaluate each of the two laser seekers by using their HWIL facility and determining which system performs best under simulated flight conditions.

The G&C Analysis Group's HWIL simulation facility has the capability of permitting that group to meet its assigned HELLFIRE mission of evaluating and comparing the two competing laser seekers. As such, it can provide information which will enable the group to determine which system has the best chance of meeting the total system requirements.

The flight table used in the HWIL simulation facility is a modified 2-axis (pitch and yaw) Carco model. The bandwidth of that table has been found to be adequate for the class of seekers being tested. For example, a 30° phase shift existed at 2 Hz in the original uncompensated flight table. However, for several years the flight table has been compensated to provide the proper (i.e., 0°) phase shift at that frequency. Performance has been established over a 60 db range, which meets the specification.

4. Proposed Hardware-in-the-Loop Modifications

In addition to the existing modifications, laboratory conditions surrounding the HWIL are constantly evaluated with the objective of improving facility performance in a cost conscious manner.

I

Modest improvements have been incorporated from time to time, such as the recent addition of anti-reflective material (for the wave length we are using) for use on the floor. A list of other modifications under consideration follows. Several of these improvements could be implemented in time for the impending seeker evaluation.

(1) The room containing the facility could be renovated to remove contaminating inputs to the systems being evaluated. Where feasible, mobile equipment that does not need to be in the room (such as work benches and consoles) could be removed and placed outside the room. The ceiling and walls could be covered with an anechoic material to absorb unwanted inputs. A sliding screen could be installed to separate the laser area from the seeker - Carco table area. Personnel not absolutely needed in the room during simulation runs should remain outside the room. Those who remain in the room should remove, cover, or mask light-colored reflective clothing. This entire set of improvements could be implemented in a short time period.

(2) A "Warm-up" period could be used to heat up equipment, build up energy levels, and in general permit transients to die out. This should be done before using laser pulses in order to provide better repeatability of results. This improvement could be implemented immediately.

(3) A study could be made for improving the dynamic response of the Carco table when the roll fixture is attached.

(4) A similar (to the above item) study could be instigated to determine if the mirror system dynamics should be improved.

(5) An analytical study of a means of improving the dynamic range of the Carco table is being conducted recently by Dr. S. M. Seltzer (a consultant to the G&C Analysis Group).

5. Conclusions

The hardware-in-the-loop facility will continue to be used to support the HELLFIRE program. Selected scenarios and trajectories that are within the capabilities, geometry, and optics of existing equipment will be utilized. It is felt that by so doing, the stated HELLFIRE mission can be accomplished by the Guidance and Control Analysis Group.

REFERENCES:

¹"Low Cost Laser Seeker Evaluation Test Plan," contained in a DF to Roger Comer, HELLFIRE Project Office, dated 13 March 1978, signed by Jere D. Ducote, Sr., Chief, Optical Guidance Technology, Advanced Sensors Directorate.

²Pastrick, H. L., Will, C. M., Jr., Isom, L. S., Jolly, A. C., Hazel, L. H., and Vinson, R. J., "Hardware-in-the-Loop Simulation: A Guidance System Optimization Tool," AIAA Paper No. 74-929, Anaheim, California, August 5 - 9, 1974.

RESEARCH ON FUTURE US ARMY MODULAR MISSILE

"ADVANCED GUIDANCE AND CONTROL"

S. M. SELTZER

10 MAY 79

PURPOSE OF BRIEFING

1. ASSESSMENT OF PROGRAM STATUS
2. PROGRAM PLANS

BRIEFING FORMAT

- 1. OBJECTIVES**
- 2. PROGRAM PLAN**
- 3. INITIAL ACHIEVEMENTS/STATUS**
- 4. PROJECTED ACCOMPLISHMENTS**
- 5. PROGRAM IMPLEMENTATION**

PROGRAM OBJECTIVES

1. EXTEND SYSTEM TECHNOLOGY THAT "LEAPFROGS"
CURRENT DESIGN BASE
2. PROVIDE AND VALIDATE RESEARCH ENABLING
DIGITAL OPTIMAL G&C OF FUTURE
US ARMY MODULAR MISSILE

REQUIREMENTS FOR PROGRAM

1. PREDICTED FUTURE TARGETS
2. WEAPON SYSTEM CAPABILITIES
 - A. EXISTING
 - B. UNDER DEVELOPMENT

PROGRAM PLAN

	FY	FUNDS (\$K)	
		6.1	6.2
1. DEFINE PROGRAM	79		
2. DEFINE POTENTIAL DIGITAL G&C ELEMENTS	79	185	100
3. DEFINE CANDIDATE MISSILES & SUBSYSTEMS	80	200	250*
4. EVALUATE CANDIDATES	81	?	250*
5. SELECT & VALIDATE SELECTED CANDIDATES	82	?	625

*DARCOM CORE

PROGRAM DEFINITION

	<u>IN-HOUSE</u>	<u>CONTRACT</u>
1. TARGET/MISSILE SCENARIOS & DYNAMICS	PASTRICK, McLEAN, MAPLES, THACKER	
2. MISSILE PLANT CHARACTERISTICS	HERBERT, KALANGE WASHINGTON	
3. AERODYNAMICS	McCOWAN	
4. ERROR SOURCES		
5. GUIDANCE LAWS	PASTRICK, KELLY McCOWAN, DICKSON	SELTZER, WARREN (U OF FL), YORK (W KY U)
6. DISTURBANCE ACCOMMODATING CONTROL (DAC)	KELLY, McCOWAN	JOHNSON (UAH)
7. SENSOR CHARACTERISTIC	MURDOCK	
8. COMPUTER-AIDED DESIGN TOOLS	MILL	
9. MICROPROCESSOR SOA	ISOM	
10. DIGITAL DESIGN TOOL DEVELOPMENT		SELTZER
11. COORDINATION		SELTZER

1. TARGET/MISSILE SCENARIOS & DYNAMICS

1. PRINCIPAL INVESTIGATORS

J. McLEAN

R. MAPLES

J. THACKER

2. MAJOR TARGETS (THREATS)

A. AIRCRAFT

B. CRUISE MISSILES

C. TBMs

3. CONFIRMATION BY OSD, USAF

4. TASK COMPLETED - UPDATE IF REQUIRED

2. MISSILE PLANT CHARACTERISTICS

1. PRINCIPAL INVESTIGATORS

E. HERBERT

M. KALANGE

2. ACHIEVEMENTS

PRELIMINARY MISSILE DESIGN EQUATIONS

3. PROJECTED ACCOMPLISHMENTS--DETAILED ANALYTICAL MODELS

A. MISSILES (SPRINT, PATRIOT?, AS UPDATED)

B. EFFECTORS

C. AUTOPILOTS

3. AERODYNAMICS

1. PRINCIPAL INVESTIGATOR

D. WASHINGTON

2. ACHIEVEMENTS

PLAN OF ACTION

3. PROJECTED ACCOMPLISHMENTS

MANEUVERABILITY REQUIREMENTS & CAPABILITIES

DETERMINE CANDIDATE CONFIGURATION

DETERMINE PERFORMANCE DATA

4. ERROR SOURCES

1. PRINCIPAL INVESTIGATOR

McCOVAN

2. ACHIEVEMENTS

A. CATEGORIZED ERROR SOURCES

- (1) MISSILE
- (2) AERODYNAMIC
- (3) INSTRUMENT
- (4) EXTERNAL
- (5) SUBSYSTEM

B. PRELIMINARY EVALUATION OF DAC APPLICABILITY

3. PROJECTED ACCOMPLISHMENTS

TASK COMPLETED

5. GUIDANCE LAWS

1. PRINCIPAL INVESTIGATORS

PASTRICK

SELTZER (CDC)

KELLY

WARREN (U OF FL)

DICKSON

YORK (W KY U)

MCCOWAN

2. ACHIEVEMENTS

A. CATEGORIZED (AIAA AEROSPACE SCIENCES PAPER)

B. OPTIMAL GUIDANCE LAW EVALUATION

C. DAC APPLICATIONS

3. PROJECTED ACCOMPLISHMENTS

A. COMPARE CANDIDATE GUIDANCE LAWS (USING PLANT MODELS)

B. DIGITAL (SAMPLED-DATA) FORMULATIONS

C. EXTENSION OF GARBER'S WORK

D. GUIDANCE LAW DESIGN VIA DAC THEORY - KELLY & MCCOWAN

6. DISTURBANCE ACCOMMODATING CONTROL (DAC)

1. PRINCIPAL INVESTIGATORS

KELLY

MCCOWAN

C. D. JOHNSON (UAH)

2. ACHIEVEMENTS

A. BILL KELLY'S DISSERTATION: UTILIZING DAC WITH APPLICATIONS TO HOMING MISSILES

B. MCCOWAN: APPLICATIONS TO VARIOUS PORTIONS OF MISSILE

(1) GUIDANCE

(2) SENSORS

C. INITIAL "DIGITIZATION"

3. PROJECTED ACCOMPLISHMENTS

A. EXTEND DIGITAL APPLICATIONS

B. SEARCH FOR FURTHER APPLICATIONS

7. SENSOR CHARACTERISTICS

1. PRINCIPAL INVESTIGATOR

MURDOCK

2. ACHIEVEMENTS

IDENTIFIED TRADE STUDIES

3. PROJECTED ACCOMPLISHMENTS

- A. IDENTIFY FUTURE SENSOR REQUIREMENTS
- B. PERFORM IDENTIFIED TRADE STUDIES - DETERMINE
PREFERRED DESIGN DIRECTION(S)
- C. DEVELOP MATH MODELS OF CANDIDATE SENSORS

8. COMPUTER-AIDED DESIGN TOOLS

1. PRINCIPAL INVESTIGATOR

WILL

2. ACHIEVEMENTS

PROGRAMS NOW CODED:

- A. STABILITY ANALYSIS: ROOT LOCUS, BODE, NICHOLS
- B. RANDOM NOISE ANALYSIS: FFT, PSD, COVARIANCE
- C. DIGITAL MANIPULATION: Z-, W-TRANSFORMS

3. PROJECTED ACCOMPLISHMENTS

- A. DESIGN AND CODE EXECUTIVE ROUTINES
- B. DIGITAL ANALYSIS TOOLS

9. MICROPROCESSOR SOA

1. PRINCIPAL INVESTIGATOR

ISOM

2. ACHIEVEMENTS

INVESTIGATED CAPABILITIES, SOA

3. PROJECTED ACCOMPLISHMENTS

MAINTAIN AWARENESS OF SOA

AD-A074 782

CONTROL DYNAMICS CO HUNTSVILLE AL*
APPLICATION OF DISCRETE GUIDANCE AND CONTROL THEORY. (U)
AUG 79 S M SELTZER
CDC-79-2

F/G 17/7

DAAK40-78-C-0226

UNCLASSIFIED

NL

3 OF 3

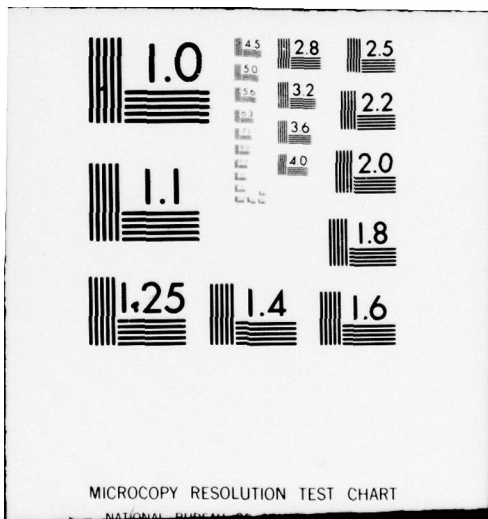
ADA
074782



END
DATE
FILMED

11 -79

DDC



MICROCOPY RESOLUTION TEST CHART

NATIONAL BUREAU OF STANDARDS-1963-A

10. DIGITAL DESIGN TOOL DEVELOPMENT

1. PRINCIPAL INVESTIGATOR
SELTZER (CONSULTANT)
2. ACHIEVEMENTS
 - A. DIGITAL CONTROL SYSTEM DESIGN SEMINAR: "CLASSICAL"
 - B. SAM--A SIGNAL FLOW GRAPH ALTERNATIVE
 - C. CROSS MULTIPLICATION-ANALYTICAL DETERMINATION OF DIGITAL SYSTEM RESPONSE
3. PROJECTED ACCOMPLISHMENTS
 - A. PARAMETER SPACE--FOR DIGITAL SYSTEM DESIGN & ANALYSIS
 - B. DIGITAL OPTIMAL CONTROL LAWS
 - C. DIGITAL CONTROL SYSTEM DESIGN SEMINAR: "MODERN"

11. COORDINATION

1. PRINCIPAL INVESTIGATORS

GAMBILL

SELTZER (CONSULTANT)

2. ACHIEVEMENTS

A. USAF (EGLIN)

B. BM/DSC

C. DoD

D. AIAA 17TH AEROSPACE SCI. MTG: "GUIDANCE LAWS FOR SHORT RANGE TACTICAL MISSILES"

E. AIAA ANNUAL G&C CONF.: "US ARMY FUTURE G&C SYSTEMS"

3. PROJECTED ACCOMPLISHMENTS

A. MEMO OF UNDERSTANDING: USAF EGLIN AFB & MIRADCOM

B. PROGRAM DOCUMENTATION

C. ADVERTISE!

FY79 PROGRAM IMPLEMENTATION

IN-HOUSE	6.1	6.2	OUT-OF-HOUSE	6.1	6.2
AERO	\$35K		DR. SELTZER, CONSULTANT	\$10K	\$63K
G&C (TGN)	\$15K	\$35K	PROF. C. D. JOHNSON, UAH	\$ 8K	
			PROF. WARREN, U OF FLA	\$ 8K	
			PROF. YORK, W. KY. U.	\$73K	
			SAI		
	<u>\$50K</u>	<u>\$35K</u>		<u>\$99K</u>	<u>\$63K</u>

Σ6.1: \$149K

Σ6.2: \$ 98K

FY80 PROGRAM IMPLEMENTATION PLANS

IN-HOUSE	6.1	6.2	OUT-OF-HOUSE	6.1	6.2
G&C (TGN)	\$100K		SELTZER		\$70K
		\$145K	WARREN	\$20K	
OTHER LABS	<u>\$ 30K</u>	<u> </u>	JOHNSON	<u>\$20K</u>	<u> </u>
	\$130K	\$145K		\$40K	\$70K

Σ6.1: \$170K

Σ6.2: \$215K

SUMMARY

- 1. ACCOMPLISHMENTS**
- 2. G&C ANALYSIS GROUP**
 - A. EXTENDING SYSTEM ANALYSIS/DESIGN CAPABILITIES**
 - B. LEARNING DIGITAL SYSTEM ANALYSIS/SKILLS**
- 3. TEAM**

APPENDIX J. PRESENTATION TO ADVANCED SENSORS DIRECTORATE

RESEARCH ON FUTURE US ARMY MODULAR MISSILE

"ADVANCED GUIDANCE AND CONTROL"

S. M. SELTZER

JUNE 79

(2)

PURPOSE OF BRIEFING

1. DESCRIBE ADVANCED G&C PROGRAM
2. DESCRIBE PREDICTED TARGETS OF THE 1990'S
3. PERMIT PREDICTION OF ADVANCED SENSOR REQUIREMENTS

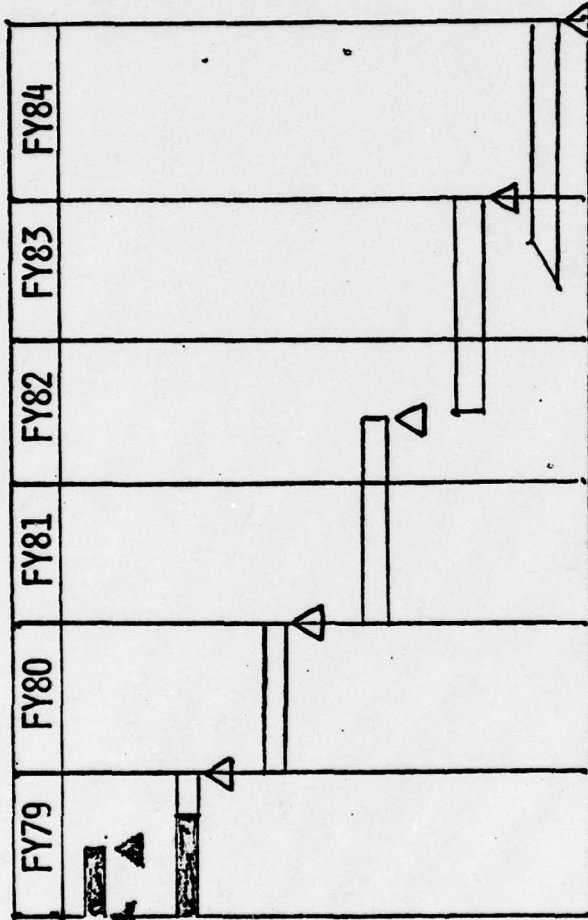
AGENDA

- | | |
|--------------------------------------|---------|
| 1. PROGRAM DEFINITION | SELTZER |
| 2. TARGET SCENARIO & DYNAMICS | MAPLES |
| 3. GUIDANCE LAWS | SELTZER |
| 4. DISTURBANCE ACCOMMODATING CONTROL | SELTZER |
| 5. DIGITAL DESIGN TOOL DEVELOPMENT | SELTZER |
| 6. SUMMARY | SELTZER |

PROGRAM OBJECTIVES

1. EXTEND SYSTEM TECHNOLOGY THAT "LEAPFROGS" CURRENT DESIGN BASE
2. PROVIDE AND VALIDATE RESEARCH ENABLING DIGITAL OPTIMAL G&C OF FUTURE US ARMY MODULAR MISSILE
3. PROVIDE MEANS OF DEFEATING PREDICTED FUTURE TARGETS

PROGRAM PLAN



1. DEFINE PROGRAM

2. COLLECT G&C ELEMENTS

3. DEFINE CANDIDATE SYSTEMS

4. EVALUATE CANDIDATES

5. DESIGN & FABRICATE

6. PROOF OF CONCEPT

PROGRAM DEFINITION

- *1. TARGET/MISSILE SCENARIOS & DYNAMICS
2. MISSILE PLANT CHARACTERISTICS
3. AERODYNAMICS
4. ERROR SOURCES
- *5. GUIDANCE LAWS
- *6. DISTURBANCE ACCOMMODATING CONTROL (DAC)
7. SENSOR CHARACTERISTICS
8. COMPUTER-AIDED DESIGN TOOLS
9. MICROPROCESSOR SCA
10. DIGITAL DESIGN TOOL DEVELOPMENT

GUIDANCE LAWS

PREDICTED FUTURE TARGETS (1990's AND BEYOND)

- **PRESENT WEAPON SYSTEM PERFORMANCE MAY BE SERIOUSLY DEGRADED IN BATTLEFIELD ENVIRONMENT OF 1990's**
- **CURRENT GUIDANCE LAWS: INADEQUATE**
- **CURRENT MISSILE AIRFRAME AND PROPULSION SYSTEMS: MAY BE INADEQUATE**

GUIDANCE LAWS

LITERATURE SEARCH

- TO ESTABLISH TECHNOLOGY BASE STARTING POINT
- OVER 100 PERTINENT REFERENCES

GUIDANCE LAWS

COMPARISON CRITERIA

- o ABILITY TO ENGAGE TARGETS
- o COMPLEXITY AND RELIABILITY
- o COST
- o SENSOR REQUIREMENTS
- o MISSILE AIRFRAME AND PROPULSION REQUIREMENTS
- o TACTICAL CONSIDERATIONS, e.g. "FIRE AND FORGET"

GUIDANCE LAWS

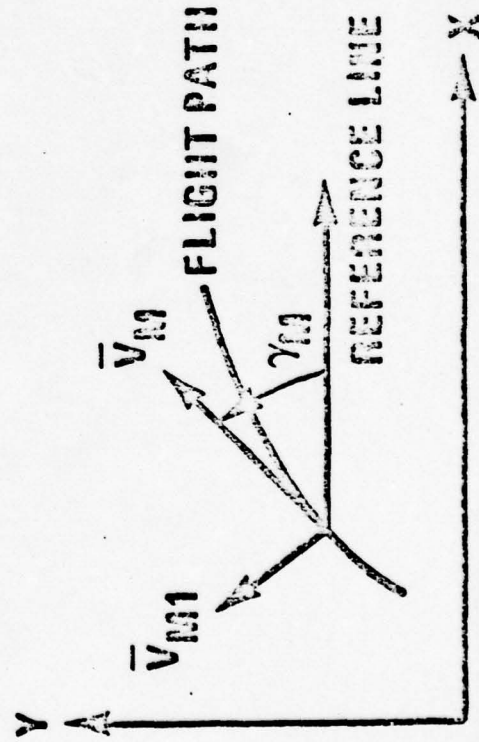
PROPORTIONAL NAVIGATION GUIDANCE (PNG): DESCRIPTION

$$\dot{\gamma}_M = N\dot{\lambda}$$

λ : LOS w.r.t. FIXED REFERENCE

N : "NAVIGATION RATIO"

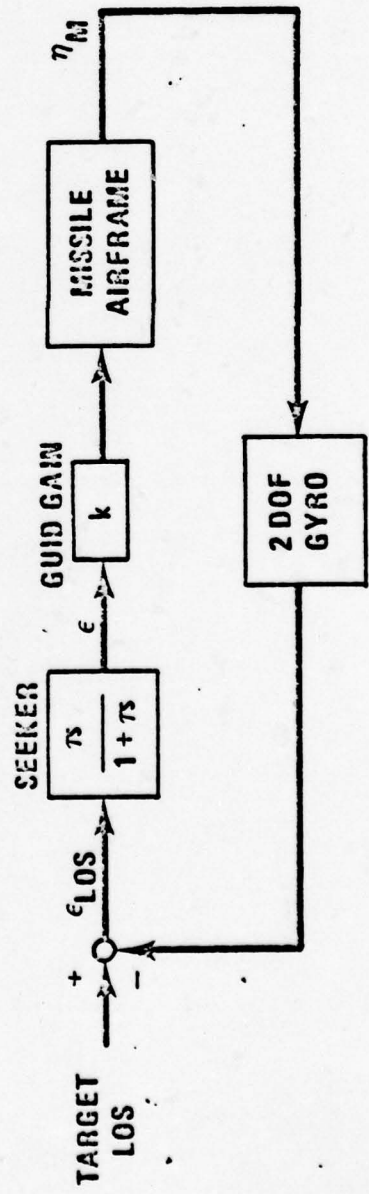
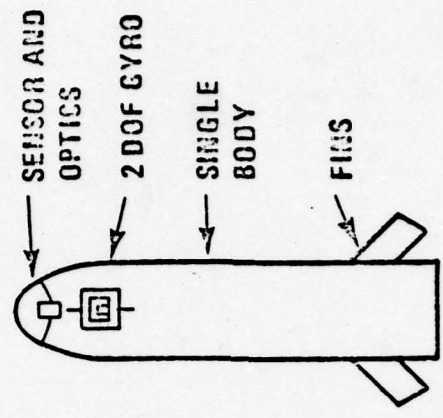
γ_M : FLIGHT PATH w.r.t. FIXED REFERENCE



GUIDANCE LAWS

PROPORTIONAL NAVIGATION GUIDANCE (PNG): MECHANIZATION

$$\eta_M(s) = k\epsilon(s) = \frac{[k\tau s\lambda(s)]}{(1 + \tau s)}$$



GUIDANCE LAWS

PROPORTIONAL NAVIGATION GUIDANCE (PNG): CHARACTERISTICS

- PERFORMANCE
 - EXCELLENT
 - ALMOST ALWAYS RESULTS IN CONSTANT VELOCITY TARGET INTERCEPT
- REQUIRED CONTROL EFFORT - LOW TURNING ACCELERATION
- CAN "FIRE AND FORGET"

PNG: EXAMPLES OF USAGE

- HELLFIRE
- COPPERHEAD
- PATRIOT

GUIDANCE LAWS

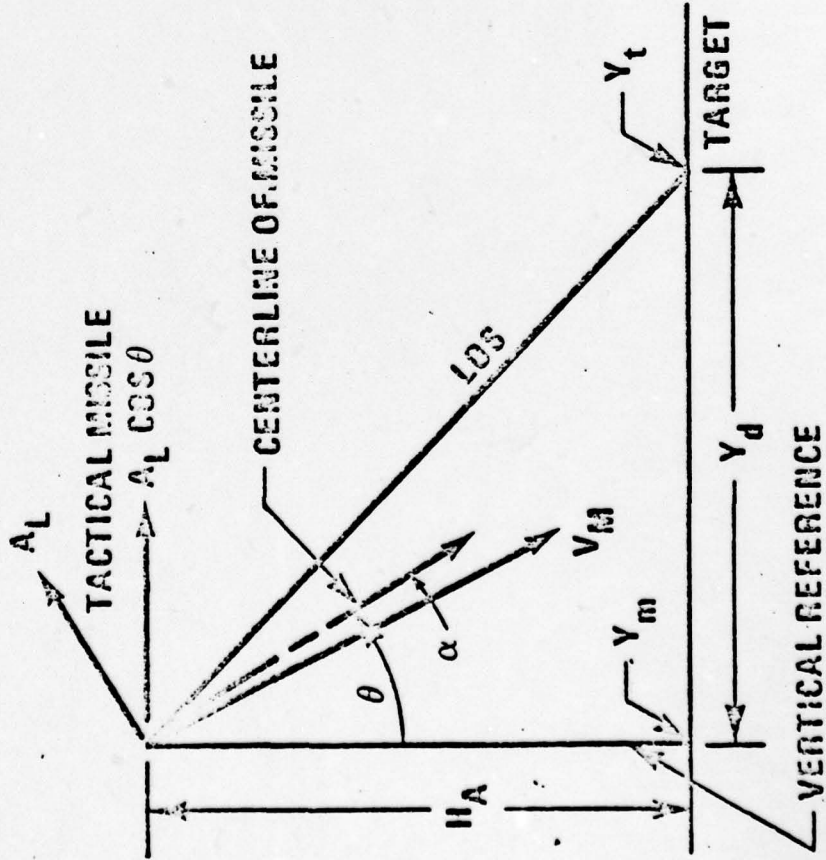
OPTIMAL LINEAR GUIDANCE: DESCRIPTION

- BACKGROUND – SINCE MID-60's, MISSILE GUIDANCE LITERATURE INCREASINGLY PERMEATED W/OPTIMAL CONTROL TECHNIQUES
- TYPICAL OPTIMAL CONTROL LAW FORMULATION
 - ASSUME SMALL $\angle\alpha$ AND IGNORE
 - STATE

$$\bar{x} = \begin{bmatrix} Y_d, \dot{Y}_d, A_L, \theta \end{bmatrix}^T \equiv \begin{bmatrix} Y_t - Y_m, Y_t - Y_m, A_L, 0 \end{bmatrix}^T$$

GUIDANCE LAWS

OPTIMAL LINEAR GUIDANCE: DESCRIPTION (CONT'D)



Y_d : POSITION VARIABLE FROM MISSILE TO TARGET, PROJECTED ON GROUND

Y_t : POSITION VARIABLE OF TARGET

Y_m : POSITION VARIABLE OF MISSILE, PROJECTED ON GROUND

A_L : MISSILE LATERAL ACCELERATION

θ : MISSILE BODY ATTITUDE \angle

GUIDANCE LAWS

OPTIMAL LINEAR GUIDANCE: DESCRIPTION (CONT'D)

o TYPICAL OPTIMAL CONTROL LAW FORMULATION (CONT'D)

- CONTROLLER

$$u = C_Y Y_d + C_{\dot{Y}} \dot{Y}_d + C_{\theta} \theta + C_{A_L} A_L$$

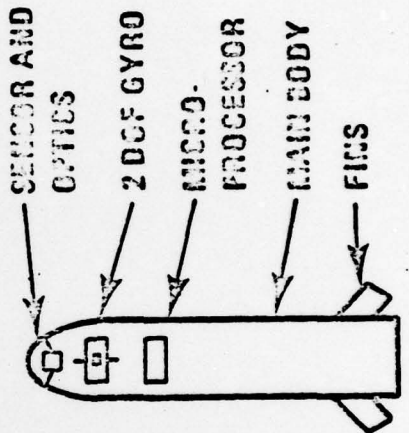
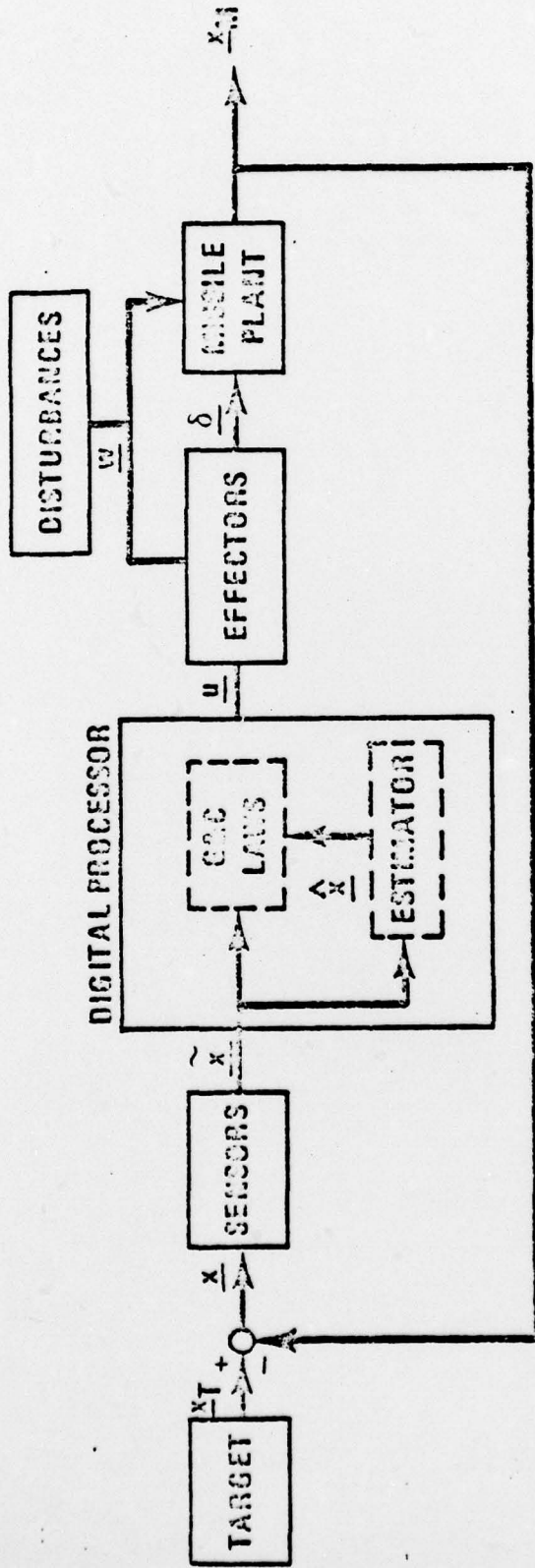
C_Y, C _{\dot{Y}} , C _{θ} , C_{A_L} : TIME-VARYING COEFFICIENTS CHOSEN TO MINIMIZE J

- COST FUNCTIONAL

$$J = Y_d(t_f) + \gamma \theta(t_f) + \beta \int_0^{t_f} u^2(t) dt$$

GUIDANCE LAWS

OPTIMAL LINEAR GUIDANCE: MECHANIZATION



- x : SYS STATE
- x_T : TARGET STATE
- x_M : MSL STATE
- \hat{x} : SENSED STATE
- \hat{x} : ESTIMATED STATE
- u : CONTROL
- δ : EFFECTOR(S) STATE

12

GUIDANCE LAWS

OPTIMAL GUIDANCE: CHARACTERISTICS

- PERFORMANCE – EXCELLENT
- REQUIRED CONTROL EFFORT – HIGH TURNING ACCELERATION
- CAN "FIRE AND FORGET"

19)

GUIDANCE LAWS

OPTIMAL GUIDANCE: SPECIAL CONSIDERATIONS

- o TIME-TO-GO
- o SENSITIVITY TO INITIAL CONDITIONS
 - NEED ACCURATE MODELING OF SYSTEM
 - IMPORTANCE OF SELECTING NUMERICAL VALUES FOR MATRICES IN J
- o COMPLEXITY → COMPUTER ROTS
- o CAN CONSIDER ADDITIONAL (w.r.t. MISS DISTANCE) PERFORMANCE CRITERIA
- o ABILITY TO ENGAGE HIGHLY MANEUVERABLE TARGET(S)

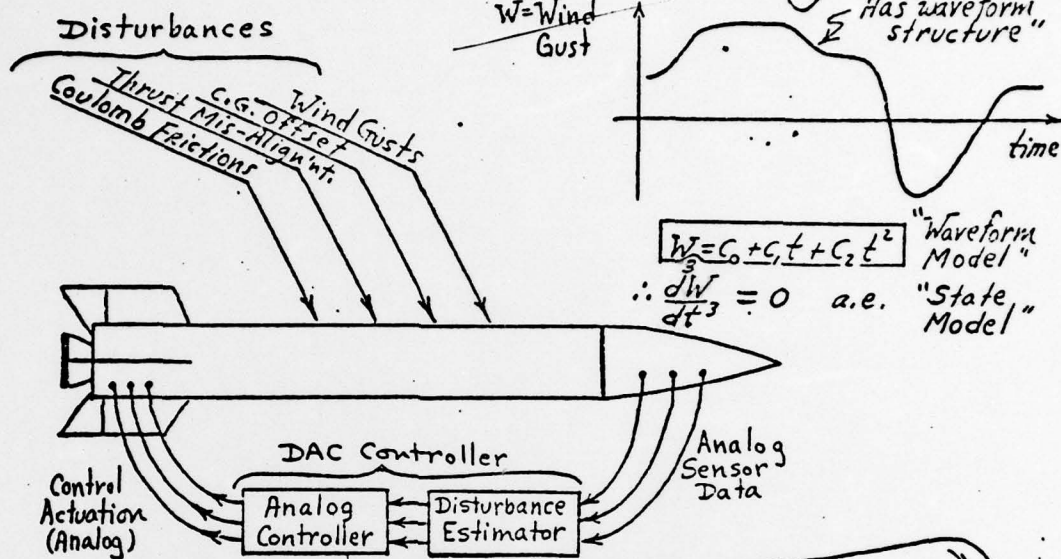
GUIDANCE LAWS

CONCLUSIONS

- o SELECTED CANDIDATE: OPTIMAL GUIDANCE
 - TARGET ENGAGEMENT CAPABILITIES
 - RELATIVE COMPLEXITY
 - CURRENT IMPLEMENTATION DIFFICULTIES
 - STRONGEST SHORTCOMING: TIME-TO-GO (t_{GO}) ROT.

- o STRONG CONTENDER: PNG
 - SIMPLICITY
 - TARGET ENGAGEMENT LIMITATIONS

Brief Review of Continuous-Time DAC Theory (4)



Nature of DAC Controller (Disturbance-Absorption Mode)

The DAC Controller generates a real-time on-line estimate of the actual (instantaneous) disturbance waveform and creates a special control action that exactly cancels-out the disturbance effect on the missile, [like classical idea of "crabbing into the wind" to cancel-out the wind-drift effect; ditto for boating example].

(22) (10)

Composite Discrete-Time Model for Plant + Disturbance

Remark: The disturbance $w(t)$ is typically NOT coupled to the plant dynamics through a sample-and-hold arrangement. Thus, the composite model for plant + disturbance must not assume that $w(t) = w(nT)$, but rather that $w(t) = w(t)$.

- Review of Composite Model for Continuous-Time Case

$$\begin{cases} \dot{x} = Ax + Bu + Fw \\ y = Cx \\ \dot{w} = Hz \\ \dot{z} = Dz \end{cases}$$

$$\begin{pmatrix} \dot{x} \\ \dot{z} \end{pmatrix} = \begin{bmatrix} A & | & FH \\ \hline 0 & | & D \end{bmatrix} \begin{pmatrix} x \\ z \end{pmatrix} + \begin{bmatrix} B \\ 0 \end{bmatrix} u ; y = [C \ | \ 0] \begin{pmatrix} x \\ z \end{pmatrix}$$

- Composite Model for Discrete-Time Case (Time-Invariant Case)

(Use Laplace Transform for
the DAC block)

$$\begin{pmatrix} Ex \\ Ez \end{pmatrix} = \begin{bmatrix} \overset{\tilde{A}}{e^{AT}} & | & \overset{\tilde{F}_H}{\int_0^T e^{A(T-\tau)} F H e^{D\tau} d\tau} \\ \hline 0 & | & \overset{\tilde{D}}{e^{DT}} \end{bmatrix} \begin{pmatrix} x(nT) \\ z(nT) \end{pmatrix} + \begin{bmatrix} \overset{\tilde{B}}{\int_0^T e^{A(T-\tau)} B d\tau} \\ 0 \end{bmatrix} u(nT)$$

$$y(nT) = [C \ | \ 0] \begin{pmatrix} x(nT) \\ z(nT) \end{pmatrix}$$

DIGITAL DESIGN TOOL DEVELOPMENT

1. ACHIEVEMENTS
 - A. DIGITAL CONTROL SYSTEM DESIGN SEMINAR: "CLASSICAL"
 - B. SAM--A SIGNAL FLOW GRAPH ALTERNATIVE
 - C. CROSS MULTIPLICATION--ANALYTICAL DETERMINATION OF DIGITAL SYSTEM RESPONSE
2. PROJECTED ACCOMPLISHMENTS
 - A. PARAMETER SPACE--FOR DIGITAL SYSTEM DESIGN & ANALYSIS
 - B. DIGITAL OPTIMAL CONTROL LAWS
 - C. DIGITAL CONTROL SYSTEM DESIGN SEMINAR: "MODERN"

SUMMARY

1. REVIEW OF PROGRAM
2. STATUS OF FUTURE TARGET PREDICTIONS
3. STATUS OF GUIDANCE LAW SELECTION & DEVELOPMENT
 - A. PNG
 - B. OPTIMAL
 - C. DAC
4. DIGITAL IMPLEMENTATION
5. DESIRED SENSOR CHARACTERISTICS
 - A. MISSILE STATE MEASUREMENT/ESTIMATION
 - B. TARGET STATE MEASUREMENT/ESTIMATION
 - C. TIME-TO-GO ESTIMATE

APPENDIX K. PLANT MODEL FOR ADVANCED GUIDANCE AND CONTROL SYSTEM

DISPOSITION FORM

For use of this form, see AR 340-15, the proponent agency is TAGCEN.

Dr. Seltzer

REFERENCE OR OFFICE SYMBOL

SUBJECT

DRDMI-TGN

Plant Model for Advanced G&C System

TO SEE DISTRIBUTION

FROM DRDMI-TGN

DATE 18 Jun 79

CMT 1

Dr. Seltzer/dt/6-5954

1. As a result of target predictions and meetings among the G&C Analysis Group and the Aeroballistics Directorate personnel, the following decisions regarding the Advanced G&C System have been arrived at:

a. As a design goal, the shape of the missile that is to carry the Advanced G&C System is to be as clean aerodynamically as possible. Three possible shapes are to be considered by the Aeroballistics Directorate in their studies supporting the development of the Advanced G&C System. They are:

- 1) Low aspect ratio long-cord delta configuration (Fig. 1). This shape is similar in appearance to a dart. Maneuvering is provided by hinged aft-tabs.
- 2) Flared-skirt extendable wing surfaces configuration (Fig. 2). This configuration derives its stability from the flared aft-body. Wing surfaces are extended when control (maneuver) authority is desired -- typically at the terminal phases of the trajectory.
- 3) Lifting body configuration (Fig. 3). This is to obtain more efficient coordinated ("bank-to turn") control maneuvers. Body lift is achieved by using elliptical or triangular half cross-sections.

b. Design Point.

The following design point will be used by Messrs. Dave Washington and Jimmie Derrick (Aeroballistics Directorate) to generate aerodynamic coefficients for G&C Analysis Group simulations.

- 1) MACH No: 4
- 2) Lateral g's: 12
- 3) Altitude: 70,000 ft

It is expected that these values will be exceeded by a significant margin, e.g. perhaps 20 g's.

2. When the Aeroballistics studies have been completed, the G&C Analysis Group's simulation development will begin. The analytical models of the plant developed by

DRDMI-TGN

18 Jun 79

SUBJECT: Plant Model for Advanced G&C Systems

Ed Herbert and Mike Kalange (to be reported upon in the first annual report on our progress and achievements, due 1 October 1979) will be used in conjunction with the aerodynamic data as the basis for the simulation.

Russell T. Gambill

RUSSELL T. GAMBILL
Guidance and Control Analysis
Guidance and Control Directorate
Technology Laboratory

DISTRIBUTION:

DRDMI-TR, R. Hartman

-TDK, D. Washington

-TDW, J. Derrick

R. Dickson

-TGN, All Personnel

Research and Training Corporation, ATTN: C. D. Johnson

University of Florida, ATTN: M. Warren

Western Kentucky University, ATTN: R. York

Control Dynamics Company, ATTN: S. Seltzer

Science Applications Incorporated

LOW-ASPECT-RATIO LONG-CHORD DELTA MISSILE CONFIGURATION

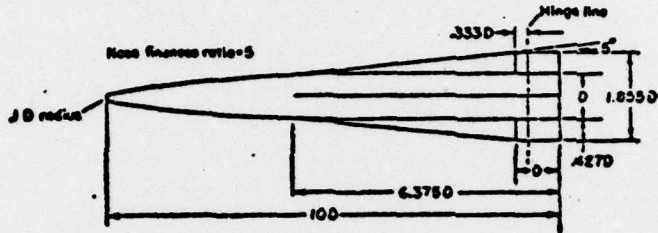


Figure 1

FLARED-SKIRT-STABILIZED MISSILE CONFIGURATION WITH ALL-MOVABLE FORWARD SURFACE

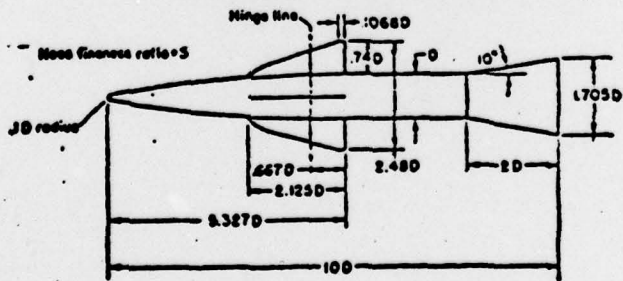


Figure 2

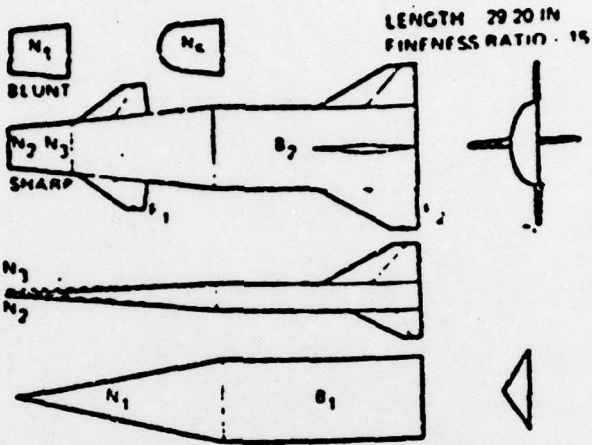


FIGURE 2 NON CIRCULAR BODY CONCEPTS

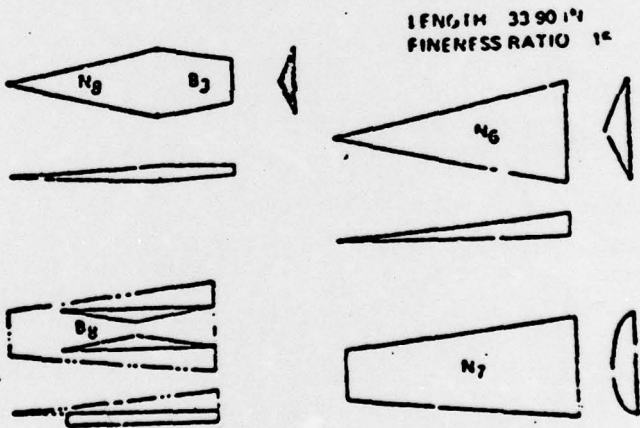


FIGURE 3 LIFTING BODY AND FAVORABLE INTERFERENCE CONCEPTS